Roles of Disordered Volume Regulation in Apoptosis

Emi Maeno

Department of Physiological Sciences

School of Life Science

The Graduate University for Advanced Studies

and

Department of Cell Physiology

National Institute for Physiological Sciences

Okazaki 444-8585, Japan

2000

Summary

A major hallmark of apoptosis is normotonic shrinkage of cells. Here, we studied the relation between apoptotic cell shrinkage and apoptotic cell death. Induction of the apoptotic volume decrease (AVD) under normotonic conditions was found to be coupled to facilitation of the regulatory volume decrease (RVD), which is known to be attained by parallel operation of Cl and K^+ channels, under hypotonic conditions. Both the AVD induction and the RVD facilitation were found to precede cytochrome c release, initiator caspase (-8, -9) activation, effector caspase (-3) activation, DNA laddering and ultrastructural alterations in four cell types (human lymphoid U937, epithelial HeLa, rat pheochromocytoma PC12 and mouse neuroblastoma×rat glioma hybrid NG108-15 cells) after apoptotic insults with two distinct apoptosis inducers. Also, the AVD was not prevented by a broad-spectrum caspase inhibitor. When the AVD induction and the RVD facilitation were prevented by blocking volume-regulatory Cl or K^+ channels, these cells did not show succeeding apoptotic biochemical and morphological events and were rescued from death. Thus, it is concluded that the AVD, which is caused by disordered cell volume regulation, is an early prerequisite to apoptotic events leading to cell death. It was previously reported that hypertonic stress triggers apoptosis in cell types that lack the regulatory volume increase (RVI). In fact, in Na^+/H^+ antiporter-deficient CCL39 cells, which were found to lack the RVI mechanism, hypertonic stimulation was found to induce persistent cell shrinkage without following volume recovery, and then lead to succeeding apoptotic events and cell death. When the RVI ability was conferred by transfection of the gene of NHE1 isoform of Na^+/H^+ antiporter, this cell line failed to exhibit apoptosis under hypertonic stimulation. Taken together, it is concluded that disorderd or altered cell volume regulation is associated with apoptosis.

Introduction

Apoptosis is accompanied by characteristic morphological changes, including cell shrinkage and nuclear condensasion, chromatin margination, and the formation of membrane-bound remnants (apoptotic bodies) (Kerr et al. 1972). However, despite the universal prominence of cell volume loss in cells undergoing apoptosis, the relationship between this event and about biochemical events remains uncertain.

The normotonic cell shrinkage, here termed to apoptotic volume decrease (AVD), which is a major hallmark of apoptosis and starts before cell fragmentation (Wyllie et al. 1980), is known to be coupled to K^+ release from the cells (Barbiero et al. 1995; Benson et al. 1996; Bortner et al. 1997), presumably via K^+ channels (Yu et al. 1997; Wang et al. 1999; Colom et al. 1998). To drive the net efflux of water, which leads to cell shrinkage, release of anions should take place in parallel with K^+ release to restrain electroneutrality. Stimulation of CD95 receptor (Fas) has actually been shown to induce activation of outwardly rectifying Cl channels (Szabo et al. 1998), which were also activated by osmotic swelling (Lepple-Wienhues et al. 1998), in lymphoid Jurkat cells. Recently, hepatoma cells exposed to tumor necrosis factor were found to exhibit activation of both K^+ and Cl currents (Nietsch et al. 2000). Thus, there exists a possibility that volume regulation mechanisms (Okada & Hazama, 1989; Hoffmann & Simonseen, 1989; Okada, 1997), including volume-regulatory Cl and K^+ channels, are disordered, thereby inducing the AVD during the apoptotic process. Thus, the first purpose of the present study is to answer the question as to whether AVD is induced by operation of volume-regulatory K^+ and Cl^- channels.

Since Bortner and Cidlowski (1996) previously reported that persistent physical shrinkage induced by hyperosmotic stress leads to apoptosis in lymphoid cells, it is also possible that the AVD is a prerequisite to apoptotic

cell death. The second purpose of this study is to examine this possibility.

In recent years much has been learned about the molecular underpinnings of apoptosis, including the release of cytochrome c from mitochondria, modulation by Bcl-2 and related genes, and a central role for caspase activation in triggering final events (Li &Yuan, 1999). Both a receptor-mediated and a mitochondria-mediated pathways to caspase activation have been described, as summalized in Figure 1. In the receptor-mediated pathway, Fas ligand or tumor necrosis factor α (TNF α) binds to its receptor, causing receptor aggregation and recruitment of death adapter molecules on the cytoplasmic side of the membrane. Procaspase-8 and/or -10 are recruited to the complex, where it can undergo proximity-induced processing to the active form of a p20/p10 heterotetramer (Muzio et al. 1998). The activated caspase-8 (or -10) can then cleave procaspase-3 into caspase-3, which serves as an efficient executioner to cleave multiple targets within the cell, including caspase-activated DNase (Liu et al. 1997). Caspase-8 also targets the mitochondria through the proteolytic activation of Bid. The C-terminal fragment translocates to the mitochondria, where it mediates cytochrome c release. Although anti-apoptotic Bcl-2 family members may prevent the amplification mediated by cytochrome c release, they are generally ineffective in preventing the direct activation of caspase-3 by caspase-8 after Fas ligation (Huang et al. 1999). This has led to classification of cell lines as type I or type II based on whether they can generate enough caspase-3 directly or whether they depend upon the Bcl-2-inhibitable step of mitochondrial amplication (Peter et al. 1998). In the type II cells, caspsase activation is mediated by mitochondria and is activated in response to variety of cellular stresses, including DNA damage, protein kinase inhibition, and loss of survival signaling. In this pathway, termed the mitochondrial pathway, a pro-apoptotic member of the Bcl-2 family, such as Bax or Bid, associates with the mitochondria and directs the dissociation and eventual release of cytochrome c to the cytosol (Li et al. 1997). Apaf-1 binds cytochrome c, dATP

or ATP, and forms a large (~700 kDa) multimeric complex, termed the apoptosome, which also includes molecules of caspase-9 and -3 (Cain et al. 2000). Caspase-9 is activated when bound to Apaf-1, where it processes caspase -3 to its active form (Stennicke et al. 1999). While caspases are abundant in the cytoplasm of transformed cell lines, it appears that caspase-9 may be restricted to the mitochondria in neurons and cardiomyocytes (Krajewski et al. 1999). Caspases and another pro-apoptotic molecule, AIF, are released from mitochondria along with cytochrome c in response to stimuli that induce the permeability transition (Patterson et al. 2000). Although it is established that caspase activation is considered to be the *sine qua non* of apoptosis, it is not known whether AVD is an event upstream or downstream to caspase activation. The third porpose of this study is to answer this question.

The regulatory volume decrease (RVD) and regulatory volume increase (RVI) processes involve, respectively, loss of KCl as well as organic solutes and gain of NaCl as well as organic solutes through concerted activation of a number of channels and transporters (Hoffman & Simonsan, 1989; Okada, 1997). NaCl uptake during RVI is accomplished either by parallel operation of Na^+/H^+ and Cl^-/HCO_3^- antiporters or by operation of either Na^+-K^+-$2Cl^-$ or Na^+-Cl^- symporters. Accumulated Na^+ is then exchanged for extracellurar K^+ by the Na^+-K^+ pump. Different transport pathways have been reported to be responsible for the RVD-associated KCl loss, depending on the cell types. Electroneutral cotransporters such as K^+-Cl^- symporters and K^+/H^+ and Cl^-/HCO_3^- antiporters are reported to play a volume regulatory role in a number of cell types such as erythrocytes and gallbladder epithrlial cells. In most cell types, however, RVD involves activation of K^+ and Cl^- channels. Pallarel activation of Ca^{2+}-activated K^+ channels and Ca^{2+}-independent, volume-sensitive Cl^- channels was observed for the first time during the RVD process in human epitherial Intestine 407 cells (Hazama & Okada, 1988). It was previously reported that hypertonic stress triggers apoptosis in cell types

that lack the regulatory volume increase (RVI) mechanism (Bortner & Cidlowski, 1996). The Na^+/H^+ antiporter -deficient CCL39-derivative cells (PS120) lack the RVI mechanism(S. Wakabayashi, unpublished data: personal communication). The Na^+/H^+ exchanger isoform 1 (NHE1) is a plasma membrane transporter that regulates the intracellular pH (pH_i) and cell volume in virtually all cells. It is activated in response to a variety of stimuli including growth factors, Ca^{2+}-mobilizing agonists, and hyperosmotic stress (Wakabayashi et al. 2000). These stimuli that lead to cytosolic acidification activate NHE1 thereby attaining the RVI. Fas-induced apoptosis is paralleled by marked cytosolic acidification (Lang et al. 2000) which partially results from activation of HCO_3-permeable anion channels. The cytosolic acidification should activate the Na^+/H^+ exchanger. Rather, it was found that a decline of Na^+/H^+ exchange activity parallels the decline of cytosolic ATP (Lang et al. 2000). Inhibition of the Na^+/H^+ exchange most likely plays a permissive role in receptor triggered apoptosis. Beyond that nuclear acidification may promote DNA fragmentation as DNase II has its pH optimum in the acidic range. Along those lines, Fas-induced apoptosis is observed to be accelerated by inhibition of Na^+/H^+ exchange (Lang et al. 2000). In these cells hypertonic stimulation induces cell shrinkage without following volume recovery (RVI), and then sustained cell shrinkage may switch on the AVD-inducing machinery, thereby inducing further shrinkage, leading to succeeding apoptotic events and cell death. The fourth purpose of the present study is to answer the question whether RVI dysfunction is actually associated with apoptosis.

Materials and Methods

Cell culture and apoptosis induction.

HeLa cells were cultured in MEM medium. U937, SKW6.4, WEHI231 and Bcl-2-transfected WEHI231 (WEHI/Bcl-2) cells were cultured in RPMI 1640 medium, supplemented with 10% fetal bovine serum (FBS). WEHI231 and WEHI/Bcl-2 cells were gifts from Dr. Takeshi Tsubata (Tokyo Med. Dent. Univ.). PC12 and NG108-15 cells were cultured in DMEM medium supplemented with 10% FBS and provided for experiments without inducing neuronal differentiation. SKW6.4 cells were purchased from American Type Culture Collection. The Chinese hamster lung fibroblast line CCL39 (American Type Culture Collection), its Na^+/H^+ antiporter-deficient derivative PS120 cells, and the corresponding transfectants (PS120/NHE1) were maintained in DMEM medium containing 25 mM $NaHCO_3$ supplemented with 7.5% FBS. PS120 and PS120/NHE1 cells were gifts from Dr. Shigeo Wakabayashi (Natl. Cardiovas. Centr. Res. Insti). Cells were maintained at 37℃ in the presence of 5% CO_2.

To induce apoptosis, these cells in the log-growing phase were treated with bacterial alkaloid staurosporine (STS: Sigma, Tokyo: 1, 4, 4 and 8 ΠM for U937, HeLa, NG108-15 and PC12 cells, respectively), as previously described (Ishizaki et al. 1993), or TNFΔ (Endogen, Woburn, : 2, 10, 10 and 20 ng ml ^{1} for U937, PC12, NG108-15 and HeLa cells, respectively) plus cycloheximide (CHX: WAKO, Kyoto, Japan: 0.1, 1, 1 and 10 Πg ml ^{1} for U937, PC12, NG108-15 and HeLa cells, respectively), as previously reported (White et al. 1992), or anti-Fas monoclonal antibody (MBL,CH-11, Tokyo: 0.5 Πg ml ^{1} for U937, HeLa and SKW6.4 cells), as previously reported (Eguchi et al. 1999), or 45°C (for 10 min for WEHI and WEHI/Bcl-2) or H_2O_2 (50 μ M for WEHI and WEHI/Bcl-2) or hypertonic solution (adding NaCl or mannitol).

Cell volume measurements.

Cell volume was measured by an electronic sizing technique using a Coulter-type cell size analyser (CDA-500, Sysmex, Kobe, Japan), as previously described (Hazama & Okada, 1988). The mean volume of the population was calculated by a computer from the cell volume distribution based on those of latex beads with known volume. Hypotonic, isotonic or hypertonic solution consisted of (mM) 95 NaCl, 4.5 KCl, 1 $MgCl_2$, 1 $CaCl_2$, 0, 110 or 400 mannitol, and 5 HEPES/NaOH (pH 7.3; 200, 300 or 600 mosmol $kg \cdot H_2O^{-1}$). Hypertonic solution also contained 10 mM $NaHCO_3$.

Cytochrome c release assay.

Loss of cytochrome c from mitochondria was observed by immunostaining under a confocal, laser scanning fluorescence microscope (BioRad MRC-1024, Hercules, CA), as previously reported (Deshmukh & Johnson, 1998), using an anti-cytochrome c monoclonal antibody (6H2.B4: Pharmingen, San Diego, CA). Propidium iodide was used as a counterstain. Cytochrome c release to cytosol was monitored by Western blot analysis using an anti-cytochrome c monoclonal antibody (7H8.2C12: Pharmingen, San Diego, CA) for cytosolic fractions, as previously described (Liu et al. 1996).

Caspase activity measurements.

Caspase-3 activity was measured using a fluorometric assay (Thornberry, 1994). To exclude an involvement of other related proteases, the difference between fluorescence in the absence and presence of the specific inhibitor of caspase-3 was observed. The fluorogenic substrate, which was labeled with the fluorochrome 7-amino 4-methyl coumarin (AMC), for caspase-3 (Ac-DEVD-AMC) and the tetrapeptide inhibitor of caspase-3 (Ac-DEVD-CHO) were provided in the CaspASE^{TM} Assay System (Promega, Madison, WI). The substrate (Ac-IETD-AMC) and inhibitor (Ac-IETD-CHO)

of caspase-8 were from BIOMOL Reseach Laboratories, Inc. CA, and substrate (Ac-LEHD-AMC) and inhibitor (Ac-LEHD-CHO) of caspase-9 were from Quality Controlld Biochemicals, Inc. Hopkinton.

DNA fragmentation assay.

Internucleosomal DNA fragmentation was detected by DNA ladder, as previously described (Shiokawa et al. 1994). Briefly, cells were digested in lysis buffer (10 mM EDTA, 0.5% Na-N-lauroylsarcosinate, 500 Πg ml ^{1} RNAse, and 50 mM Tris-HCl, pH 7.8) at 37ΘC for 1 h and treated with 500 Πg ml ^{1} proteinase K at 37ΘC for 1 h. The chromosomal DNA was analyzed by agarose gel electrophoresis (2%), followed by staining with ethidium bromide.

Transmission electron microscopy.

Electron microscopical observations were made by a JEM 100CX (Tokyo, Japan). Cell cultures were prefixed by modified Karnovsky fixative (Karnovsky, 1965) using 0.1 M Na-phosphate buffer without adding $CaCl_2$. After postosmification with 1% OsO_4 in water, cells were dehydrated in a graded ethanol series, and embedded in Epon.

Cell viability assay.

Viability of cells cultured in the 96-well culture plates was assessed by mitochondrial dehydrogenase activity using the colorimetric MTT assay, based on the fact that viable cells (but not dead cells) can reduce 3-(4,5-dimethylthiazol-2-yl)-2,5-diphenyl tetrazolium bromide (MTT) (Mossman, 1983), using the Cell Counting Kit (Dojindo, Kumamoto, Japan) according to the manufacturer's instructions. Cell viability was also assessed by trypan blue exclusion after 5-min incubation with 0.4% trypan blue.

Radioisotope efflux measurements.

HeLa cells in the log-growing phase were loaded with 5 μ Ci ^{42}K for 2 h in MEM medium at 37℃ in the presence of 5% CO_2. Before the experiments the cultures were washed three times with phosphate-buffered saline (PBS). Isotope efflux was determined by replacing with the MEM medium (control) or that containing STS or anti-Fas monoclonal antibody at 10-min intervals. Radioactivity in the media was determined by γ -radiation counting.

Intracellular Cl^- concentration measurements using a Cl^--sensitive fluorescent dye (MAQE).

HeLa cells in the log-growing phase were loaded with 5 mM Cl^--sensitive dye, N-ethoxycarbonylmethyl-6-methoxyquinolinium bromide (MAQE; Dojindo, Kumamoto, Japan) for 90 min in MEM medium at room tempreture. The MAQE fluorescence was monitored at excitation wavelength of 360 nm with an emission wavelength of 510 nm every 5 min and digitized by an image processor (Argus-50; Hamamatsu Photonics, Hamamatsu, Japan) through a SIT camera.

Patch-clamp experiments.

Whole-cell recordings were performed, as reported previously (Kubo and Okada, 1992; Liu et al. 1998), The patch electrodes were fabricated from borosilicate glass capillaries (outer diameter=1.4 mm, inner diameter=1.0 mm, Asahi Techniglass Co., Tokyo, Japan) using a micropipette puller (P-2000, Sutter Instrument, Novato, USA). The wide-tipped electrodes had a resistance of around 2 MΩ, when filled with pipette solution. Series resistance (<5 MΩ) was compensated (to 70－80%) to minimize voltage errors. Currents were recorded using an Axopatch 200A amplifier (Axon Instruments, Foster City, CA). Current signals were filtered at 1 kHz using a four-pole Bessel filter and digitized at 4 kHz. The pClamp software (version 6.0.2; Axon Instruments) was

used for command pulse control, data acquisition and analysis. The time couse of current activation and recovery was monitored by repetitively applying (every 15 s) alternating step pulses (2 s duration) from a holding potential of –25 mV to +30 and –80 mV. To observe voltage dependence of the current profile especially inactivation kinetics at large positive potentials, stepping pulses (2 s duration) were applied from –80 to +30 mV in 11 mV increments after attaining steady activation of STS-induced current. The amplitude of instantaneous current was measured at 1.25 ms after the step pulse onset.

The control isotonic external solution contained (in mM): 20 NaCl, 9 NaHEPES, 6 HEPES, 5 KCl, 1 MgCl, 0.5 CaCl and 222 mannitol (pH 7.5, 305 mosmol kg $\cdot$ H_2O^{-1}). The osmolality of solution was measured using a freezing-point depression osmometer (OM802, Vogel, Germany). The pipette (intracellular) solution contained (in mM): 90 KCl, 30 K-Aspartate, 1.5 $MgCl_2$, 1.5 Na_2ATP, 5 HEPES, 5 Tris, 1 ethylene glycol bis(β -aminoethylether) -N,N,N', N',-tetraacetic acid (EGTA), and 32 mannitol (pH 7.3, 300 mosmol kg $\cdot$ H_2O^{-1}). The osmolality of the pipette solution was set lower (by 5 mosmol kg $\cdot$ H_2O^{-1}) than that of the control isotonic bathing solution in order to prevent spontaneous cell swelling after attaining the whole-cell mode (due to poorly diffusible cytosolic constituents: Worrell et al. 1989).

Chemicals.

Bumetanide, 4,4'-diisothiocyanatostilbene-2,2'-Disulfonicacid (DIDS) (Sigma,), glibenclamide (Sigma), phloretin (Sigma), niflumic acid (Sigma) and 4-acetamido-4'-isothiocyanatostilbene-2, 2'-disulfonic acid (SITS) (Sigma), furosemide (Nacalai Tesque, Kyoto, Japan), 5-nitro-2-(3-phenylpropylamino) benzoic acid (NPPB) (Nacalai Tesque), 4-aminopyridine (Nacalai Tesque) and quinine hydrochloride (Nacalai Tesque) were added to extracellular solution after solubilizing with a minimal amount of dimethylsulfoxide (DMSO). Balium chloride (WAKO, Kyoto, Japan) were after solubilizing with a minimal

amount of H_2O. Broad-spectrum caspase inhibitors, carbobenzoxy-L-aspart-1-yl-[(2,6-dichlorobenzoyl)oxy]methane (zD-dcb) (Peptide Institute, Inc., Osaka, Japan) and carbobenzoxy-Val-Ala-Asp (O-me)-fluoromethyl ketone (zVAD-fmk) (Enzyme Systems Products, Livermore, CA) were gifts from Dr. Yasuki Ishizaki (Kobe Univ.).

Statistical analysis

Data are given as means±S.E.M of observations (n). Statistical differences of the data were evaluated by Student's paired or unpaired t-test and considered significant at $P < 0.05$.

Results

Ⅰ. AVD is induced by operation of volume regulatoly K^+ and Cl channels.

AVD induction and its sensitivity to channel blockers.

Treatment with STS, TNFα/CHX and anti-Fas monoclonal antibody resulted in significant reduction of mean cell volume within 1 h in lymphoid U937 (Figure 2A), epithelial HeLa (Figure 2B), neuronal PC12 (Figure 2C) and NG108-15 (Figure 2D) cells. Within 3 h after apoptogenic stimulation, cell volume distribution exhibited no additional population with smaller cell size due to apoptotic body formation, and electron microscopic studies indicated that no cell fragmentation started (data not shown).

This early-phase cell shrinkage associated with apoptosis, termed AVD, was completely inhibited by a Cl channel blocker, DIDS or NPPB (0.5 mM: Figure 2). Other Cl channel blockers, SITS, niflumic acid and glibenclamide, were also effective (0.5 mM: data not shown, n=6－10 each). Since these chemicals are commonly known to block volume-sensitive Cl channels (Okada, 1997), which are activated by cell swelling in a large variety of cell types, I tested another drug, phloretin, which has been recently shown to block at low concentrations (below 100 ΓM), volume-sensitive Cl channels but not cAMP- or Ca^{2+}-activated Cl channels in epithelial cells (Fan et al. 1999). Phloretin (30 ΓM) could also prevent the AVD induced by STS, TNFα/CHX and anti-Fas monoclonal antibody (Figure 2) in U937, HeLa, PC12 and NG108-15 cells. A known blocker of volume-regulatory K^+ channels (Okada & Hazama, 1989), Ba^{2+} (5 mM: Figure 2) or quinine (0.5 mM: Figure 2), also abolished the AVD in U937, HeLa, PC12 and NG108-15 cells (Figure 2) treated with STS, TNFα/CHX or anti-Fas monoclonal antibody. These results indicate that AVD is induced either by a mitochondrial-mediated apoptotic stimulant or by a death receptor- mediated stimulant, and also suggest that AVD is accomplished by

KCl efflux via K^+ and Cl channels.

Channel-mediated KCl efflux in response to an apoptosis inducer.

Whole-cell patch-clamp studies showed that HeLa cells responded to STS application with increases in both K^+ and Cl currents (Figure 3). Fluorescence measurements using the Cl -sensitive dye, N-ethoxycarbonylmethyl-6-methoxyquinolinium bromide (MQAE) indicated that STS decreased $[Cl]_i$ in HeLa cells (Figure 4). Furthermore, treatment with STS immediately induced an increase in the ^{42}K efflux rate from HeLa cells, compared to that in control cells (Figure 5).

These data clearly demonstrate that HeLa cells immediately respond with increased KCl efflux through K^+ and Cl channels to an apoptotic inducer, STS.

RVD facilitation and its block by pretreatment with channel blockers.

To examine a possible involvement of the same ion mechanism in both RVD and AVD, I next measured the RVD. U937 and HeLa cells could respond with osmotic swelling to a hypotonic challenge (65% osmolality) and thereafter exhibited RVD (Figure 6). PC12 and NG108-15 cells also responded with swelling to a hypotonic challenge, but there after little showed RVD. The RVD is known to be attained by activation of both K^+ and Cl conductances in most mammalian cell types (Okada & Hazama, 1989; Okada, 1997). Actually, the RVD was abolished in these cells, when a blocker of volume-sensitive Cl channels (0.5 mM DIDS, 0.5 mM NPPB or 30 ΓM phloretin) or K^+ channels (5 mM Ba^{2+} or 0.5 mM quinine) was added during cell volume measurements.

U937, HeLa, PC12 and NG108-15 cells undergoing apoptosis also responded with swelling and RVD to hypotonic stress, but the RVD time course in these apoptotic cells was found to be hastened (Figure 6), compared to that in control cells. Control PC12 cells showed little RVD within 10 min (Figure 6C). After induction of apoptosis, however, PC12 cells exhibited distinct RVD (Figure 6C).

Similar observations were also obtained in NG108-15 cells (Figure 6D). Such facilitation of the RVD response was never observed in these cells, when either DIDS, NPPB or phloretin had been simultaneously applied during application of an apoptotic inducer and then removed immediately before cell volume measurements (Figure 6). Similar effects were also observed by pretreatment with another volume-sensitive Cl channel blocker, SITS, glibenclamide or niflumic acid (0.5 mM) (deta not shown; n=5) and with a K^+ channel blocker, quinine (0.5 mM: Figure 6) or Ba^{2+} (5 mM: Figure 6).

Taken together, it is concluded that stimulation with an apoptotic inducer may somehow, even under normotonic conditions, lead to activation of volume-regulatory Cl and K^+ channels that can usually partake in the RVD process under hypotonic conditions.

Ⅱ. AVD is an early prerequisite to apoptotic cell death.

Cytochrome c release and its block by channel blockers.

Both immunocytochemistry and Western blot demonstrated that either 4- to 8-h application of STS or TNF α /CHX induces release of cytochrome c from mitochondria in HeLa (Figure 7A) and to cytosol in HeLa, U937 and PC12 cells (Figure 7B). Apoptotic cytochrome c release was prevented by a Cl channel blocker, DIDS, NPPB or phloretin. There may exist a possibility that Cl channel blockers inhibited mitochondrial VDAC/porin anion channels, which are likely to mediate cytochrome c release (Green et al. 1998; Tsujimoto et al. 2000). However, a K^+ channel blocker, quinine (0.5mM: Figure 6B) or Ba^{2+} (5 mM: Figure 6B), was also effective in suppressing STS- or TNF α /CHX- induced cytochrome c release.

Caspase activation, DNA laddering and their prevention by channel blockers.

Activation of caspase-9, -8 and -3 as well as laddering of DNA were evoked by application of STS or TNFα/CHX or anti-Fas monoclonal antibody in all the cell types employed, as shown in Figures 8, 9, 10 and 11, respectively. These two biochemical signs indicative of apoptosis, however, were abolished by simultaneous application of a Cl channel blocker, DIDS, NPPB or phloretin (Figures 8, 9, 10 and 11), or of SITS, glibenclamide or niflumic acid (data not shown, n=4 each), with either apoptotic inducer, STS or TNFα/CHX. A K^+ channel blockers, Ba^{2+} or quinine (Figures 8, 9, 10 and 11) also prevented STS-, TNFα/CHX- or anti-Fas monoclonal antibody-induced activation of caspase-9, -8, -3 and laddering of DNA in U937 cells (Figures 7, 8, 9 and 10), as well as other cell types (data not shown, n=6 each). Thus, it appears that AVD or AVD-inducing KCl efflux is a necessary step for caspase activation and DNA laddering in apoptotic cells. This is in agreement with a recent report that internucleosomal DNA fragmentation was inhibited by reducing Cl efflux in leukemia cells exposed to apoptotic stimulants (Rosola et al. 1999).

Apoptotic morphology and its prevention by channel blockers.

As demonstrated in Figure 12 (A, B), treatment of U937 and HeLa cells with STS induced ultrastructural alterations characteristic of apoptosis (Wyllie et al. 1980), such as chromatin condensation at the periphery of the nucleus, leaky nuclear envelopes and intracellular vacuolation within 4 h, as gauged by transmission electron microscopy. These morphological signs of apoptosis were largely abolished by simultaneous treatment with a Cl channel blocker, DIDS, NPPB (Figure 12C). Also, a K^+ channel blocker (5 mM Ba^{2+} or 0.5 mM quinine) was found to be effective in blocking the morphological changes induced by TNF α /CHX in PC12 cells (data not shown). These results suggest that ultrastructual alterations in apoptotic cells are downstream to AVD.

Apoptotic cell death and its prevention by channel blockers.

Treatment with STS resulted in marked reduction of cell survival assessed by the MTT assay in HeLa, U937, PC12 and NG108-15 cells (Figure 13). Application of TNFα/CHX or anti-Fas monoclonal antibody also induced cell death in U937, HeLa and PC12 and NG108-15 cells (Figure 13). Simultaneous application of a known Cl channel blocker, DIDS, NPPB or phloretin, was found to prevent cell death in U937, HeLa, PC12 and NG108-15 cells (Figure 13). Other Cl channel blockers, SITS, niflumic acid and glibenclamide, were also effective (0.5 mM: data not show, n=10 each). Apoptotic cell death was blocked by a K^+ channel blocker, Ba^{2+} (5 mM) or quinine (0.5 mM). Essentially the same results were obtained, when cell survival was assessed by trypan blue exclusion in U937, HeLa, PC12 and NG108-15 cells (deta not shown, n=12 each). In contrast, neither anthracene-9-carboxylate (1 mM), which is a known blocker of cAMP-activated (CFTR) Cl channels, nor furosemide (0.5 mM), which blocks not only Na^+-K^+-2Cl or Na^+-Cl symporters but also epithelial Ca^{2+}-activated Cl channels (Evans et al. 1986), prevented STS-induced death of HeLa and U937 cells (data not shown, n=10 each for MTT assay and n=4 each for trypan blue assay). These data suggest that AVD or AVD-inducing KCl efflux is an prerequisite to apoptotic cell death.

AVD induction prior to known biochemical apoptotic events.

The time courses of AVD, biochemical apoptotic events and cell death induced by STS were compared in U937, HeLa, PC12 and NG108-15 cells. As shown in Figure 2a (filled circles), cell shrinkage started as early as 30 min after application of STS. In contrast, activation of caspase-9, -8 and -3 (Figure 8a, 9a and 10a) and cell death (Figure 13a) were not observed within 1 h after STS treatment, respectively. Cytochrome c release was not observed within 2 h after stimulation with STS in all cell types tested (data not shown, n=4 each). When stimulated with TNF α /CHX, cell shrinkage was found to start within 30

min (Figure 2b, filled circles), whereas cytochrome c release (data not shown), caspase activation (Figure 8b, 9b and 10b), DNA laddering (Figure 11b) and cell death (Figure 12b) were never observed within 30 min in U937 (A), HeLa (B), PC12 (C) and NG108-15 (D) cells. Essentially similar results were obtained with another death receptor stimulant, anti-Fas monoclonal antibody (Figure 2C, 8C, 9C, 10C and 12C). Taken together, it appears that the AVD is an event upstream to cytochrome c release, caspase activation, DNA laddering and cell death.

Ⅲ. AVD is independent of mitochondrial events and caspase activation.

Apoptotic mitochondrial events are not involved in the AVD induction.

Since the mitochondrial anion channel, VDAC, is known to be involved in apoptotic cytochrome c release (Liu et al. 1996, Yang et al. 1997, Kluck et al. 1997), these arises a possibility that Cl channel blocker-induced rescue from apoptotic cell death is due to its action to VDAC. To test this possibility, I made experiments using additional two cell lines: SKW6.4 and WEHI/Bcl-2.

SKW6.4 cells are classified into the type I cell, which does not depend on Bcl-2-inhibitable mitochondrial apoptotic events (Eguchi et al. 1999). Stimulation with anti-Fas monoclonal antibody induced not only activation of caspase-3 and induction of cell death but also AVD induction and RVD facilitation in this cell line (Figure 14). These results indicate that Fas-mediated AVD induction is totally independent of mitochondria. Furthermore, Cl channel blockers prevented Fas-induced AVD induction, RVD facilitation, caspase-3 activation and cell death (Figure 14). Therefore, it is clear that inhibition of VDAC is not responsible for the rescue of Fas-induced cell death by Cl channel blockers.

This conclusion was also supported by the following experiment with WEHI231 cells transfected with a VDAC closer protein, Bcl-2 (WEHI/Bcl-2),

in which apoptotic cell death induced by H_2O_2 or heat stress (45°C) is known to be rescued (T. Tsubata, unpublished data: private communication). Either stimulation with H_2O_2 or heat stress was actually ineffective in activating caspase-3 but still effective in inducing AVD in WEHI/Bcl-2 cells (Figure 15). Taken together, it is concluded that AVD induction is independent of mitochondria and that rescue of apoptosis by Cl^- channel blockers is not due to its inhibitory action to mitochondrial anion channels (VDAC).

Activation of caspases are not responsible for the AVD induction.

Administration of a broad-spectrum caspase inhibitor, benzyloxycarbonyl-Val-Ala-Asp-fluoromethyl ketone (zVAD-fmk) or boc-aspartyl(OMe)-fluoromethylketone (zD-dcb) blocked STS-induced caspase-3 activation (Figure 16a) and cell death (data not shown) in U937(A), PC12 cells (C). However, both AVD induction and RVD facilitation induced by STS were not prevented by the caspase inhibitor (Figure 16a). Essentially similar results were observed in U937 cells after stimulation with TNF α /CHX (Figure 16 Ab) or anti-Fas antibody (Figure 16 Ac), in HeLa cells stimulated with STS (Figure 16Ba) or TNF α /CHX (Figure 16Bb) and in PC12 cells stimulated with STS (Figure 16C). These results are in good agreement with following previous observations: A caspase blocker benzyloxycarbonyl-Val-Ala-Asp-fluoromethyl ketone (zVAD-fmk) or boc-aspartyl (OMe)-fluoromethylketone (zD-dcb), failed to block AVD in sympathetic neurons stimulated by removal of nerve growth factor (Deshmukh et al. 1997) and in lymphoma cells treated with a Ca^{2+} ionophore or thapsigargin (Bortner & Cidlowski, 1999). Therefore, it is concluded that AVD induction is an upstream events of and not dependent on caspase activation.

IV. Dysfunction of RVI is associated with apoptosis.

Apoptotic cells failed to exhibit the RVI.

Since apoptotic processes are associated with persistent cell shrinkage, it is likely that the RVI mechanism is overridden by AVD or somehow impaired in cells undergoing apoptosis. Figure 17 shows that control HeLa cells can respond with slow RVI after osmotic shrinkage to a hypertonic challenge (open symbols), but apoptotic HeLa cells little exhibited RVI (filled symbols). These results indicate that not only AVD induction but also RVI dysfunction are involved in progressive cell shrinkage in apoptotic cells.

Osmotic cell shrinkage triggers apoptosis in RVI-lacking cells.

Apoptotic cell death has been reported to be induced by hypertonic stress in many cell types (Bortner & Cidlowski, 1996; Matthews & Feldman, 1996; Orlov et al. 1996; Singleton et al. 1996; Qin et al. 1997; Edwards et al. 1998; Bilney & Murray, 1998; Rosola et al. 1999). Borter & Cidlowski (1996) pointed out that hypertonic stress is able to trigger apoptosis only into cells that lack the RVI mechanism. I first tested this concept using U937 and HeLa cells that cannot and can respond, respectively, with the RVI to hypertonic stimulation (Figure 18a). Actually, hypertonic stress (600 mosM added with 300 mM mannitol or 150 mM NaCl) triggered activation of caspase-3 in RVI-lacking U937 cells but not in RVI-possessing HeLa cells (Figure 18b).

To further test the hypothesis raised by Bortner and Cidlowski (1996), I made experiments using NHE1-deficient PS120 cells and PS120 cells overexpressing NHE1, because PS120 cells lack RVI but restore it after NHE1 transfection (S. Wakabayashi, unpublished data: private communication). As shown in Figure 19a, hypertonic stimulation consistently induced caspase-3 activation in PS120 cells. In contrast, when the RVI ability was conferred by overexpression with the Na^+/H^+ antiporter, hypertonic stress failed to induce caspase-3 activation

(Figure 19b) and apoptotic cell death (data not shown).

Taken together, it is concluded that RVI dysfunction plays a causative role in induction of apoptosis. Also, it is suggested that persistent cell shrinkage itself leads to apoptotic cell death.

Discussion

Cell volume regulation is an important cell function supporting cell survival. Apoptosis occurs in response to various stimuli under physiological and pathological circumstances. A major hallmark of apoptosis is shrinkage of cells. Cell shrinkage undergoes in two distinct stages: before and after cell fragmentation (Benson et al. 1996). It was supposed that this normotonic shrinkage of cells was due to a number of cytoskeletal protein, including fodolin and F-actin, cleavage by effector caspase during apoptosis (Tan & Wang, 1998). Consistently, a broad-spectrum caspase inhibitor zVAD-fmk, was found to block apoptotic cell shrinkage in ML-1 cells exposure to etoposide (Wolf et al. 1997), thymocytes after exposure to glucocorticoids (Hughes & Chidrowski, 1998), Jurkat T cells exposure to anti-Fas antibody (Bortner & Cidlowski, 1999) and lymphoma cells exposure to TGF β (Schrantz et al. 1999). However these studies, no quantitive or statistical evaluation was made for cell size changes. Here, I measured the size of STS-, TNF α /CHX- or anti-Fas monoclonal antibody-treated U937, HeLa cells and STS- treated PC12 cells with or without zVAD-fmk and zD-dcb. A broad-spectrum inhibitor of caspase, zVAD-fmk or zD-dcb, failed to prevent the early-phase of cell volume decrease during apoptosis, although they completely prevented caspase activation and DNA laddering (see Figure 16). This early-phase shrinkage was here termed an apoptotic volume decrease (AVD).

All the apoptotic events (AVD, cytochrome c release from mitochondria) caspase activation, DNA laddering, morphological change, cell viability loss) were found to be prevented by NPPB, DIDS, SITS, niflumic acid, glibencamide and phloretin, which are known as blockers of volume-regulatory Cl channels (Okada, 1997; Fan et al. 1999). Similarly, previous studies showed that, at a much higher concentration (2 mM), DIDS exhibited an inhibitory effect on an STS-induced DNA fragmentation monitored by terminal dUTP nick-end

labeling (TUNEL) in rat cerebellar granule neurons (Himi et al. 1995), and also that a low concentration of glibenclamide (0.1 mM), DIDS (0.1 mM), IAA (0.1 mM) or DPC (1 mM), though only in part, reduced DNA fragmentation and annexin binding in Fas antigen-treated Jurkat lymphoid cells (Szabo et al. 1998). These drugs are known to be effective blockers of volume-sensitive Cl channels (Okada, 1997). In contrast, blockers of cAMP-activated (CFTR) Cl channels and that of epithelial Ca^{2+}-activated Cl channels were found to be ineffective (Maeno & Okada, unpublished data). These results suggest that volume-regulatory Cl channels are involved in the AVD.

In fact, the cells exhibiting the AVD responded to a hypotonic challenge with a faster RVD, which is known to involve volume-regulatory Cl channels. In addition, Szabo and collaborators (1998) have recently shown that stimulation of Fas receptors induced activation of outwardly rectifying Cl channels in lymphoid Jurkat cells. In the present study, the whole-cell patch clamp study showed that STS increased Cl currents compared with control, and the study using a Cl -sensitive fluorescent dye (MQAE) showed that a significant decrease in the intracellular Cl concentration, was observed within 1 h after treatment with STS in HeLa cells. Taken together, it is concluded that apoptotic cell death can be rescued by preventing the early-phase apoptotic cell shrinkage (AVD) by blocking the volume-regulatory Cl channel in lymphoid, epithelial and neuronal cells.

Ba^{2+} and quinine, which are known blockers of volume-regulatory K^+ channels (Okada & Hazama, 1989), also prevented all the apoptotic events examined in this study. This is in good agreement with previous observations that another K^+ channel blocker, TEA or 4-aminopyridine, blocked apoptotic cell death in other cell types (Yu et al. 1997; Wang et al. 1999; Colom et al. 1998). Thus, it is possible that some K^+ channel is activated in apoptotic cells. In fact, upregulation of voltage-dependent K^+ channels was observed in neuronal and myelobastic cells undergoing apoptosis (Yu et al. 1997; Wang et

al. 1999, Colom et al. 1998). In the present study, the whole-cell patch clamp study showed that STS increase K^+ currents compared with control, and the $^{42}K^+$ efflux study showed that an increase in $^{42}K^+$ efflux was observed within 1 h after treatment with STS in HeLa cells. Thus, it appears that the K^+ channel activity is implicated in the AVD in concert with the Cl channel activity.

Although its mechanism remains to be elucidated, it is noted that physical shrinkage itself was reported to induce apoptosis in lymphoid cells (Bortner et al. 1996) and activation of mitogen-activated protein kinases (MAPK) (Roger et al. 1999), which are possibly involved in the apoptosis signaling (Ichijo et al. 1997, Ashkenazi et al. 1998, Gotoh et al. 1998). Also, a decrease in the intracellular K^+ concentration, which is coincident with apoptotic cell shrinkage (Tsujimoto et al. 2000), was shown to be necessary for apoptotic cell death (Hughes et al. 1997). In fact, the cells exhibiting the AVD failed to respond to a hypertonic challenge with RVI, which is known to involve Na^+/H^+ exchanger isoform 1 (NHE1).

Inhibition of the volume regulatory Na^+/H^+ exchange by subsequent alkalization most likely plays a permissive role in receptor triggered apoptosis. Beyond that nuclear acidification may promote DNA fragmentation as DNase II has its pH optimum in the acidic range. Fas-induced apoptosis is observed to be accelerated by inhibition of Na^+/H^+ exchange (Lang et al. 2000). In the present study, NHE1 expression prevented hypertonicity-induced apoptosis by conferring the RVI ability on in PS120 cells. Thus, it is likely that in NHE1-lacking cells hypertonic stimulation induces cell shrinkage without following volume recovery (RVI), and then sustained cell shrinkage many switch on the AVD-inducing machinery, thereby inducing further shrinkage, leading to succeeding apoptotic events and cell death.

Although early, AVD may not be the first event in apoptotic cascade. Some biochemical events including reductions in protein synthesis, glucose uptake, mitochondrial transmembrane potential, and activity of certain kinases

(mitogen-activated proyein and phosphoinositide 3-kinase kinase), as well as increased *c-jun* expression, are known to typically precede AVD (Deckwerth & Johnson, 1993: Deshmukn & Johnson, 1997; Zamzami et al. 1995). Osmotic cell shrinkage stimulates the expression of certain heat shock proteins, which may in turn protect the cell from apoptosis (Beck et al. 2000). CD95-induced apoptosis is inhibited by activation of PKC (Gomez-Angelats et al. 2000), which in several cells is activated by osmotic cell shrinkage. In medullary tubular epithelial cells osmotic shrinkage activates p53 and antisense against p53 enhances apoptosis of those cells in hypertonic enviroment (Dmitrieva et al. 2000). On the other hand, p53 may be inhibitory or stimulatory on apoptosis depending on the cell type and challenge (Pohl et al. 1999, Wagenknecht et al. 1999)

Despite accumulated knowledge, the respective apoptotic reaction component appears to be crucial for a given cell and given experimental condition. Clearly, much more has to be learned about specific pathways linking these fundamental cellular functions involving volume regulatory ion channels.

In summary, from this study, I have drawn following four conclusions: 1) The early-phase apoptotic cell shrinkage, termed the apoptotic volume decrease (AVD) is induced by operation of volume regulatory K^+ and Cl^- channels, 2) the AVD is early prerequisite to apoptotic cell death, 3) the AVD is independent of mitochondrial events and caspase activation during apoptotic processes, and 4) dysfunction of the volume regulation after cell shrinkage (regulatory volume increase: RVI) is associated with the process leading to apoptotic cell death.

References

Ashkenazi, A. & Dixit, V. M. (1998) Death receptors: Signaling and modulation. *Science* 281, 1305-1308.

Barbiero, G., Duranti, F., Bonelli, G., Amenta, J. S. & Baccino, F. M. (1995) Intracellular ionic variations in the apoptotic death of L cells by inhibitors of cell cycle progression. *Experimental Cell Research* 217, 410-418.

Beck, F. X., Neuhofer, W. & Muller E. (2000) Molecular chaperones in the kidney: bistribution, putative roles, and regulation. *American Journal of Physiology* 279, F203-F215.

Benson, R. S. P., Heer, S., Dive, C. & Watson, A. J. M. (1996) Characterization of cell volume loss in CEM-C7A cells during dexamethasone-induced apoptosis. *American Journal of Physiology* 270, C1190-C1203.

Bilney, A. J. & Murray A. W. (1998) Pro- and anti-apoptotic effects of K^+ in HeLa cells. *FEBS Letters 424*, 221-224.

Bortner, C. D. & Cidlowski, J. A. (1996) Absence of volume regulatory mechanisms contributes to the rapid activation of apoptosis in thymocytes. *American Journal of Physiology* 271, C950-C961.

Bortner, C. D., Hughes, F. M., Jr. & Cidlowski, J. A. (1997) A primary role for K^+ and Na^+ efflux in the activation of apoptosis. *Journal of Biological Chemistry* 272, 32436-32442.

Bortner, C. D. & Cidlowski, J. A. (1999) Caspase independent/dependent regulation of K^+, cell Shrinkage, and mitochondrial membrane potential during

lymphocyte apoptosis. *Journal of Biological Chemistry* 274, 21953-21962.

Cain, K., Bratton, S. B., Langlais, C., Walker, G., Brown, D. G., Sun, X. M. & Cohen, G. M. (2000) Apaf-1 oligomerizes into biologically active approximately 700-kDa and inactive approximately 1.4-Mda apoptosome complexes. *Journal of Biological Chemistry* 275, 6067-6070.

Colom, L. V., Diaz, M. E., Beers, D. R., Neely, A., Xie, W.-J. & Appel, S. H. (1998) Role of potassium channels in amyloid-induced cell death. *Journal of Neurochemistry* 70, 1925-1934.

Deckwerth, T. L. & Johnson, E. M., Jr. (1993) Temporal analysis of events associated with programmed cell death (apoptosis) of sympathetic neurons deprived of nerve growth factor. *Journal of Cell Biology* 123, 1207-1222.

Deshmukn, M. & Johnson, E. M., Jr. (1997) Programmed cell death in neurons: focus on the pathway of nerve growth factor deprivation-induced death of sympathetic neurons. *Molecular Pharmacology* 51, 897-906.

Deshmukh, M. & Johnson, E. M. Jr. (1998) Evidence of a novel event during neuronal death: development of competence-to-die in response to cytoplasmic cytochrome c. *Neuron* 21, 695-705.

Dmitrieva, N., Kultz, D., Michea L., Ferraris, J., Burg M. (2000) Protection of renal inner medullary epithelial cells from apoptosis by hypertonic stress-induced p53 activation. *Journal of Biological Chemistry* 275, 18243-18247.

Edwards, Y. S., Sutherland, L. M., Power, J. H., Nicholas, T. E., Murray & A.

W. (1998) Osmotic stress induces both secretion and apoptosis in rat alveolar type II cells. *American Journal of Physiology* 275, L670-678

Eguchi, Y., Srinivasan, A., Tomaselli, K. J., Shimizu, S. & Tsujimoto, Y. (1999) ATP-dependent steps in apoptotic signal transduction. *Cancer Research* 59, 2174-81.

Evans, M. G., Marty, A., Tan, Y. P. & Trautmann, A. (1986) Blockage of Ca-activated Cl conductance by furosemide in rat lacrimal glands. *Pflugers Arch* 406, 65-68.

Fan, H. T., Kida, H., Morishima, S., Oiki, S. & Okada, Y. (1999) Phloretin inhibits a regulatory volume decrease in human epithelial cells. *Japanese Journal of Physiology* 49 (Suppl.) S109.

Gomez-Angelats, M., Bortner, C. D. & Cidlowski, J. A. (2000) Protein kinase C (PKC) inhibits fasreceptor-induced apoptosis through modulation of the loss of K and cell shrinkage. A role for PKC upstream of caspase. *Journal of Biological Chemistry* 275, 19609-19619

Gotoh, Y. & Cooper, J. A. (1998) Reactive Oxygen Species- and Dimerization-induced activation of s-regulating kinase 1 in tumor necrosis factor- signal transduction. *Journal of Biological Chemistry* 273, 17477-17482.

Green, D. R. & Reed, J.C. (1998) Mitochondria and Apoptosis. *Science* 281, 1309-1312.

Hazama, A. & Okada, Y. (1988) Ca^{2+} sensitivity of volume-regulatory K^+ and Cl^- channels in cultured human epithelial cells. *Journal of Physiology* 402,

687-702.

Himi, T., Ishizaki, Y. & Murota, S. (1995) A caspase inhibitor blocks ischaemia-induced delayed neuronal death in the gerbil. *Annual Meeting of Society Neuroscience* 21, 812.

Hoffmann, E. K. & Simonsen, L. O. (1989) Membrane mechanisms in volume and pH regulation in vertebrate cells. *Physiological Reviews* 69, 315-382.

Huang, D. C., Hahne, M., Schroeter, M., Frei, K. Fontana, A., Villunger, A., Newton, K., Tschopp, J. & Strasser, A. (1999) Activation of Fas by FasL induces apoptosis by a mechanism that cannot be blocked by Bcl-2 or Bcl-x(L). *Proceedings of the National Academy of Sciences of the United States of America* 96, 14871-14878.

Hughes, F. M., Jr., Bortner, C. D., Purdy, G. D. & Cidlowski, J. A. (1997) Intracellular K^+ suppresses the activation of apoptosis in lymphocytes. *Journal of Biological Chemistry* 272, 30567-30576.

Hughes, F. M., Jr. & Cidlowski, J. A. (1998) Glucocorticoid-induced thymocyte apoptosis: protease-dependent activation of cell shrinkage and DNA degradation. *Journal of Steroid Biochemistry Molecular Biology* 65, 207-217.

Ichijo, H., Nishida, E., Irie, K., ten Dijke, P., Saitoh, M., Moriguchi, T., Takagi, M., Matusmoto, K., Miyazono, K. & Gotoh, Y. (1997) Induction of apoptosis by ASK1, a mammalian MAPKKK that activates SAPK/JNK and p38 signaling pathways. *Science* 275, 90-94.

Ishizaki, Y., Voyvodic, J. T., Burne, J. F. & Raff, M. C. (1993) Control of lens

epithelial cell survival. *Journal of Cell Biology* 121, 899-908.

Karnovsky, M. J. (1965) A formaldehyde-glutaraldethdefixative of high osmolarity for use in electron microscopy. *Journal of Cell Biology* 27, 137A.

Kerr, J. F. R., Wyllie, A. H. & Currie, A. R. (1972) Apoptosis: a basic biological phenomenon with wide-ranging implications in tissue kinetics. *British Journal of Cancer* 26, 239-257.

Kluck, R. M., Bossy-Wetzel, E., Green, D. R. & Newmeyer, D. D. (1997) The release of cytochrome c from mitochondria: a primary site for Bcl-2 regulation of apoptosis. *Science* 275, 1132-1136.

Krajewski, S., Krajewska, M., Ellerby, L. M., Welsh, K., Xie, Z., Deveraux, Q. L., Salvesen, G. S., Bredesen, D. E., Rosenthal, R. E., Fiskum, G. & Reed, J. C. (1999) *Proceedings of the National Academy of Sciences of the United States of America* 96, 5752-5757.

Kubo, M. & Okada, Y. (1992) Volume-regulatory Cl^- channel currents in cultured human epithelial cells. *Journal of Physiology* 456, 351-371.

Lang, F., Ritter, M., Gamper, N., Huber, S., Fillon, S., Tanneur, V., Lepple-Wienhues, A., Szabo, I. & Bulbins, E. (2000) Cell volume in the regulation of cell proliferation and apoptotic cell death. *Cell Physiological Biochemistry* 10, 417-428.

Lepple-Wienhues, A., Szabo, I., Laun, T, Kaba, K. N., Gulbins, E. & Lang, F. (1998) The tyrosine kinase p56lck mediates activation of swelling-induced chloride channels in lymphocytes. *Journal of Cell Biology* 141, 281-286.

Li, H. & Yuan, J. (1999) Deciphering the pathways of life and death. *Current Opinion in Cell Biology* 11, 261-266.

Li, P., Nijhawan, D., Budihardjo, I., Srinivasula, S. M., Ahmad, M., Alnemri, E.S. & Wang, X. (1997) Cytochrome c and dATP-dependent formation of Apaf-1/caspase-9 complex initiates an apoptotic protease cascade. *Cell* 91, 479-489.

Liu, X., Kim, C. N., Yang, J., Jemmerson, R. & Wang, X. (1996) Induction of apoptotic program in cell-free extracts: requirement for dATP and cytochrome c. *Cell* 86, 147-157.

Liu, X., Zou, H., Slaughter, C. & Wang, X. (1997) DFF, a heterodimeric protein that functions downstream of caspase-3 to trigger DNA fragmentation during apoptosis. *Cell* 89, 175-184.

Liu, Y., Oiki, S., Tsumura, T., Shimizu, T. & Okada, Y. (1998) Glibenclamide blocks volume-sensitive Cl^- channels by dual mechanism. *American Journal of Physiology* 275, C343-C351.

Matthews, C. C. & Feldman, E. L. (1996) Insulin-like growth factor I rescues SH-SY5Y human neuroblastoma cells from hyperosmotic induced programmed cell death. *Journal of Cell Physiology* 166, 323-31.

Mossman, T. (1983) Rapid colorimetric assay for cellular growth and survival: application to proliferation and cytotoxicity assays. *Journal of Immunological Methods* 65, 55-63.

Muzio, M., Stockwell, B. R., Stennicke, H. R., Salvesen, G. S. & Dixit, V. M.

(1998) An induced proximity model for caspase-8 activation. *Journal of Biological Chemistry* 273, 2926-2930.

Nietsch, H. H., Roe, M. W., Fiekers, J. F., Moore, A. L., Lidofsky, S. D. (2000) ctivation of potassium and chloride channels by tumor necrosis factor alpha. Role in liver cell death. *Journal of Biological Chemistry* 275, 20556-61.

Okada, Y. & Hazama, A. (1989) Volume-regulatory ion channels in epithelial cells. *News in Physiological Science* 4, 238-242.

Okada, Y. (1997) Volume expansion-sensing outward-rectifier Cl^- channel: fresh start to the molecular identity and volume sensor. *American Journal of Physiology* 273, C755-C789.

Orlov, S. N., Dam, T. V., Tremblay, J. & Hamet, P. (1996) Apoptosis in vascular smooth muscle cells: role of cell shrinkage. *Biochemical and Biophysical Research Communications* 221, 708-15.

Patterson, S. D., Spahr, C. S., Daugas, E., Susin, S. A., Irinopoulou, T., Koehler, C. & Kroemer, G. (2000) Mass spectrometric identification of proteins released from mitochondria undergoing permeability transition. *Cell Death and Differentiation* 7, 137-44.

Peter, M.E. & Krammer, P. H. (1998) Mechanisms of CD95 (APO-1/Fas)-mediated apoptosis. *Current Opinion in Immunology* 10, 545-555.

Pohl, U., Wagenknecht B., Naumann U. & Weller M. (1999) p53 enhances BAK and CD95 expression in human malignant glioma cells but does not enhance CD95L-induced apoptosis. *Cell Physiological Biochemistry* 9, 29-37.

Qin, S., Minami, Y., Kurosaki, T. & Yamamura, H. (1997) Distinctive functions of Syk and Lyn in mediating osmotic stress- and ultraviolet C irradiation-induced apoptosis in chicken B cells. *Journal of Biological Chemistry* 272, 17994-17999.

Roger, F., Martin, P.-Y., Rousselot, M., Favre, H. & Feraille, E. (1999) Cell shrinkage triggers the activation of mitogen-activated protein kinases by hypertonicity in the rat kidney medullary thick ascending limb of the Henle's loop. *Journal of Biological Chemistry* 274, 34103-34110.

Rosola, A., Farahi, Far, D., Hofman, P. & Rossi, B. (1999) Lack of internucleosomal DNA fragmentation is related to Cl^- efflux impairment in hematopoietic cell apoptosis. *FASEB Journal* 13, 1711-23.

Schrantz, N., Blanchard, D. A., Auffredou, M. T., Sharma, S., Leca, G. & Vazquez, A. (1999) Role of caspases and possible involvement of retinoblastoma protein during TGF β -mediated apoptosis of human B lymphocytes. *Oncogene* 18, 3511-3519.

Shiokawa, D., Ohyama, H., Yamada, T., Takahashi, K. & Tanuma, S. (1994) Identification of an endonuclease responsible for apoptosis in rat thymocytes. *European Journal of Biochemistry* 226, 23-30.

Singleton, J. R., Dixit, V. M. & Feldman E. L. (1996) Type I insulin-like growth factor receptor activation regulates apoptotic proteins. *Journal of Biological Chemistry* 271, 31791-31794.

Stennicke, H. R., Deveraux, Q. L., Humke, E. W., Reed, J. C., Dixit, V. M. & Salvesen, G. S. (1999) Caspase-9 can be activated without proteolytic

processing. *Journal of Biological Chemistry* 274, 8359-8362.

Szabo, I., Lepple-Wienhues, A., Kaba, K. N., Zoratti, M., Gulbins, E. & Lang, F. (1998) Tyrosine kinase-dependent activation of a chloride channel in CD95-induced apoptosis in T lymphocytes. *Proceedings of the National Academy of Sciences of the United States of America* 95, 6169-6174.

Tan, X. & Wang, J. Y. (1998) The caspase-RB connection in cell death. *Trends of Cell Biology* 8, 116-120.

Thornberry, N.A. (1994) Interleukin-1 beta converting enzyme. *Method in Enzymology* 244, 615-631.

Tsujimoto, Y. & Shimizu, S. (2000) Bcl-2 family: life-or-death switch. *FEBS Letters* 466, 6-10.

Wagenknecht, B., Hermisson, M., Eitel, K. & Weller, M. (1999) Proteasome inhibitors induce p53/p21-independent apoptosis in human glioma cells. *Cell Physiological Biochemistry* 9, 29-37

Wakabayashi, S., Pang, T., Su, X. & Shigekawa, M. (2000) A novel topology model of the human Na^+/H^+ exchanger isoform 1. *Journal of Biological Chemistry* 275, 7942-7949.

Wang, L., Xu, D., Dai, W. & Lu, L. (1999) An ultraviolet-activated K^+ channel mediates apoptosis of myeloblastic leukemia cells. *Journal of Biological Chemstry* 274, 3678-3685.

White, E., Sabbatini, P., Debbas, M., Wold, W. S., Kusher, D. I. & Gooding, L.

R. (1992) The 19-kilodalton adenovirus E1B transforming protein inhibits programmed cell death and prevents cytolysis by tumor necrosis factor alpha. *Molecular Cell Biology* 12, 2570-2580.

Wolf, C. M., Reynolds, J. E., Morana, S. J. & Eastman, A. (1997) The temporal relationship between protein phosphatase, ICE/CED-3 proteases, intracellular acidification, and DNA fragmentation in apoptosis. *Experimental Cell Research* 230, 22-27.

Worrell, R. T., Butt, A. G., Cliff, W. H. & Frizzell, R. A. (1989) A volume-sensitive chloride conductance in human colonic cell line T84. *American Journal of Physiology* 256, C1111-C1119.

Wyllie, A. H., Kerr, J. F. R. & Currie, A. R. (1980) Cell death: the significance of apoptosis. *International Review in Cytology* 68, 251-307.

Yang, J., Liu, X., Bhalla, K., Kim, C. N., Ibrado, A. M., Cai, J., Peng, T. I., Wolf, C. M., Reynolds, J. E., Morana, S. J. & Eastman, A. (1997) The temporal relationship between protein phosphatase, ICE/CED-3 proteases, intracellular acidification, and DNA fragmentation in apoptosis. *Experimental Cell Reseach* 230, 22-27.

Yu, S. P., Yeh, C.-H., Sensi, S. L., Gwag, B. J., Canzoniero, L. M. T., Farhangrazi, Z. S., Ying, H. S., Tian, M., Dugan, L. L. & Choi, D. W. (1997) Mediation of neuronal apoptosis by enhancement of outward potassium current. *Science* 278, 114-117.

Zamzami, N., Marchetti, P., Castedo, M., Decaudin, D., Macho, A., Hirsch, T., Susin, S. A., Petit, P. X., Mignotte, B. & Kroemer, G. (1995) Sequential

reduction of mitochondrial transmembrane potential and generation of reactive oxygen species in early programmed cell death. *Jounal of Experimental Medicine* 182, 367-377.

Acknowledgements

I gratefully thank Prof. Yasunobu Okada for his guidance and continuous support for my study. I would like to thank Drs.Toku Kanaseki, Yasuki Ishizaki, Akihiro Hazama for their collaboration and Drs. Ravshan Z. Sabirov, Shigeru Morishima, Yuko Ando-Akatsuka, Katsuya Dezaki and Takahiro Shimizu for helpful discussion. I am grateful to Mr. M. Ohara, Ms. K. Shigemoto and Ms. S. Tanaka-Kagawa for technical assistance as well as to all other members of our laboratory for their generous supports. I am grateful to all other members of our laboratory for their generous supports. I would like to thank Drs. Shigeo Wakabayashi and Takeshi Tubata for gift of cells and discussion.

Figure Legends

Figure 1. Two distinct signaling pathways leading to apoptosis. In the receptor-mediated pathway, oligomerization of death receptors recruits adaptor molecules involved in activation caspase-8, which undergoes proximity-induced promising. The activated caspase-8 can then proteolytically activate procaspase-3. Various cellular stress causes binding of a pro-apoptotic Bcl-2 family member (e.g. Bax) to the mitochondrial outer membrane, thereby leading to cytochrome c release. Bcl-2 opposes the effect of Bax. Apaf-1 binds cytochrome c and dATP or ATP, and recruits caspases to form a large complex (apotossome). There is cross-talk between these pathways, as caspase-8 can cleave Bid to generate the active truncated Bid (tBid), which can bind to mitochondria and direct the release of cytochrome c.

Figure 2. Time course of AVD induction. U937 (A), HeLa (B), PC12 (C) and NG108-15 (D) cells were stimulated by STS (a) or TNF/CHX (b) or Fas ligand (FasL), anti-Fas monoclonal antibody (c). AVD was prevented by simultaneous treatment with a channel blocker, 0.5 mM NPPB, 30 ΠM phloretin, 0.5 mM DIDS, 5 mM Ba^{2+} or 0.5 mM quinine. Each data represents the mean ρ SEM (vertical bar) of 16 observations. *P<0.05 versus corresponding control.

Figure 3. Effects of extracellular application of STS on whole-cell K^+ and Cl current in HeLa cells. Each data represents the mean ρ SEM (vertical bar) of 7 observations. A) A representative record before and after addition of 4 μ M STS during application of alternating pulses between the equilibrium potentials to K^+ and Cl (E_K= 80 mV, E_{Cl}=+30 mV) or step pulses from 80 to +30 mV in 11 mV increments (at asterisks). B) Mean peak current densities recorded at E_K and E_{Cl} before and after addition of STS. *P<0.05 versus corresponding control.

Figure 4. STS-induced [Cl]$_i$ decrease in HeLa cells. A) The time course of relative MQAE fluorescence before and after application (bar) of 4 μ M STS. B) Calibrated [Cl]$_i$ values at 1 h after application of STS and of the corresponding control. Each data represents the mean ρ SEM (vertical bar) of 20 observations. *P<0.05 versus corresponding control.

Figure 5. STS-induced enhancement of ^{42}K efflux from HeLa cells. Each data represents the mean ρ SEM (vertical bar) of 7 observations. *P<0.05 versus corresponding control.

Figure 6. Time course of RVD facilitation by STS (a) or TNF/CHX (b) or anti-Fas monoclonal antibody (FasL: c) in U937 (A), HeLa (B), PC12 (C) and NG108-15 (D) cells. RVD facilitation was prevented by simultaneous treatment with a channel blocker, 0.5 mM NPPB, 30 ΓM phloretin, 0.5 mM DIDS, 5 mM Ba^{2+} or 0.5 mM quinine. Cell volume measurements were performed in the absence of any drugs after washing out apoptotic inducers and channel blockers, and the data were normalized by those measured immediately before a hypotonic challenge. Each data represents the mean ρ SEM (vertical bar) of 16 observations. *P<0.05 versus corresponding control.

Figure 7. Release of cytochrome c from mitochondria induced by treatment with an apotogenic inducer, and its prevention by simultaneous treatment with a Cl or K^+ channel blocker. (A) Cytochrome c release from mitochondria monitored by immunocytochemistry in HeLa cells 1 (b), 2 (c) or 4 (d, e, f) h after treatment with STS in the absence (a, b, c, d) or presence of 0.5 mM NPPB (e) or of 5 mM Ba^{2+} (f). A green fluorescence: mitochondrial cytochrome c revealed by FITC-conjugated secondary antibody. A red fluorescence: counter staining with propidium iodide. Data represent triplicate experiments. Scale: 20 Γm. (B) Cytochrome c release to cytosol was monitored

by Western blot in HeLa, U937 and PC12 cells 8 h after treatment with STS or TNF α /CHX in the absence or presence of 0.5 mM DIDS, 0.5 mM NPPB, 30 ΓM phloretin or 0.5 mM quinine. Data represent triplicate experiments.

Figure 8. Time course of caspase-9 activation induced by STS (a) or TNF α /CHX (b) or anti-Fas monoclonal antibody (FasL: c) in U937 (A), HeLa (B), PC12 (C) and NG108-15 (D) cells. Caspase-9 activation was prevention by simultaneous treatment with 0.5 mM DIDS, 0.5 mM NPPB, 30 ΓM phloretin, 5 mM Ba^{2+} or 0.5 mM quinine. Each data represents the mean ρ SEM (vertical bar) of 6 observations. *P<0.05 versus corresponding control.

Figure 9. Time course of caspase-8 activation induced by STS (a) or TNF α /CHX (b) or anti-Fas monoclonal antibody (FasL: c) in U937 (A), HeLa (B), PC12 (C) and NG108-15 (D) cells. Caspase-8 activation was prevented by simultaneous treatment with 0.5 mM DIDS, 0.5 mM NPPB, 30 ΓM phloretin, 5 mM Ba^{2+} or 0.5 mM quinine. Each data represents the mean ρ SEM (vertical bar) of 6 observations. *P<0.05 versus corresponding control.

Figure 10. Time course of caspase-3 activation induced by STS (a) or TNF α /CHX (b) or anti-Fas monoclonal antibody (FasL: c) in U937 (A), HeLa (B), PC12 (C) and NG108-15 (D) cells. Caspase-3 activation was prevention by simultaneous treatment with 0.5 mM DIDS, 0.5 mM NPPB, 30 ΓM phloretin, 5 mM Ba^{2+} or 0.5 mM quinine. Each data represents the mean ρ SEM (vertical bar) of 6 observations. *P<0.05 versus corresponding control.

Figure 11. Time course of DNA laddering induced by the treatment with STS (A) or TNF α /CHX (B) or anti-Fas monoclonal antibody (FasL: C) in U937 cells. DNA laddering was prevented by simultaneous treatment with 0.5 mM DIDS, 0.5 mM NPPB, 30 ΓM phloretin,5 mM Ba^{2+} or 0.5 mM quinine.

Figure 12. Changes in morphological features under thin section electron microscopy 4 h after treatment with STS, and their prevention by simultaneous treatment with 0.5 mM NPPB and 0.5 mM DIDS in HeLa (B) and U937 (A) cells, respectively. (a) Control HeLa and U937 cells. (b) HeLa and U937 cells 4 h after treatment with STS. (c) These cells 4 h after treatment with STS simultaneously with 0.5 mM DIDS (A) and 0.5 mM NPPB (B). Scale: 2 Πm.

Figure 13. Time course of cell viability loss induced by the treatment with STS (a) or TNF α /CHX (b) or anti-Fas monoclonal antibody (FasL: c) in U937 (A), HeLa (B), PC12 (C) and NG108-15 (D) cells. Cell death was prevented by simultaneous treatment with 0.5 mM NPPB, 0.5 mM DIDS, 30 ΠM phloretin, 0.5 mM quinine. Cell viability was assessed by the MTT assay. Each data represents the mean ρ SEM (vertical bar) of 20 observations. Control data for STS or anti-Fas monoclonal antibody experiment were obtained without adding any drugs, and those for TNF α /CHX experiments were obtained with CHX alone. *P<0.05 versus corresponding control.

Figure 14. Time courses of AVD induction (A) and caspase-3 activation (B) and RVD facilitation (C) and cell viability loss (D) induced by anti-Fas monoclonal antibody in SKW6.4 cells. They are prevented by simultaneous treatment with a channel blocker, 0.5 mM SITS or 0.5 mM NPPB. Each data represents the mean ρ SEM (vertical bar) of 16 observations. *P<0.05 versus corresponding control.

Figure 15. Time courses of AVD induction (a) and caspase-3 activation (b) induced by heat shock at 45C^0 for 10 min or 50 μ M H_2O_2 in WEHI231 (A) and WEHI/Bcl-2 (B) cells. Each data represents the mean ρ SEM (vertical bar) of 16 observations. *P<0.05 versus corresponding control.

Figure 16. Effect of 100 μ M zD-dcb or 50 μ M zVAD-fmk on time courses of AVD induction(middle), caspase-3 activity (top) and RVD facilitation (bottom) induced by STS (a) or TNF α /CHX (b) or anti-Fas monoclonal antibody (FasL: c) in U937 (A), HeLa (B), PC12 (C) and NG108-15 (D) cells. Each data represents the mean ρ SEM (vertical bar) of 10 observations.

Figure 17. Inhibition of RVI by treatment with STS or TNF α /CHX or anti-Fas monoclonal antibody (FasL) in HeLa cells. Cell volume measurements were performed in the absence of any drugs after washing out apoptotic inducers and channel blockers, and the data were normalized by those measured immediately before a hypertonic challenge. Each data represents the mean ρ SEM (vertical bar) of 5－7 observations.

Figure 18. RVI changes (A) and caspase-3 activation (B) and cell viability decrease (C) induced by hypertonic stress in U937 and HeLa cells. Each data represents the mean ρ SEM (vertical bar) of 5 observations. *P<0.05 versus corresponding control.

Figure 19. Caspase-3 activation induced by hypertonic stress in PS120 (A) and PS120/NHE1 (B) cells. Each data represents the mean ρ SEM (vertical bar) of 16 observations. *P<0.05 versus corresponding control.

Figure 20. Schematic illustrations of ionic mechanisms for RVD and RVI under physiological conditions as well as for AVD under pathophysiological conditions. Three different machineries for RVD and RVI are depicted in upper right and left cells, respectively. The AVD-inducing machineries are given in the lower middle cell. Apoptotic cell death may be triggered by persistent cell shrinkage due to AVD induction and RVI dysfunction, as depicted in the lower left cell.

Two Distinct Apoptotic Signaling Pathways

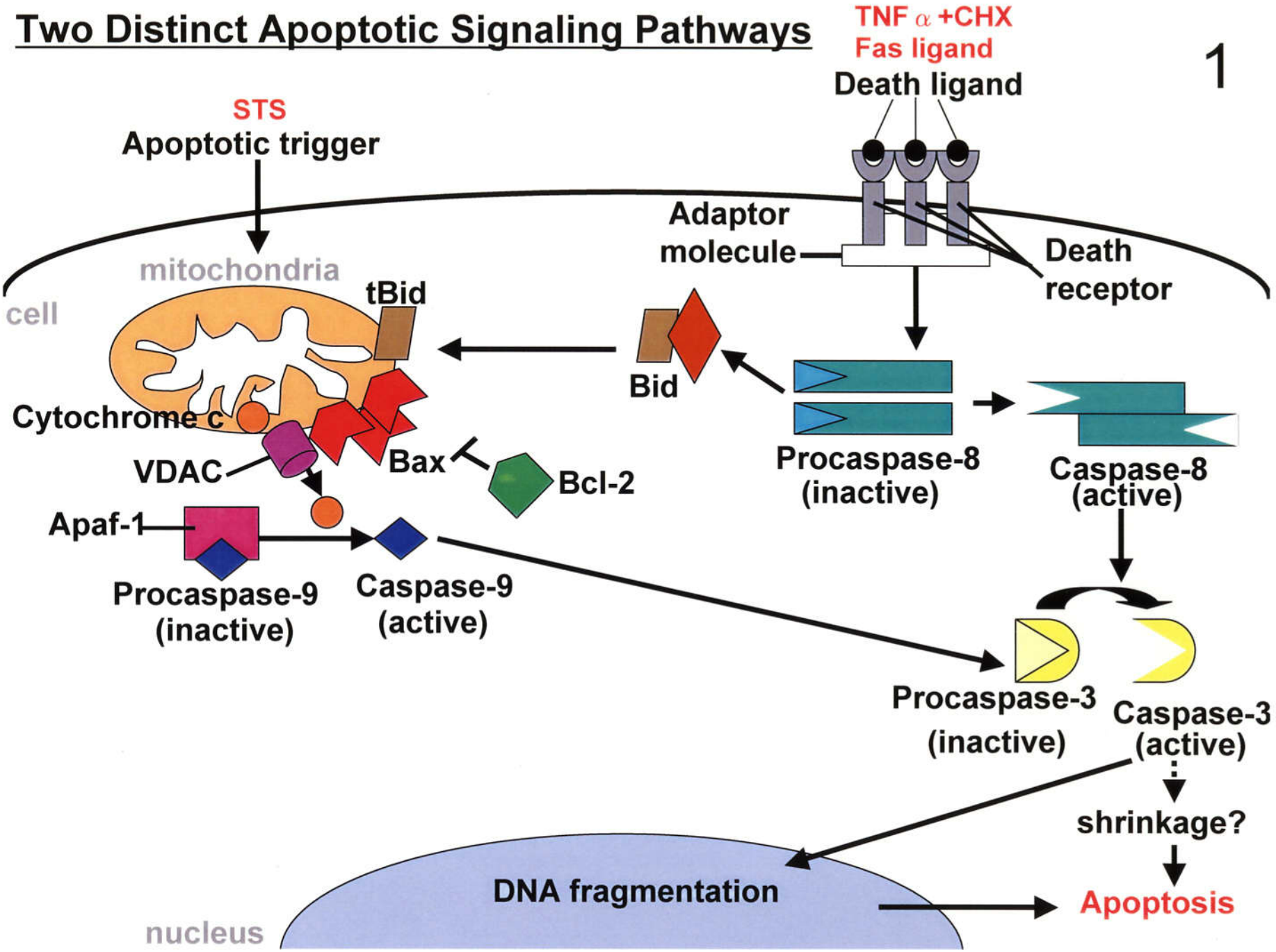

2A U937

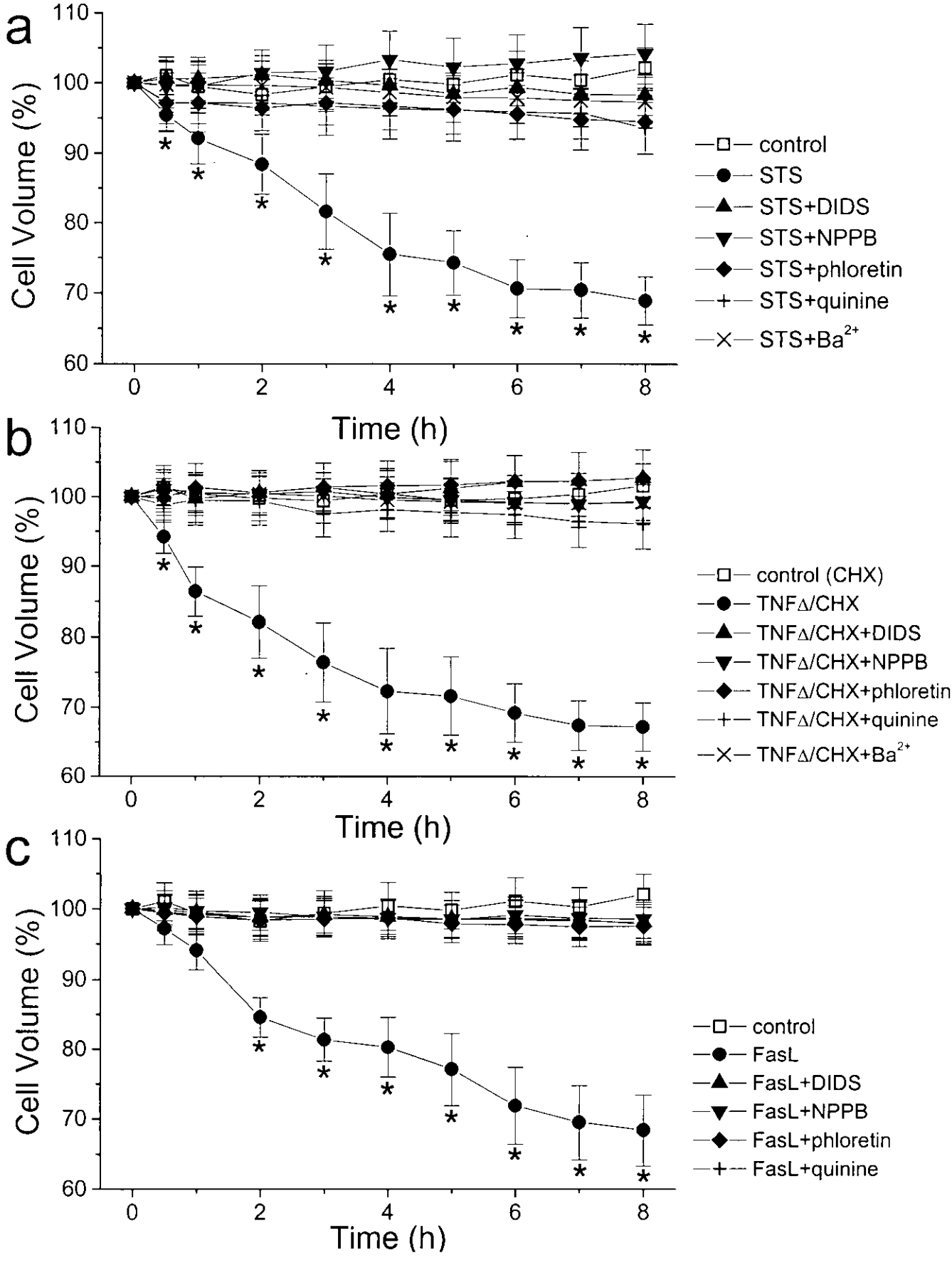
a
Cell Volume (%)
110
100
90
80
70
60
0
2
4
6
8
Time (h)
control
STS
STS+DIDS
STS+NPPB
STS+phloretin
STS+quinine
STS+Ba2+
b
Cell Volume (%)
Time (h)
control (CHX)
TNFΔ/CHX
TNFΔ/CHX+DIDS
TNFΔ/CHX+NPPB
TNFΔ/CHX+phloretin
TNFΔ/CHX+quinine
TNFΔ/CHX+Ba2+
c
Cell Volume (%)
Time (h)
control
FasL
FasL+DIDS
FasL+NPPB
FasL+phloretin
FasL+quinine

2B HeLa

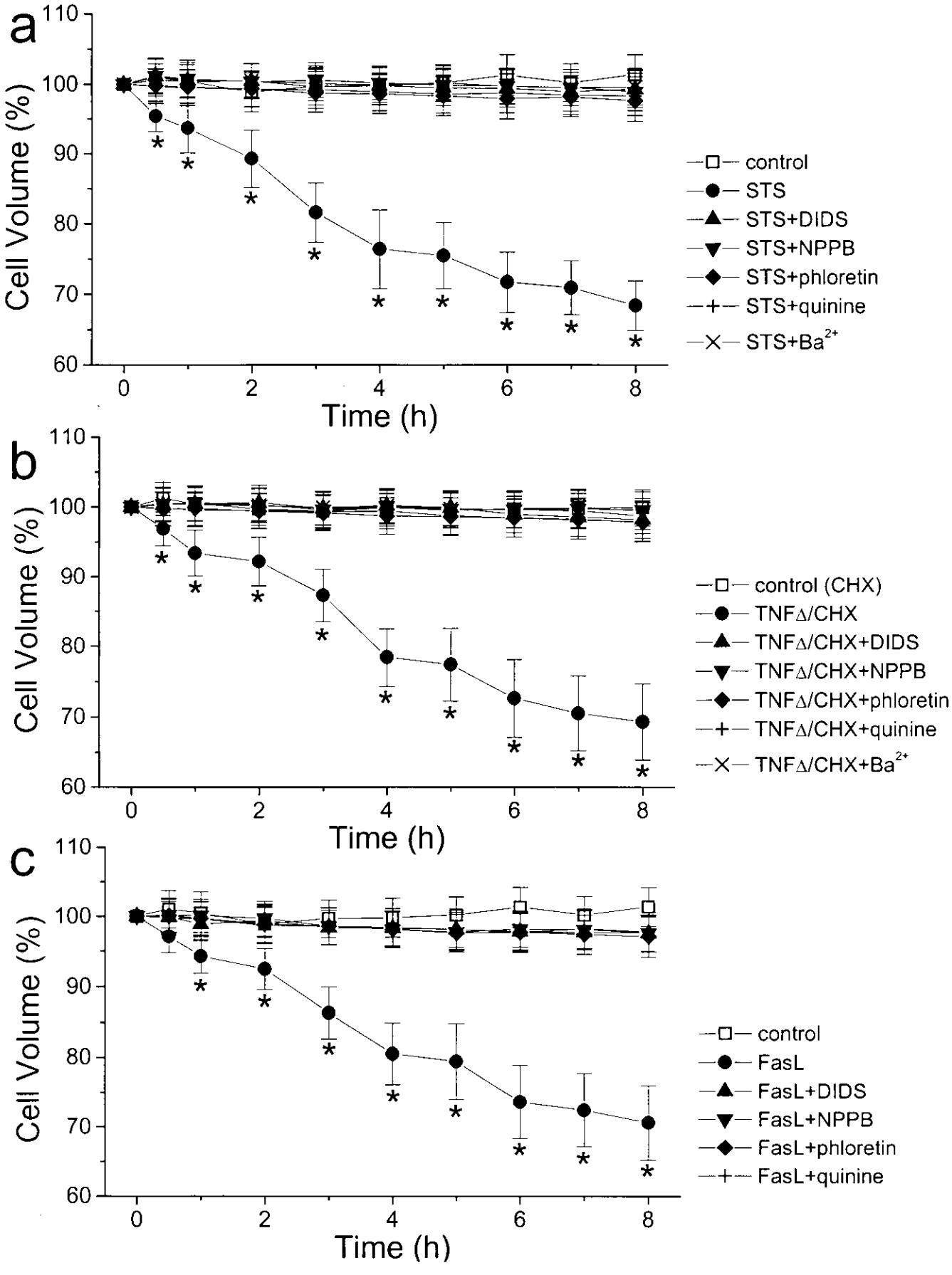
a
Cell Volume (%)
110
100
90
80
70
60
0
2
4
6
8
Time (h)
control
STS
STS+DIDS
STS+NPPB
STS+phloretin
STS+quinine
STS+Ba2+
b
Cell Volume (%)
Time (h)
control (CHX)
TNFΔ/CHX
TNFΔ/CHX+DIDS
TNFΔ/CHX+NPPB
TNFΔ/CHX+phloretin
TNFΔ/CHX+quinine
TNFΔ/CHX+Ba2+
c
Cell Volume (%)
Time (h)
control
FasL
FasL+DIDS
FasL+NPPB
FasL+phloretin
FasL+quinine

2C PC12

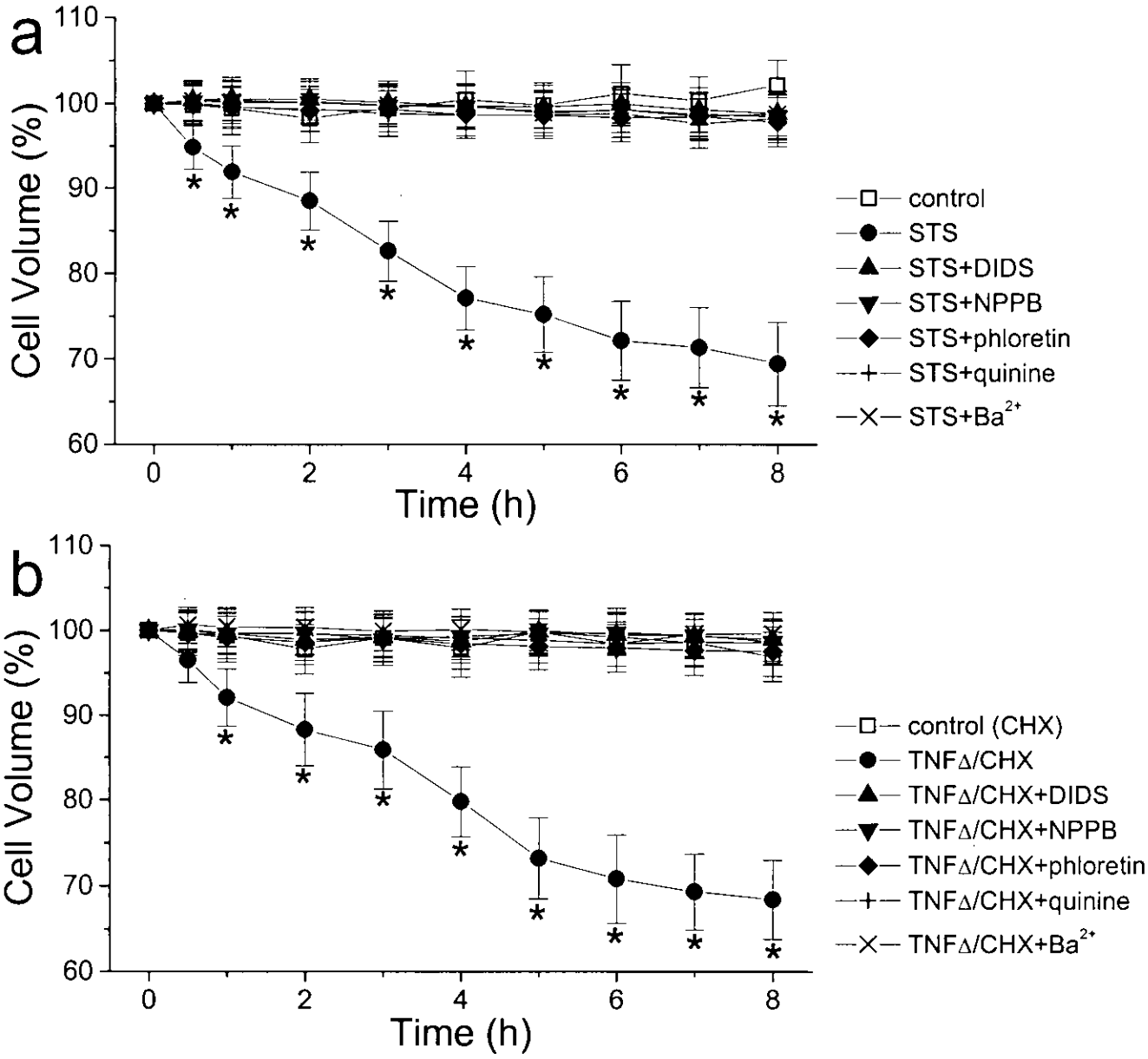
a
Cell Volume (%)
110
100
90
80
70
60
0
2
4
6
8
Time (h)
control
STS
STS+DIDS
STS+NPPB
STS+phloretin
STS+quinine
STS+Ba2+
b
Cell Volume (%)
110
100
90
80
70
60
0
2
4
6
8
Time (h)
control (CHX)
TNFΔ/CHX
TNFΔ/CHX+DIDS
TNFΔ/CHX+NPPB
TNFΔ/CHX+phloretin
TNFΔ/CHX+quinine
TNFΔ/CHX+Ba2+

2D NG108-15

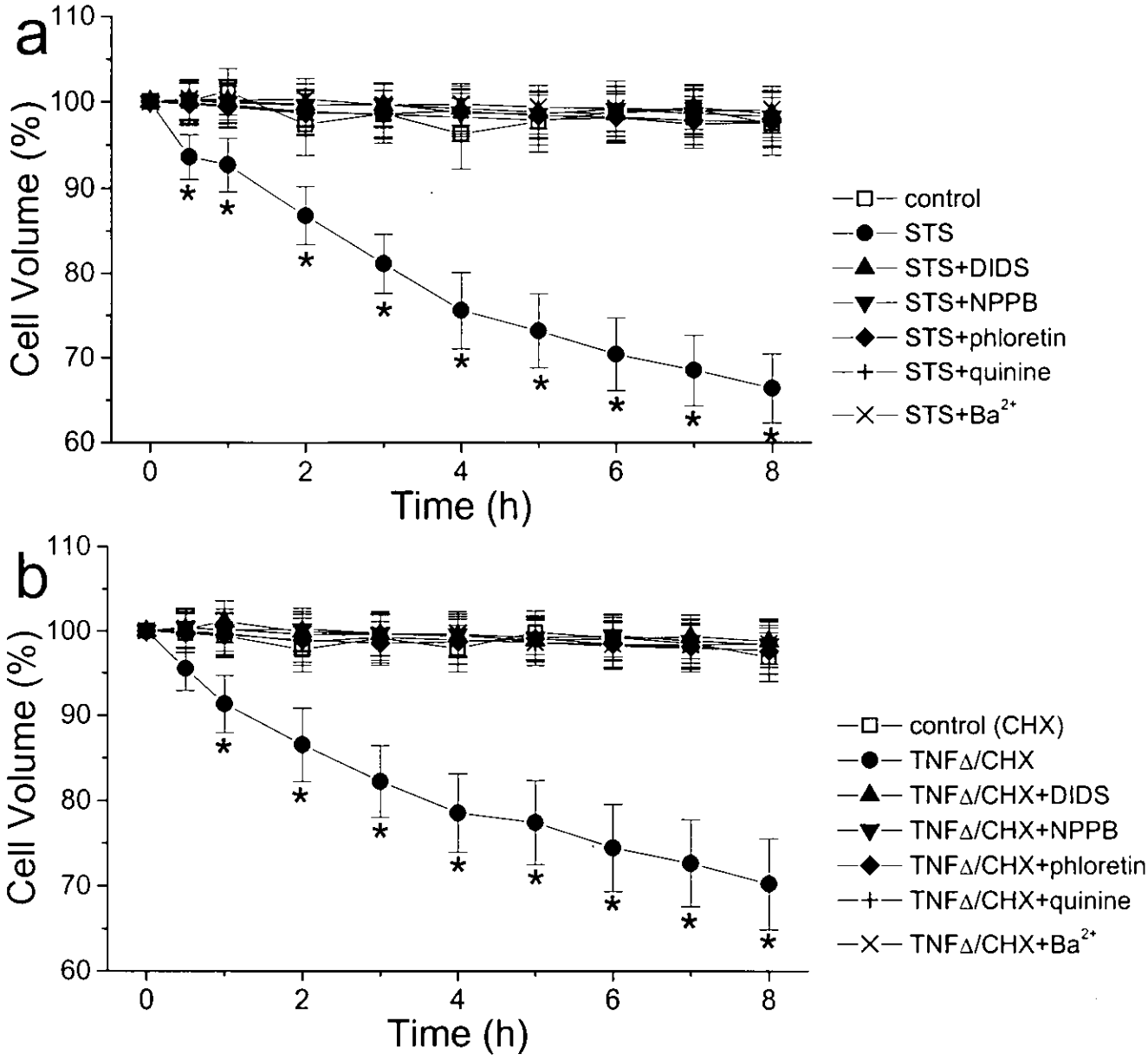
a
b
Cell Volume (%)
Time (h)
110
100
90
80
70
60
0
2
4
6
8
control
STS
STS+DIDS
STS+NPPB
STS+phloretin
STS+quinine
STS+Ba2+
control (CHX)
TNFΔ/CHX
TNFΔ/CHX+DIDS
TNFΔ/CHX+NPPB
TNFΔ/CHX+phloretin
TNFΔ/CHX+quinine
TNFΔ/CHX+Ba2+

3 HeLa

A

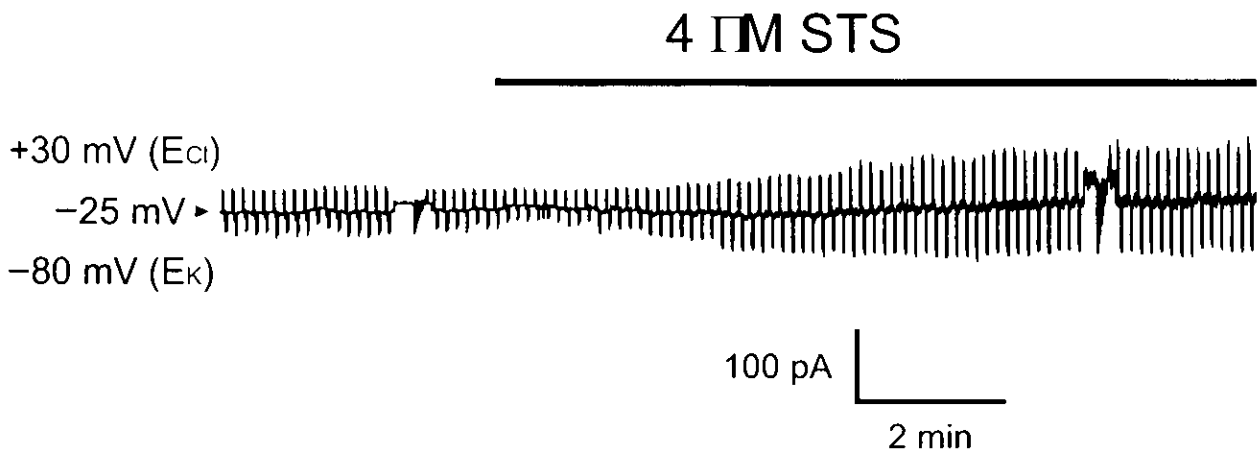
4 μM STS
+30 mV (ECl)
−25 mV
−80 mV (EK)
100 pA
2 min

B

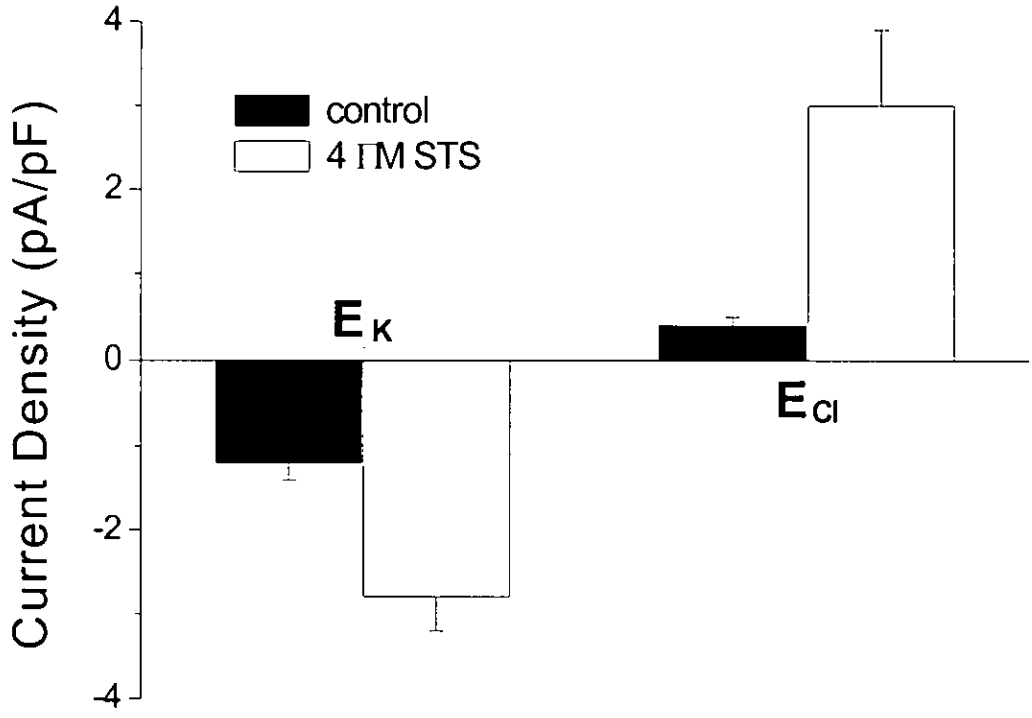
Current Density (pA/pF)
4
2
0
-2
-4
control
4 μM STS
EK
ECl

4

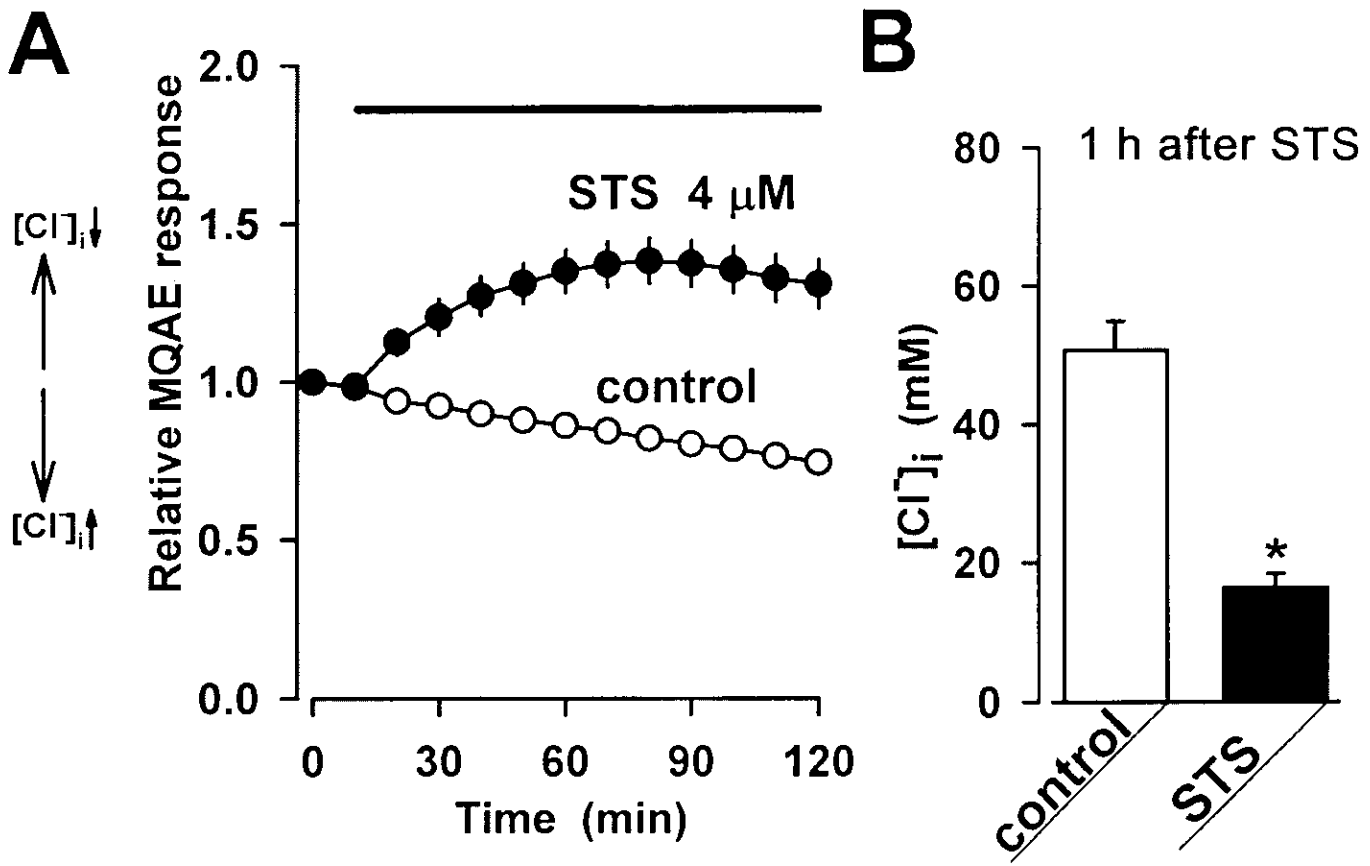

STS-induced $[Cl^-]_i$ decrease in HeLa cells.

5 HeLa

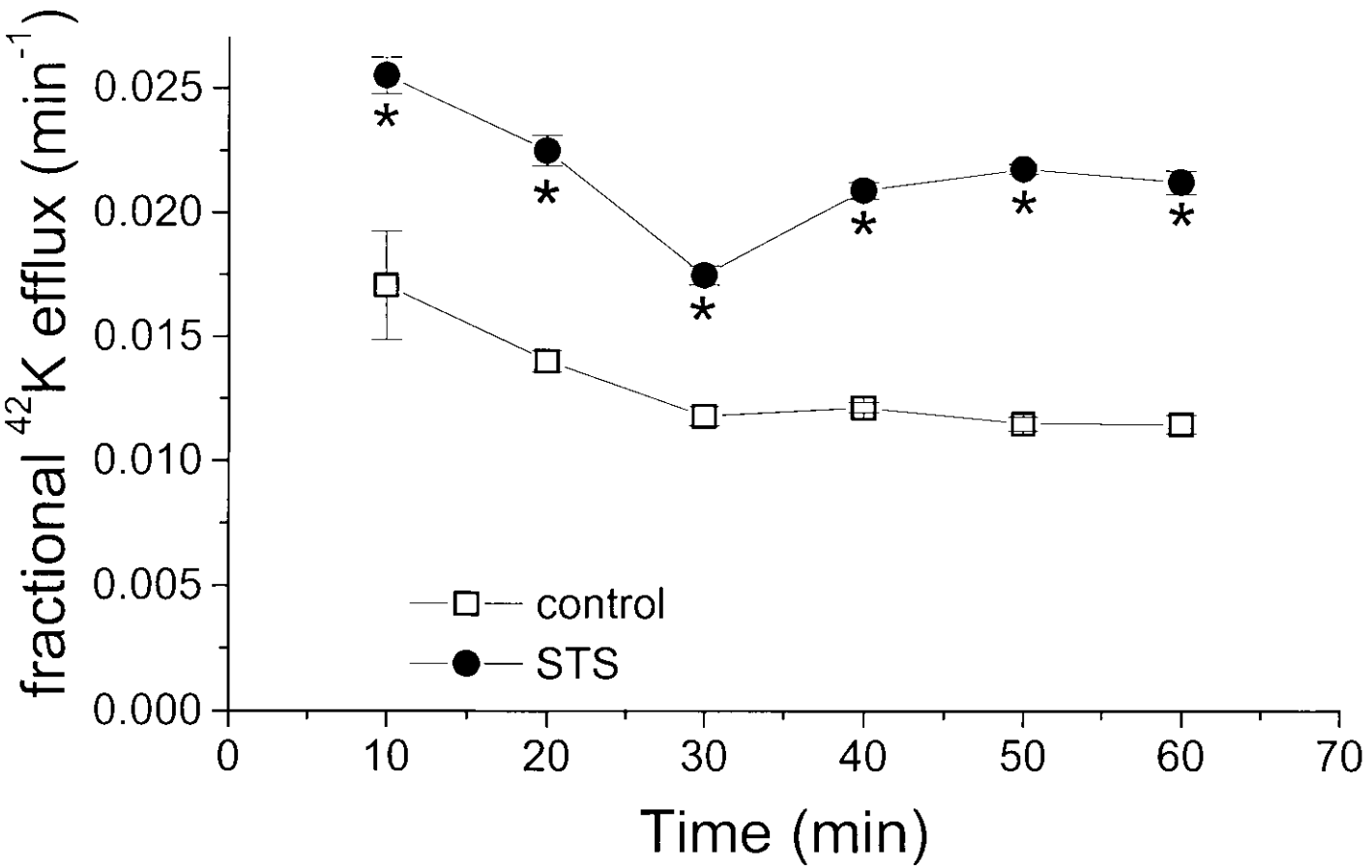
fractional ^{42}K efflux (min^{-1})
0.025
0.020
0.015
0.010
0.005
0.000
0
10
20
30
40
50
60
70
Time (min)
control
STS
*
*
*
*
*
*

6A U937

a

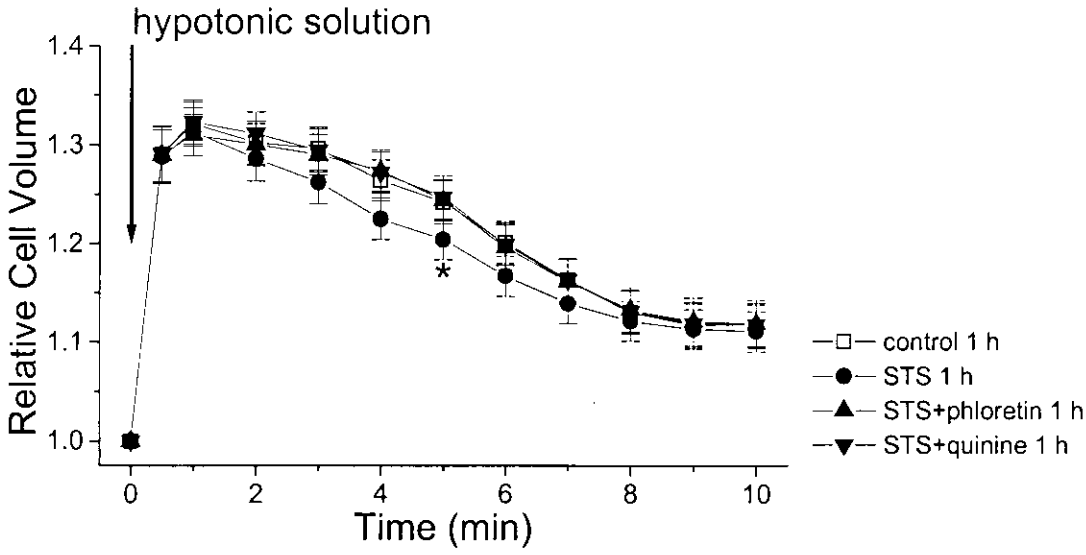
hypotonic solution
Relative Cell Volume
1.4
1.3
1.2
1.1
1.0
0
2
4
6
8
10
Time (min)
control 1 h
STS 1 h
STS+phloretin 1 h
STS+quinine 1 h

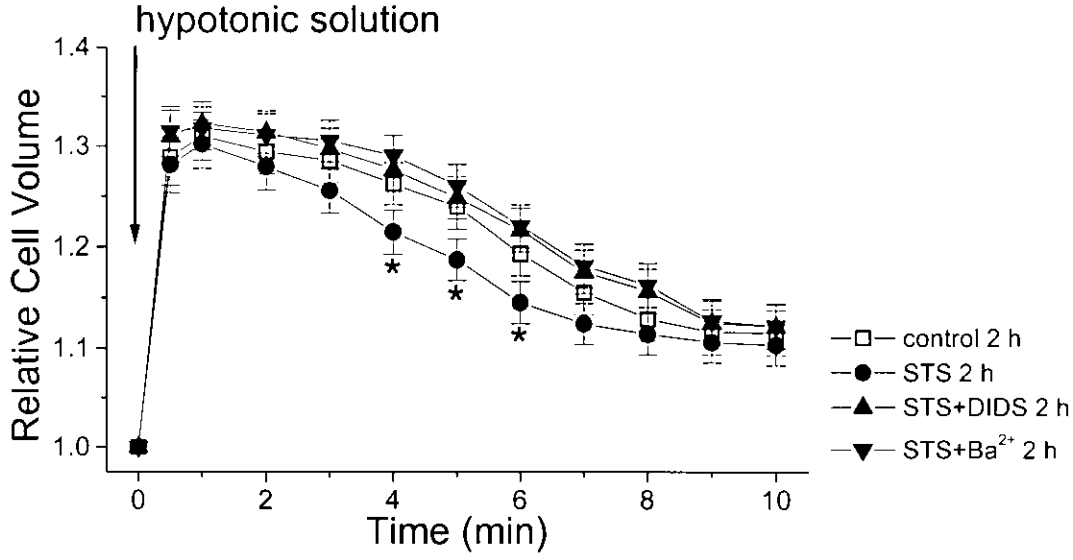
hypotonic solution
Relative Cell Volume
1.4
1.3
1.2
1.1
1.0
0
2
4
6
8
10
Time (min)
control 2 h
STS 2 h
STS+DIDS 2 h
STS+Ba2+ 2 h

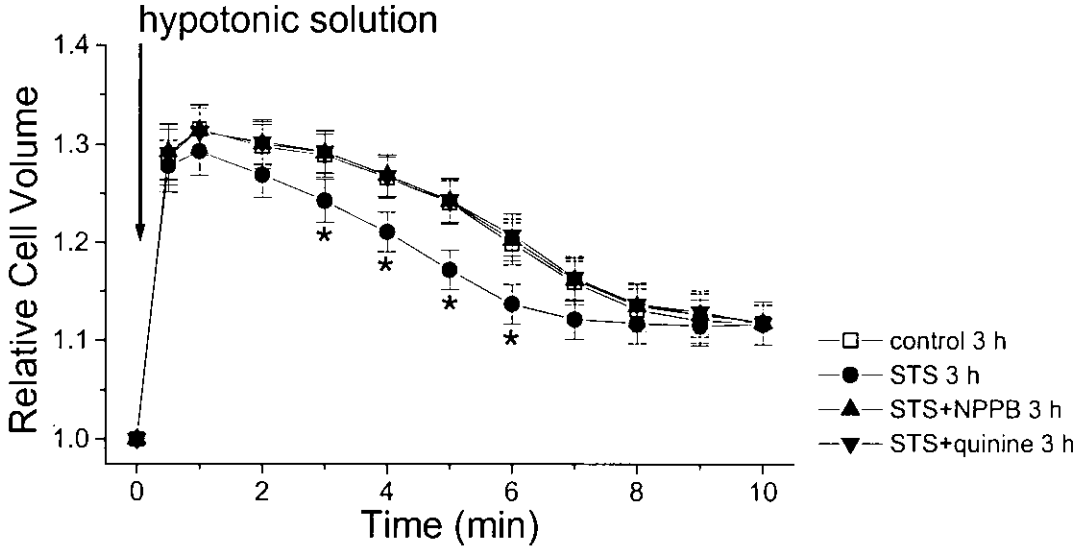
hypotonic solution
Relative Cell Volume
1.4
1.3
1.2
1.1
1.0
0
2
4
6
8
10
Time (min)
control 3 h
STS 3 h
STS+NPPB 3 h
STS+quinine 3 h

6A U937

b

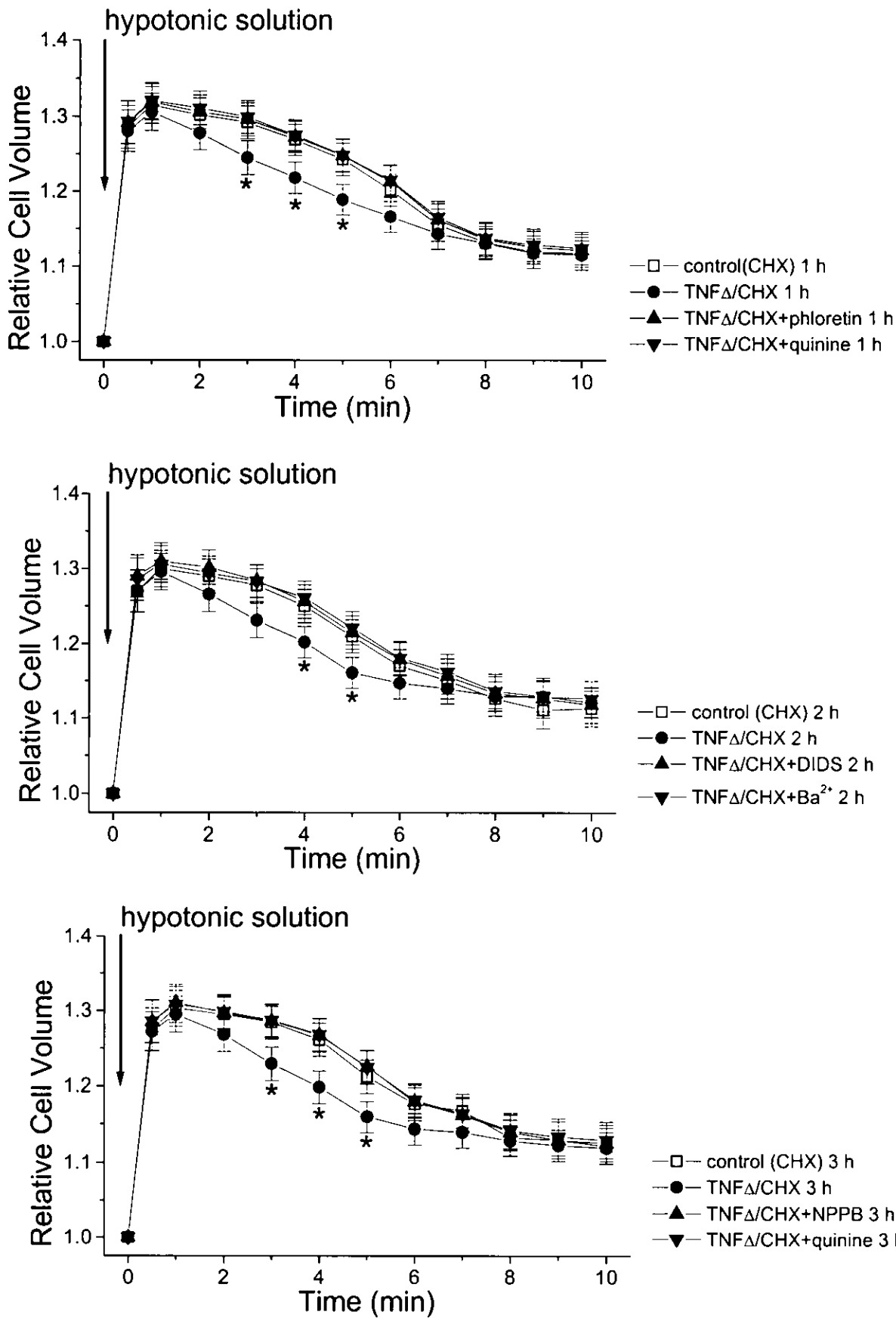
hypotonic solution
Relative Cell Volume
Time (min)
control(CHX) 1 h
TNFΔ/CHX 1 h
TNFΔ/CHX+phloretin 1 h
TNFΔ/CHX+quinine 1 h
hypotonic solution
Relative Cell Volume
Time (min)
control (CHX) 2 h
TNFΔ/CHX 2 h
TNFΔ/CHX+DIDS 2 h
TNFΔ/CHX+Ba2+ 2 h
hypotonic solution
Relative Cell Volume
Time (min)
control (CHX) 3 h
TNFΔ/CHX 3 h
TNFΔ/CHX+NPPB 3 h
TNFΔ/CHX+quinine 3 h

6A U937

c

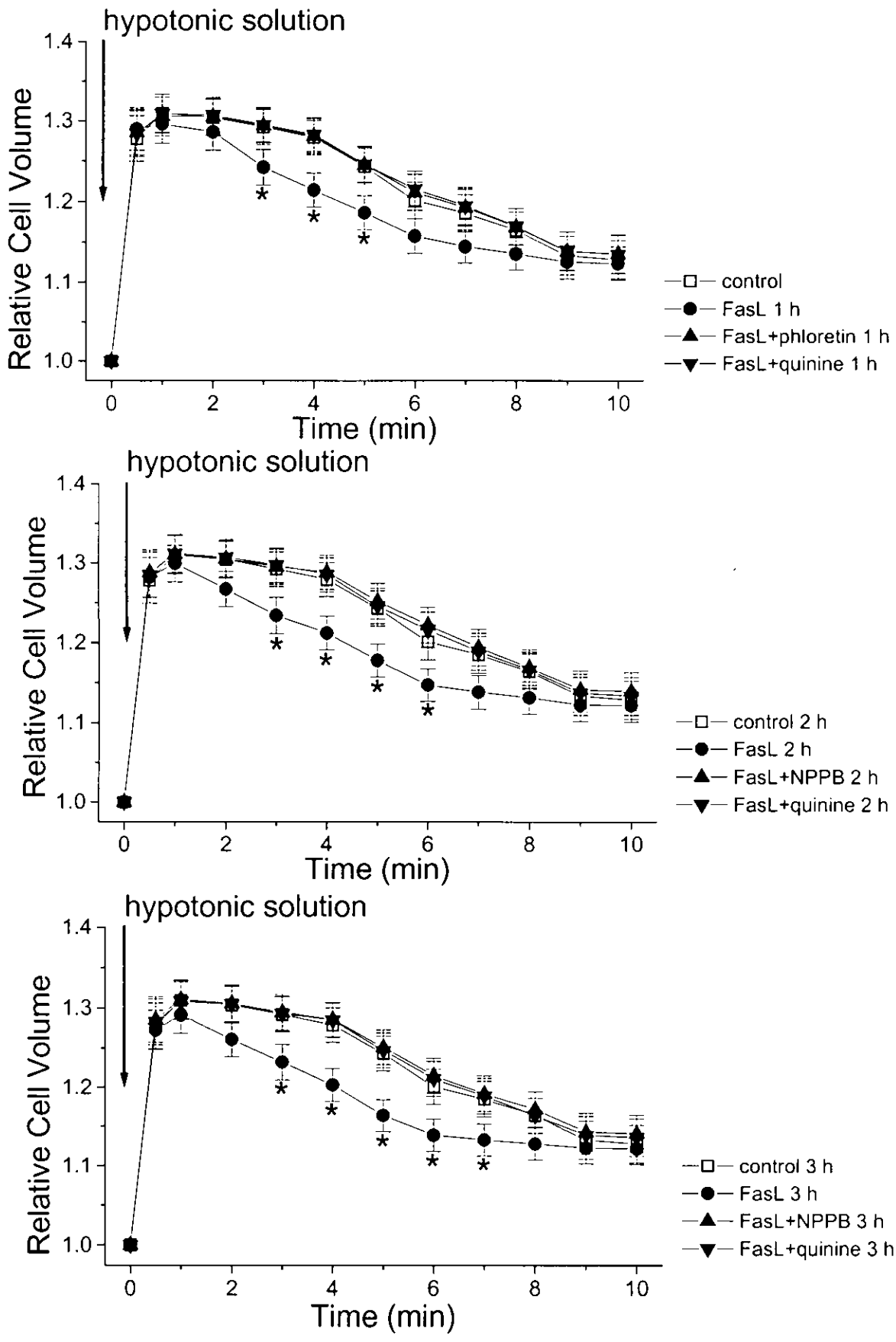
hypotonic solution
Relative Cell Volume
Time (min)
control
FasL 1 h
FasL+phloretin 1 h
FasL+quinine 1 h
hypotonic solution
Relative Cell Volume
Time (min)
control 2 h
FasL 2 h
FasL+NPPB 2 h
FasL+quinine 2 h
hypotonic solution
Relative Cell Volume
Time (min)
control 3 h
FasL 3 h
FasL+NPPB 3 h
FasL+quinine 3 h

6B HeLa

a

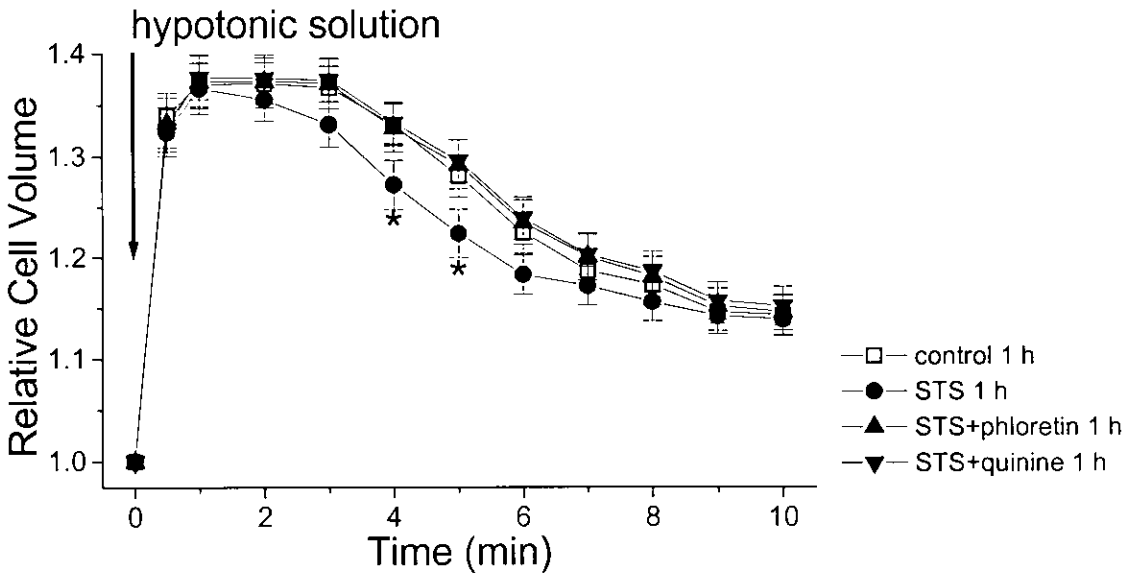
hypotonic solution
Relative Cell Volume
Time (min)
control 1 h
STS 1 h
STS+phloretin 1 h
STS+quinine 1 h

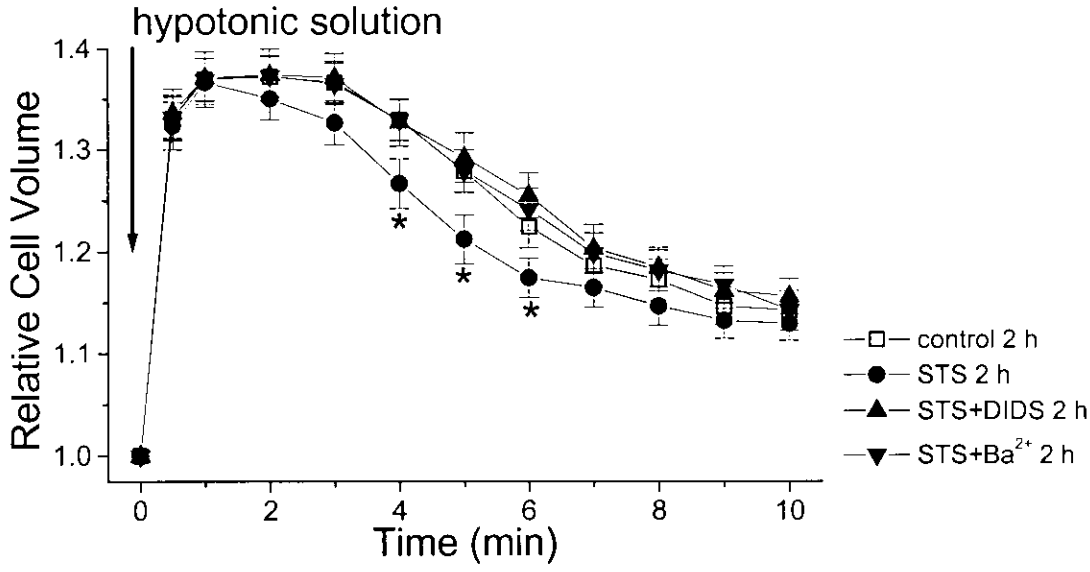
hypotonic solution
Relative Cell Volume
Time (min)
control 2 h
STS 2 h
STS+DIDS 2 h
STS+Ba2+ 2 h

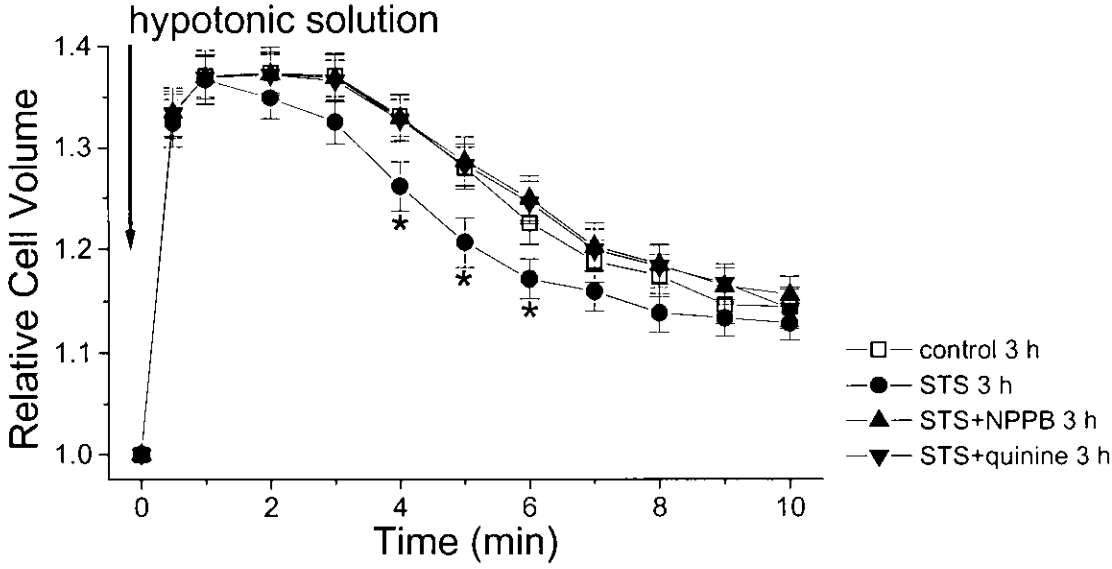
hypotonic solution
Relative Cell Volume
Time (min)
control 3 h
STS 3 h
STS+NPPB 3 h
STS+quinine 3 h

6B HeLa

b

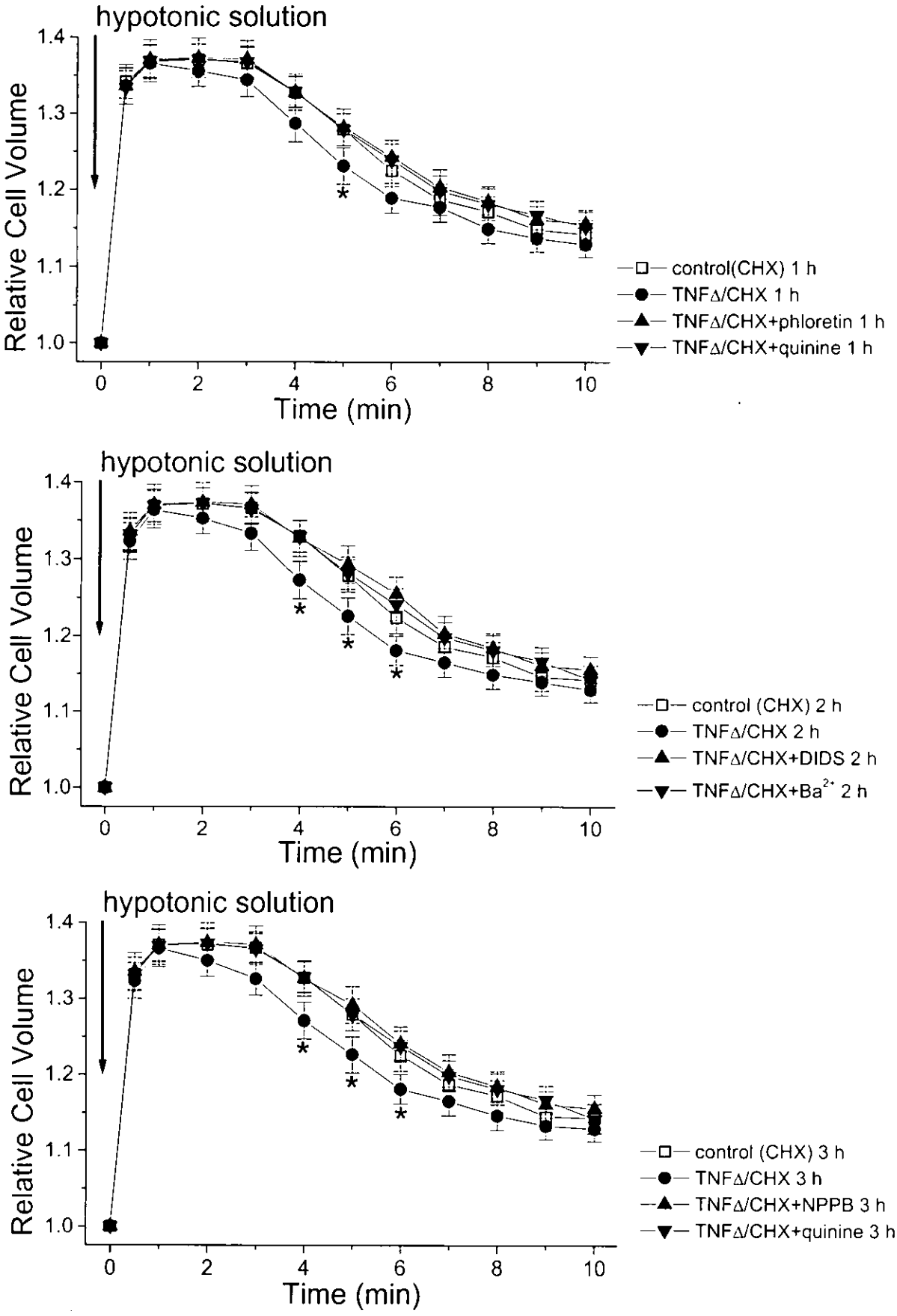
hypotonic solution
Relative Cell Volume
Time (min)
control(CHX) 1 h
TNFΔ/CHX 1 h
TNFΔ/CHX+phloretin 1 h
TNFΔ/CHX+quinine 1 h
hypotonic solution
Relative Cell Volume
Time (min)
control (CHX) 2 h
TNFΔ/CHX 2 h
TNFΔ/CHX+DIDS 2 h
TNFΔ/CHX+Ba2+ 2 h
hypotonic solution
Relative Cell Volume
Time (min)
control (CHX) 3 h
TNFΔ/CHX 3 h
TNFΔ/CHX+NPPB 3 h
TNFΔ/CHX+quinine 3 h

6B HeLa

c

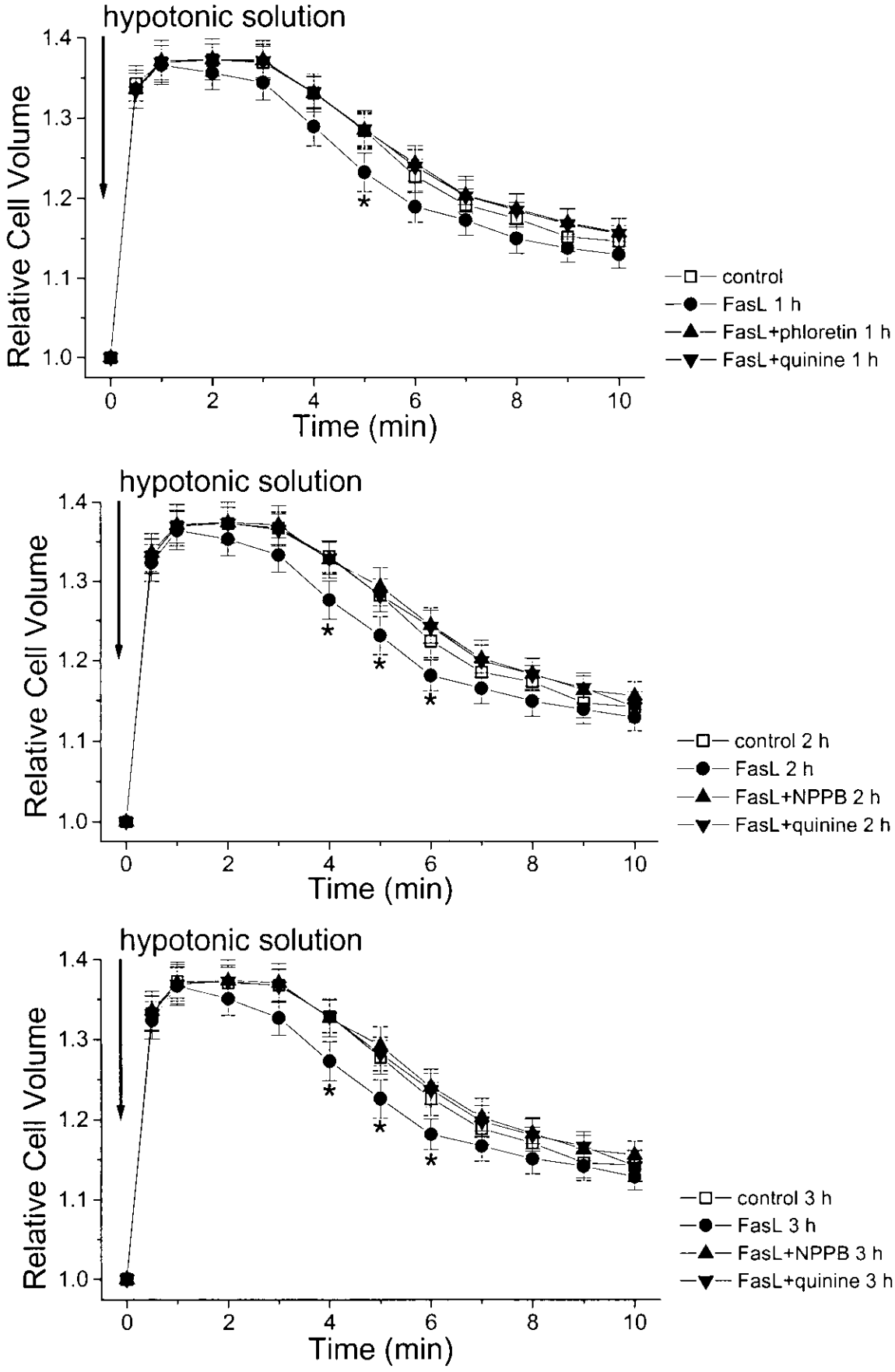
hypotonic solution
Relative Cell Volume
Time (min)
control
FasL 1 h
FasL+phloretin 1 h
FasL+quinine 1 h
hypotonic solution
Relative Cell Volume
Time (min)
control 2 h
FasL 2 h
FasL+NPPB 2 h
FasL+quinine 2 h
hypotonic solution
Relative Cell Volume
Time (min)
control 3 h
FasL 3 h
FasL+NPPB 3 h
FasL+quinine 3 h

6C PC12

a

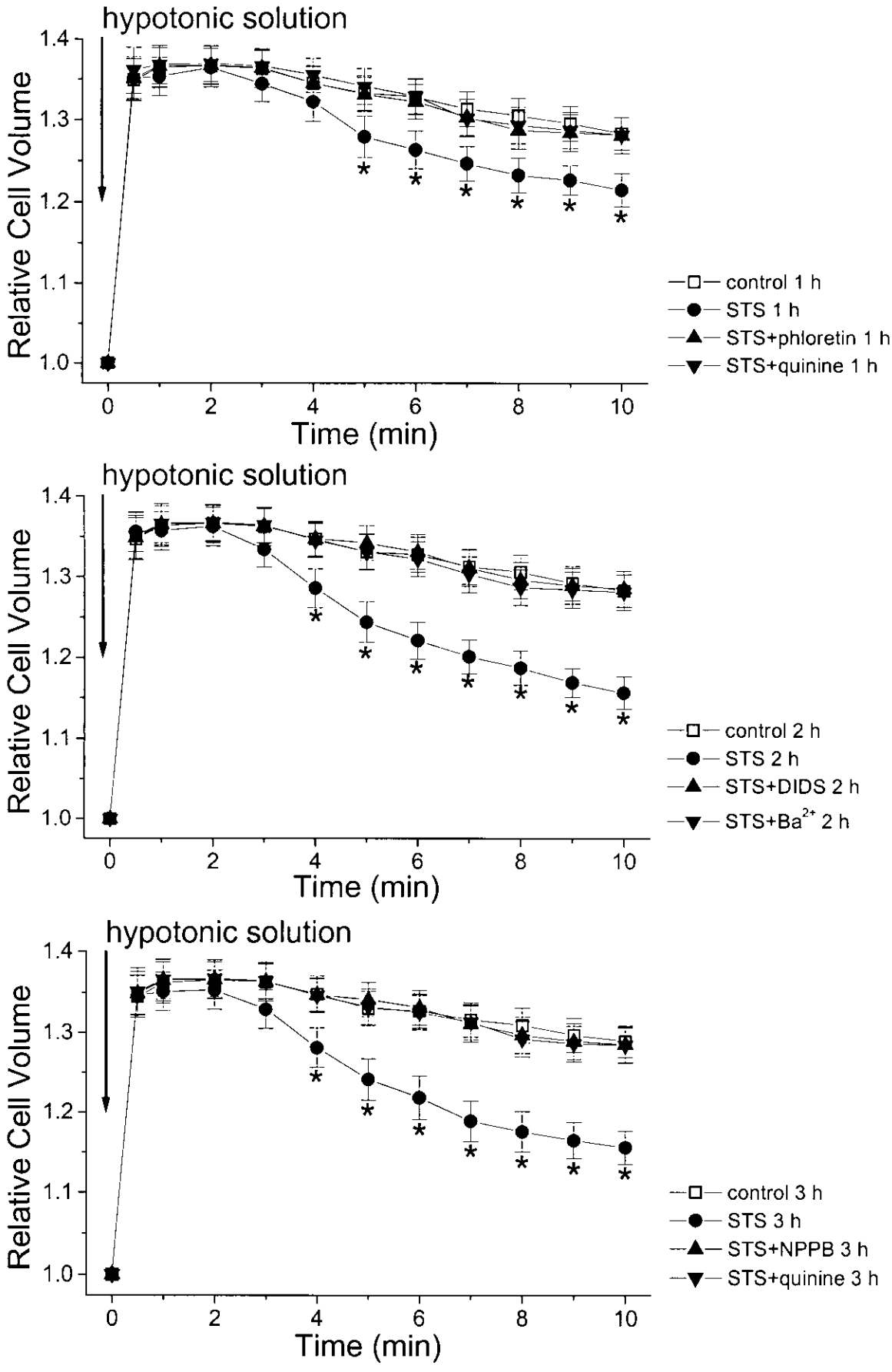
hypotonic solution
Relative Cell Volume
Time (min)
control 1 h
STS 1 h
STS+phloretin 1 h
STS+quinine 1 h
hypotonic solution
Relative Cell Volume
Time (min)
control 2 h
STS 2 h
STS+DIDS 2 h
STS+Ba2+ 2 h
hypotonic solution
Relative Cell Volume
Time (min)
control 3 h
STS 3 h
STS+NPPB 3 h
STS+quinine 3 h

6C PC12

b

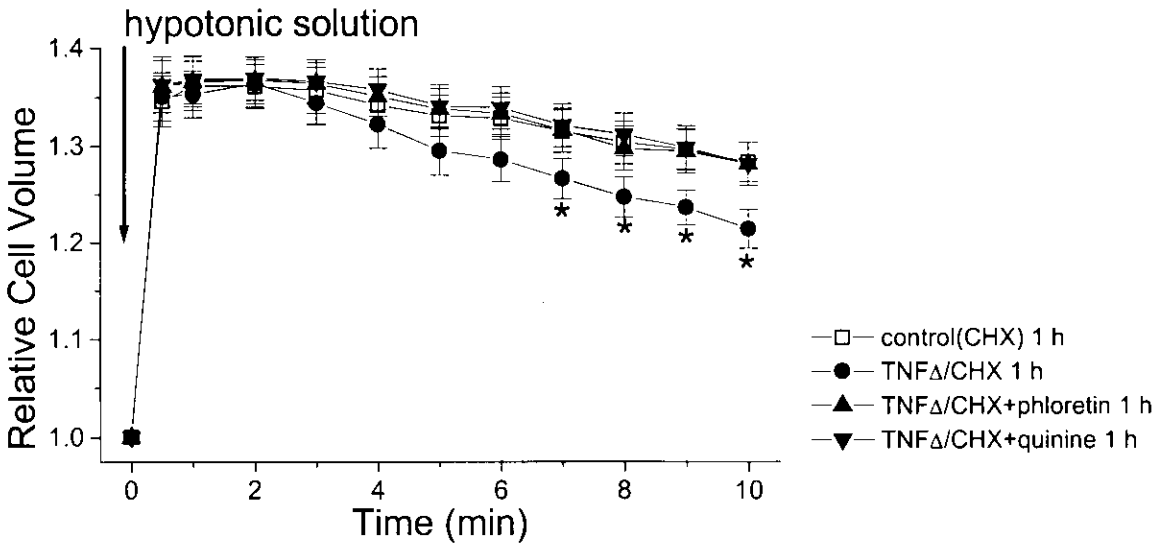
hypotonic solution
Relative Cell Volume
Time (min)
control(CHX) 1 h
TNFΔ/CHX 1 h
TNFΔ/CHX+phloretin 1 h
TNFΔ/CHX+quinine 1 h

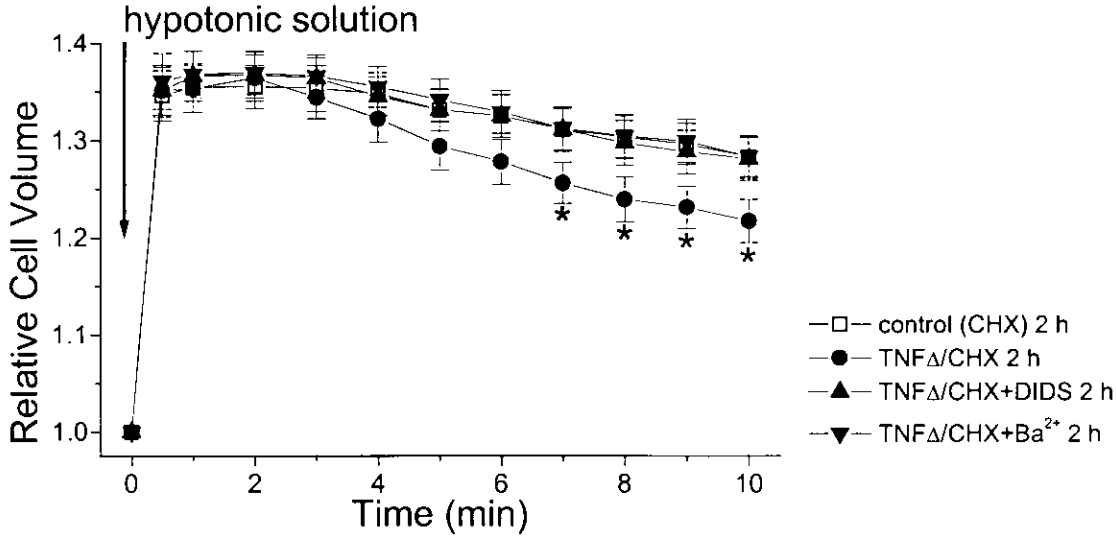
hypotonic solution
Relative Cell Volume
Time (min)
control (CHX) 2 h
TNFΔ/CHX 2 h
TNFΔ/CHX+DIDS 2 h
TNFΔ/CHX+Ba2+ 2 h

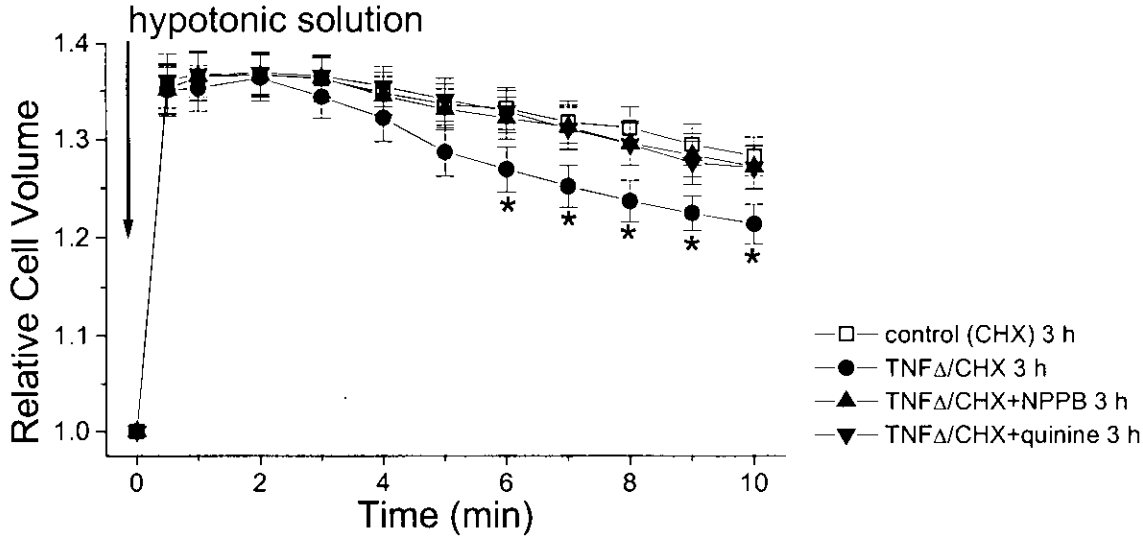
hypotonic solution
Relative Cell Volume
Time (min)
control (CHX) 3 h
TNFΔ/CHX 3 h
TNFΔ/CHX+NPPB 3 h
TNFΔ/CHX+quinine 3 h

6D NG108-15

a

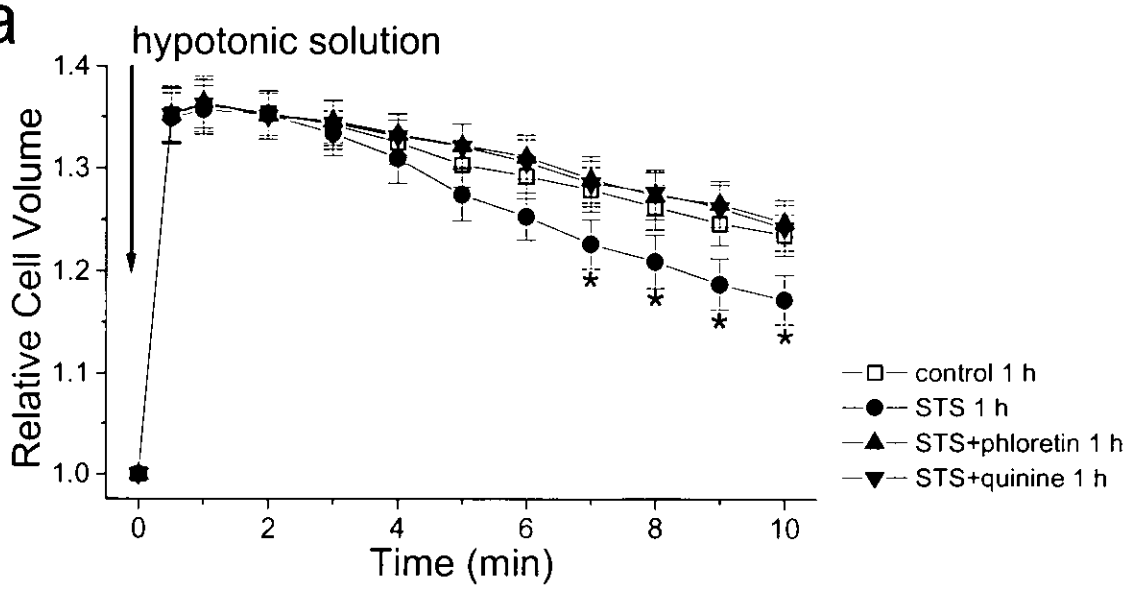
hypotonic solution
Relative Cell Volume
1.4
1.3
1.2
1.1
1.0
0
2
4
6
8
10
Time (min)
control 1 h
STS 1 h
STS+phloretin 1 h
STS+quinine 1 h

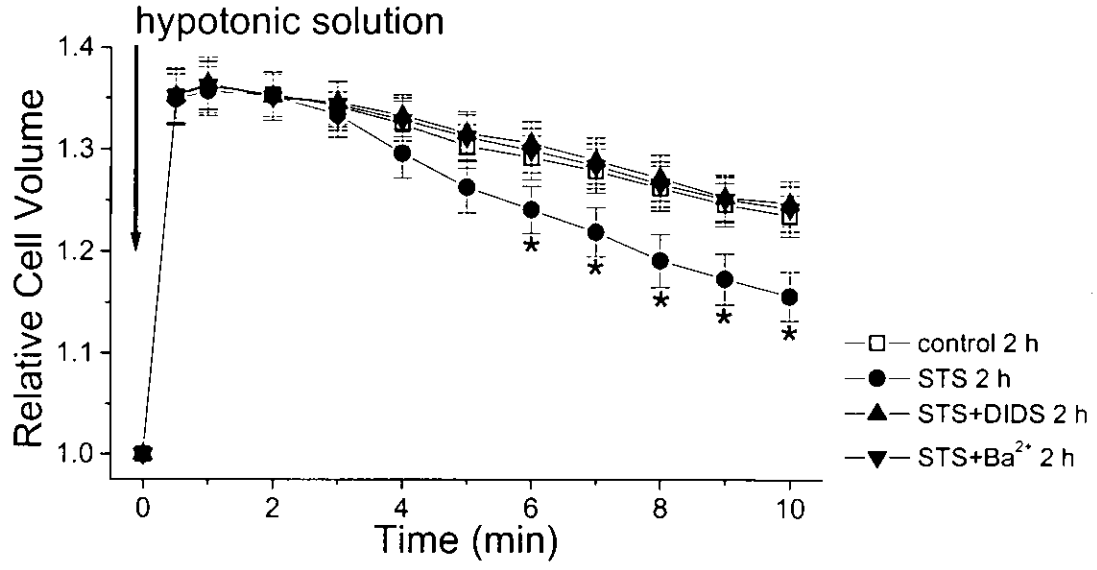
hypotonic solution
Relative Cell Volume
1.4
1.3
1.2
1.1
1.0
0
2
4
6
8
10
Time (min)
control 2 h
STS 2 h
STS+DIDS 2 h
STS+Ba2+ 2 h

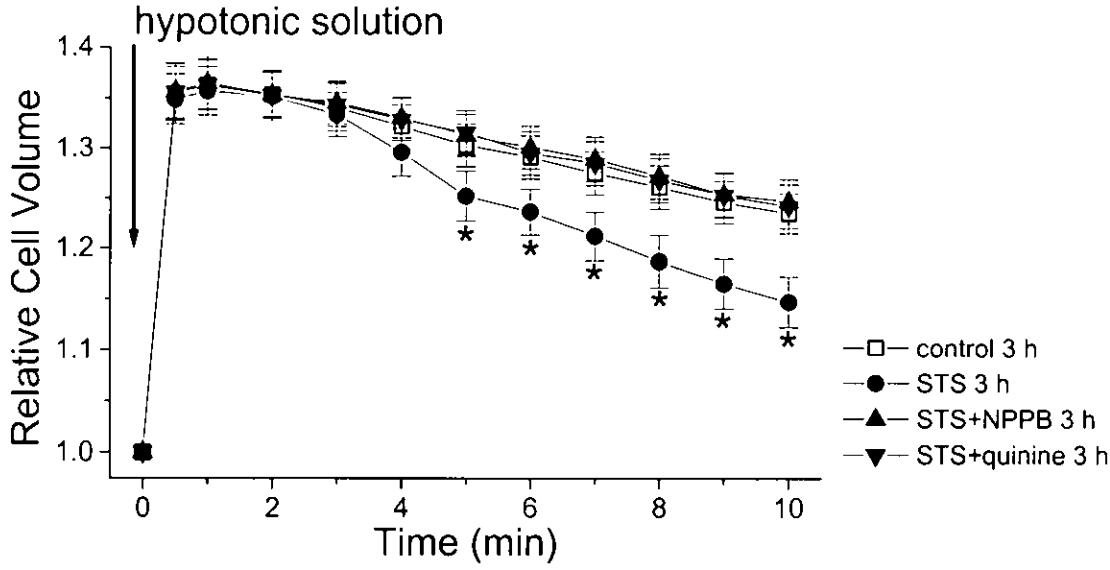
hypotonic solution
Relative Cell Volume
1.4
1.3
1.2
1.1
1.0
0
2
4
6
8
10
Time (min)
control 3 h
STS 3 h
STS+NPPB 3 h
STS+quinine 3 h

6D NG108-15

b

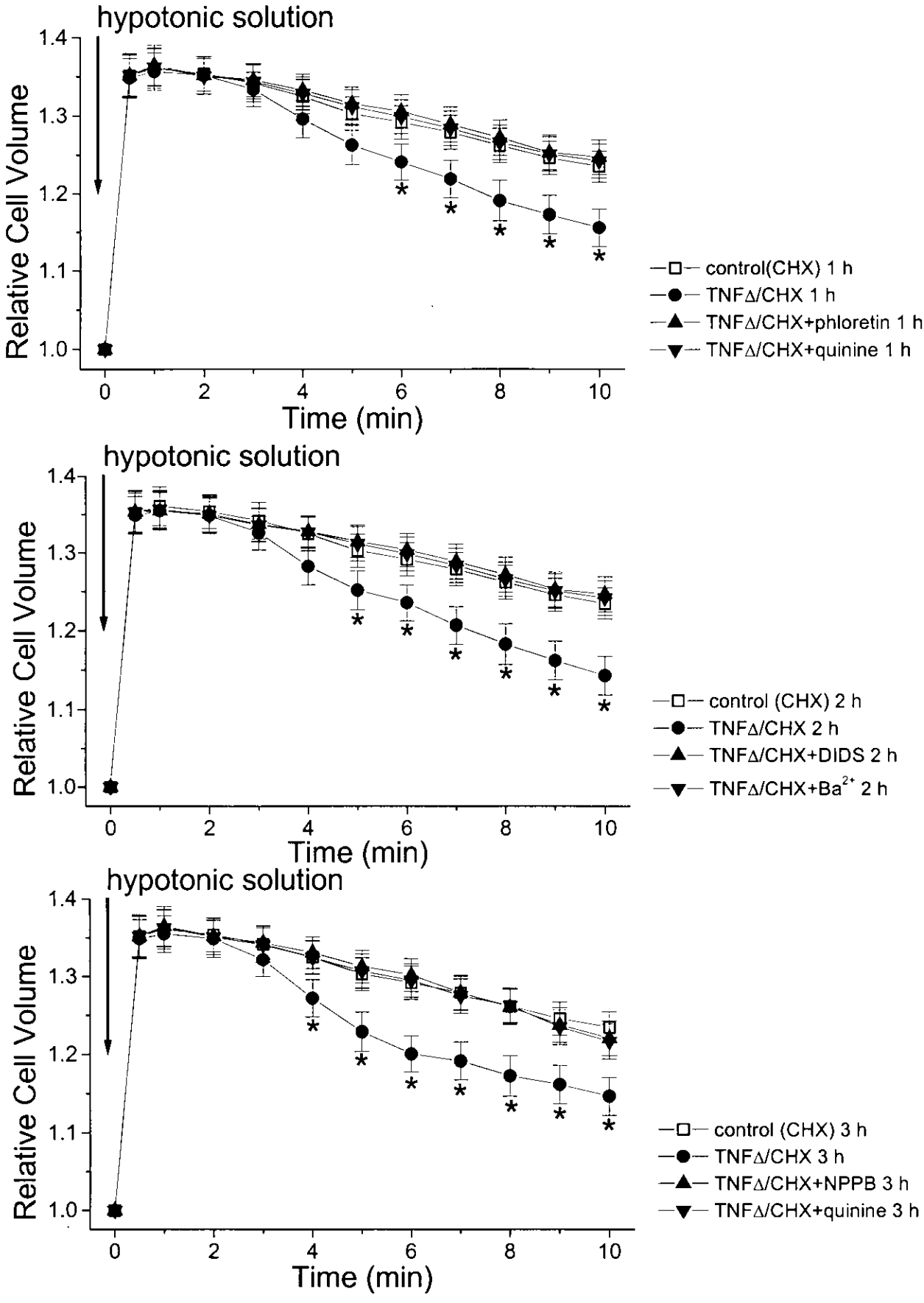
hypotonic solution
Relative Cell Volume
Time (min)
control(CHX) 1 h
TNFΔ/CHX 1 h
TNFΔ/CHX+phloretin 1 h
TNFΔ/CHX+quinine 1 h
hypotonic solution
Relative Cell Volume
Time (min)
control (CHX) 2 h
TNFΔ/CHX 2 h
TNFΔ/CHX+DIDS 2 h
TNFΔ/CHX+Ba2+ 2 h
hypotonic solution
Relative Cell Volume
Time (min)
control (CHX) 3 h
TNFΔ/CHX 3 h
TNFΔ/CHX+NPPB 3 h
TNFΔ/CHX+quinine 3 h

7 HeLa

A

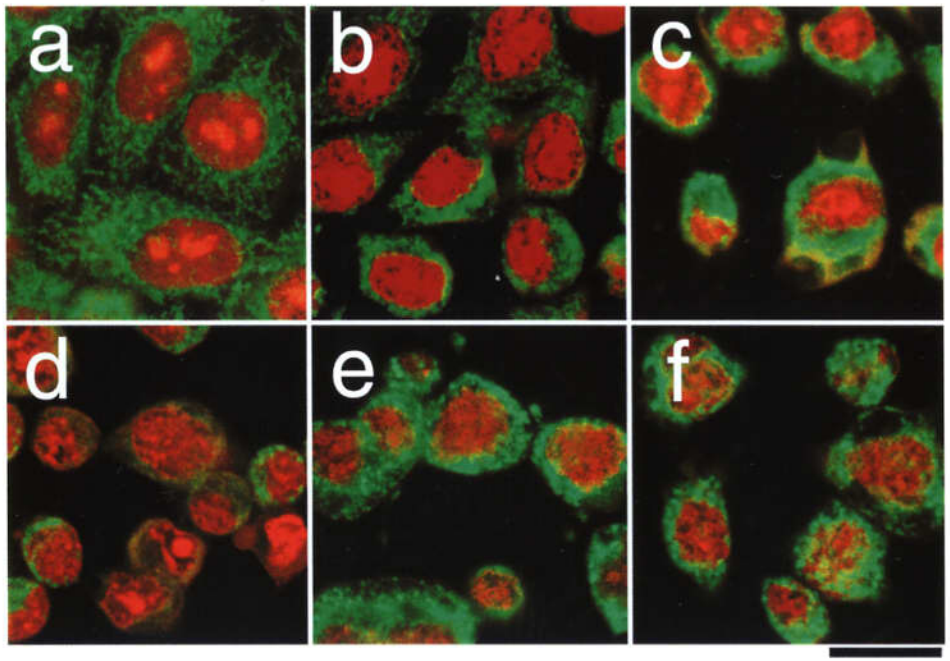
a
b
c
d
e
f

B

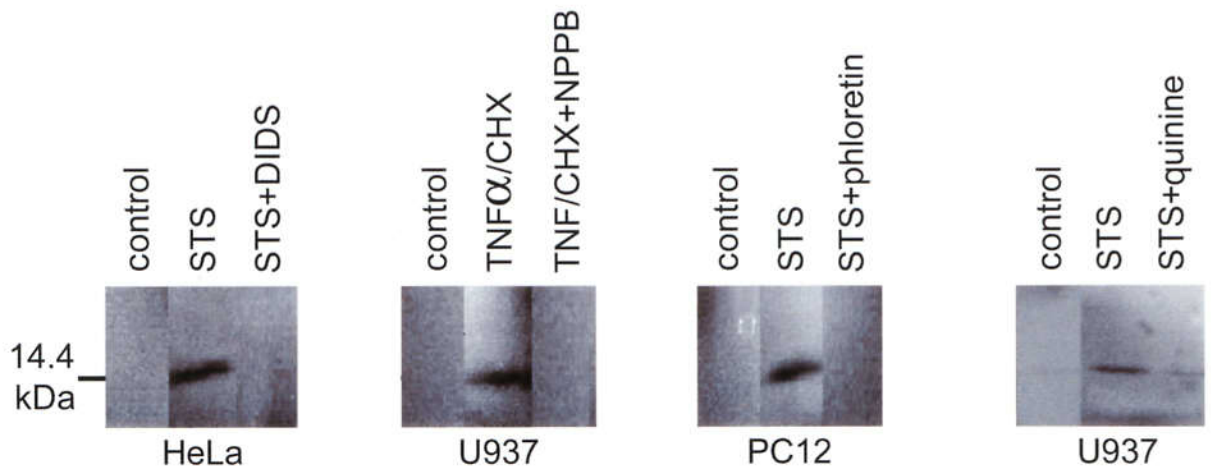
control
STS
STS+DIDS
14.4
kDa
HeLa
control
TNFα/CHX
TNF/CHX+NPPB
U937
control
STS
STS+phloretin
PC12
control
STS
STS+quinine
U937

8A U937

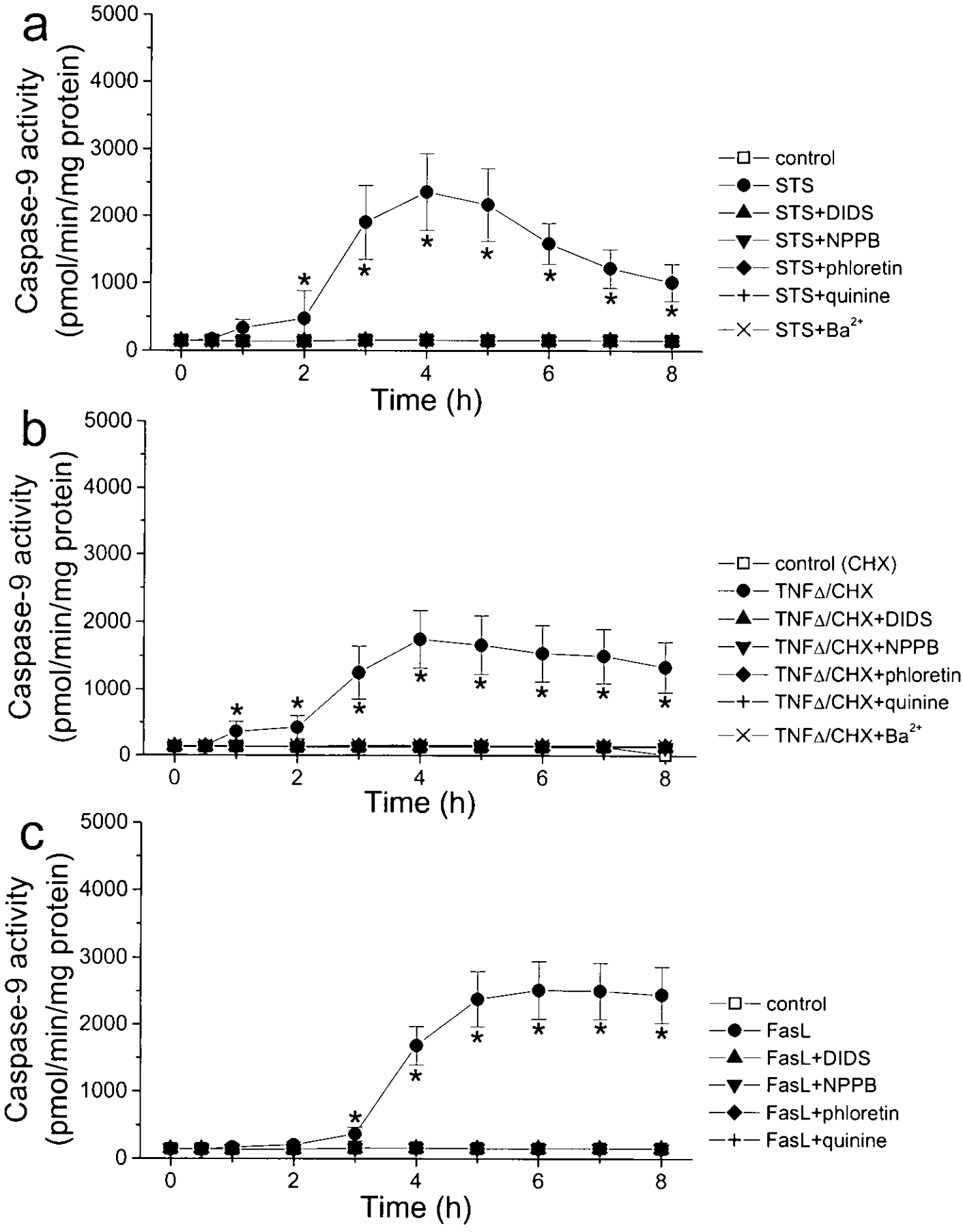
a
Caspase-9 activity (pmol/min/mg protein)
5000
4000
3000
2000
1000
0
0
2
4
6
8
Time (h)
control
STS
STS+DIDS
STS+NPPB
STS+phloretin
STS+quinine
STS+Ba2+
b
Caspase-9 activity (pmol/min/mg protein)
Time (h)
control (CHX)
TNFΔ/CHX
TNFΔ/CHX+DIDS
TNFΔ/CHX+NPPB
TNFΔ/CHX+phloretin
TNFΔ/CHX+quinine
TNFΔ/CHX+Ba2+
c
Caspase-9 activity (pmol/min/mg protein)
Time (h)
control
FasL
FasL+DIDS
FasL+NPPB
FasL+phloretin
FasL+quinine

8B HeLa

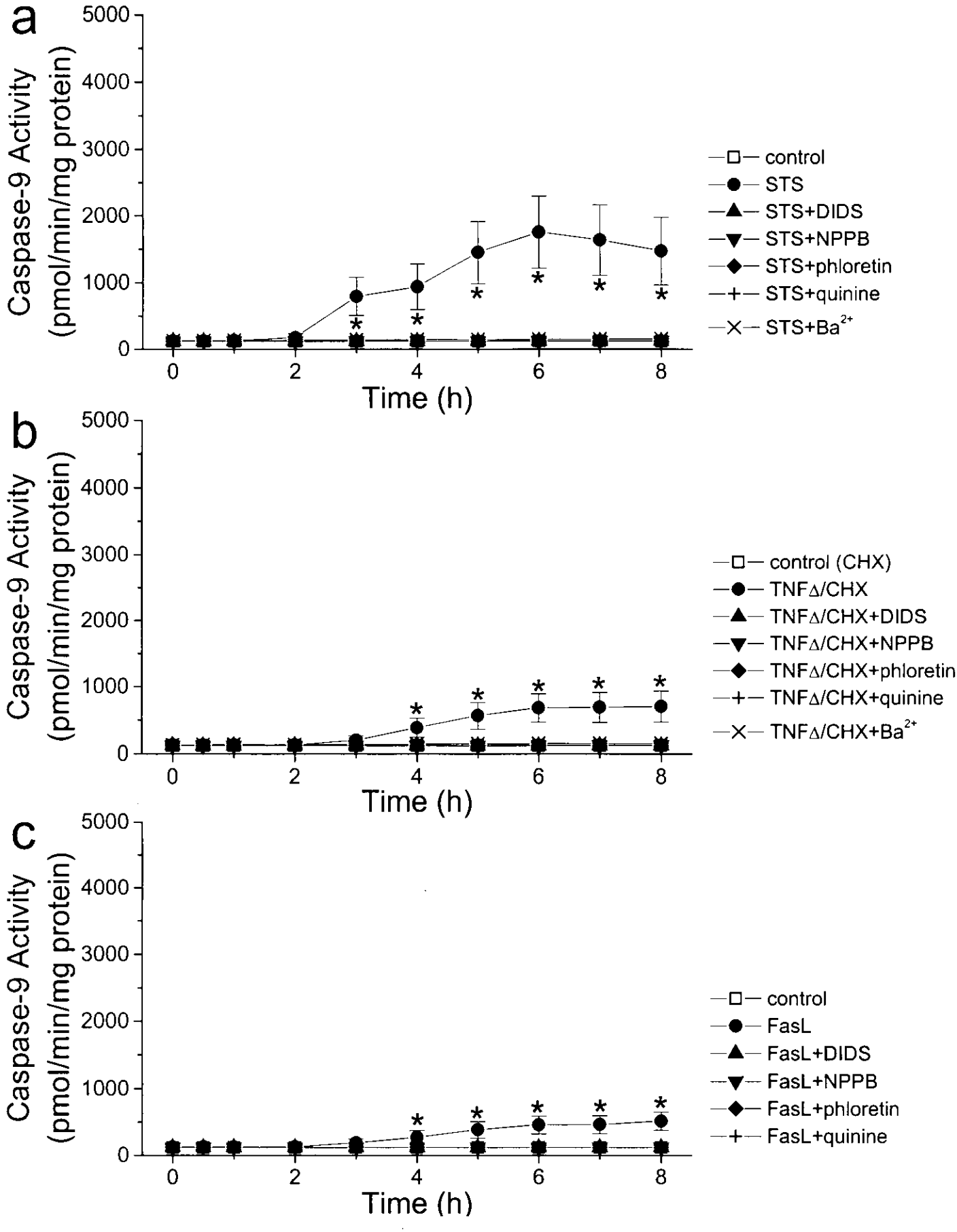
a
Caspase-9 Activity (pmol/min/mg protein)
5000
4000
3000
2000
1000
0
0
2
4
6
8
Time (h)
control
STS
STS+DIDS
STS+NPPB
STS+phloretin
STS+quinine
STS+Ba2+
b
Caspase-9 Activity (pmol/min/mg protein)
Time (h)
control (CHX)
TNFΔ/CHX
TNFΔ/CHX+DIDS
TNFΔ/CHX+NPPB
TNFΔ/CHX+phloretin
TNFΔ/CHX+quinine
TNFΔ/CHX+Ba2+
c
Caspase-9 Activity (pmol/min/mg protein)
Time (h)
control
FasL
FasL+DIDS
FasL+NPPB
FasL+phloretin
FasL+quinine

8C PC12

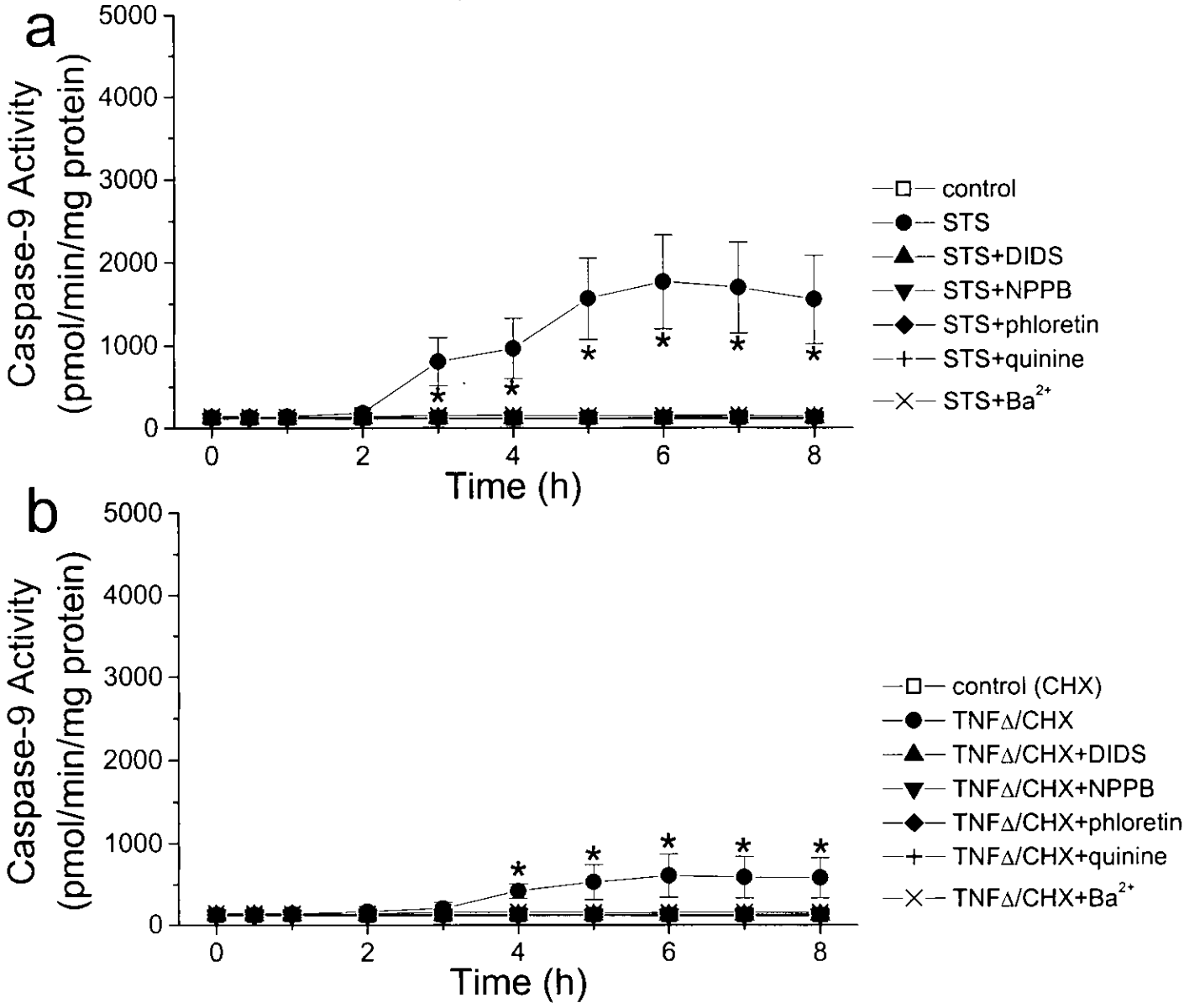
a
Caspase-9 Activity
(pmol/min/mg protein)
5000
4000
3000
2000
1000
0
0
2
4
6
8
Time (h)
control
STS
STS+DIDS
STS+NPPB
STS+phloretin
STS+quinine
STS+Ba2+
b
Caspase-9 Activity
(pmol/min/mg protein)
5000
4000
3000
2000
1000
0
0
2
4
6
8
Time (h)
control (CHX)
TNFΔ/CHX
TNFΔ/CHX+DIDS
TNFΔ/CHX+NPPB
TNFΔ/CHX+phloretin
TNFΔ/CHX+quinine
TNFΔ/CHX+Ba2+

8D NG108-15

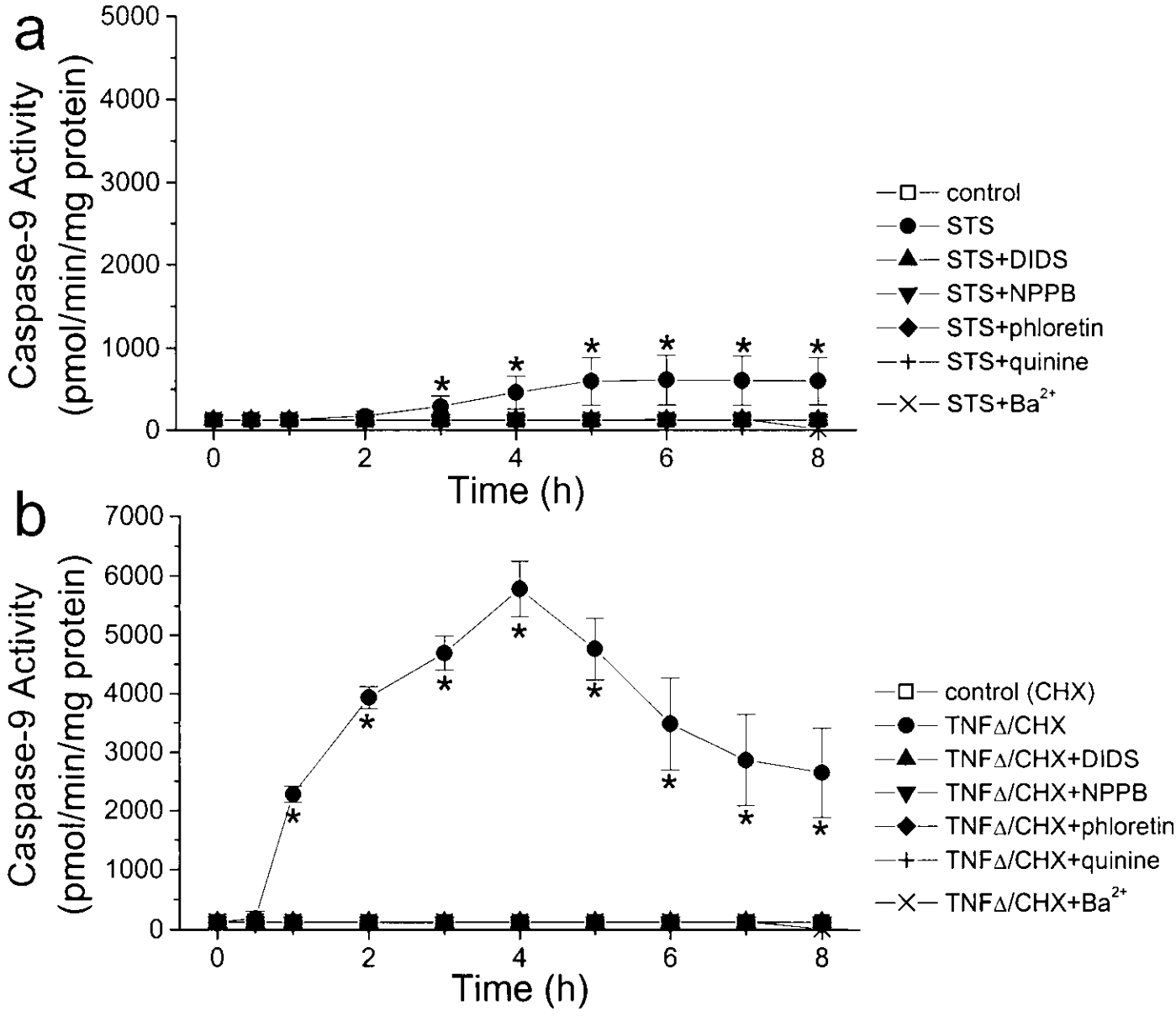
a
Caspase-9 Activity
(pmol/min/mg protein)
5000
4000
3000
2000
1000
0
0
2
4
6
8
Time (h)
control
STS
STS+DIDS
STS+NPPB
STS+phloretin
STS+quinine
STS+Ba2+
b
Caspase-9 Activity
(pmol/min/mg protein)
7000
6000
5000
4000
3000
2000
1000
0
0
2
4
6
8
Time (h)
control (CHX)
TNFΔ/CHX
TNFΔ/CHX+DIDS
TNFΔ/CHX+NPPB
TNFΔ/CHX+phloretin
TNFΔ/CHX+quinine
TNFΔ/CHX+Ba2+

9A U937

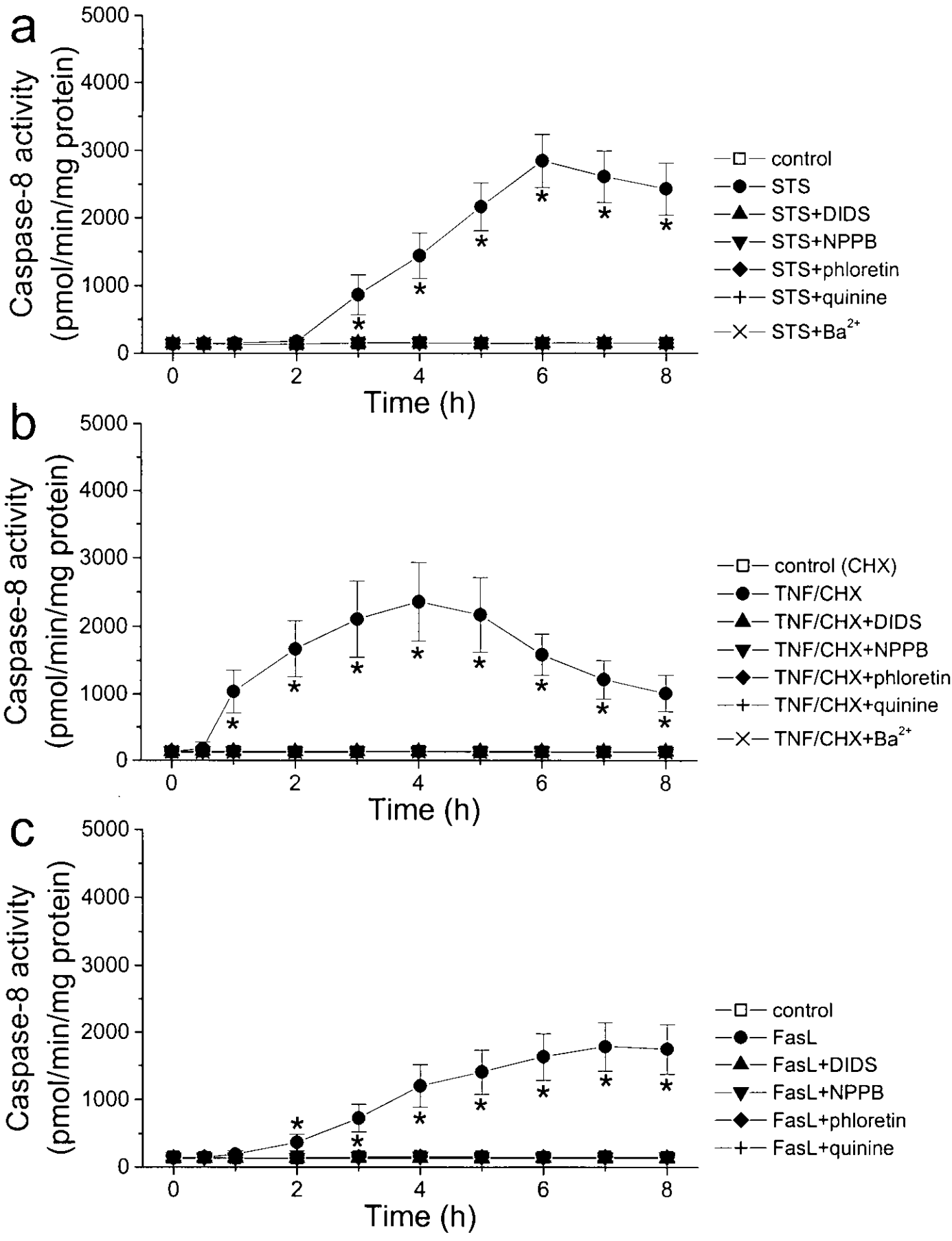
a
Caspase-8 activity (pmol/min/mg protein)
5000
4000
3000
2000
1000
0
0
2
4
6
8
Time (h)
control
STS
STS+DIDS
STS+NPPB
STS+phloretin
STS+quinine
STS+Ba2+
b
Caspase-8 activity (pmol/min/mg protein)
Time (h)
control (CHX)
TNF/CHX
TNF/CHX+DIDS
TNF/CHX+NPPB
TNF/CHX+phloretin
TNF/CHX+quinine
TNF/CHX+Ba2+
c
Caspase-8 activity (pmol/min/mg protein)
Time (h)
control
FasL
FasL+DIDS
FasL+NPPB
FasL+phloretin
FasL+quinine

9B HeLa

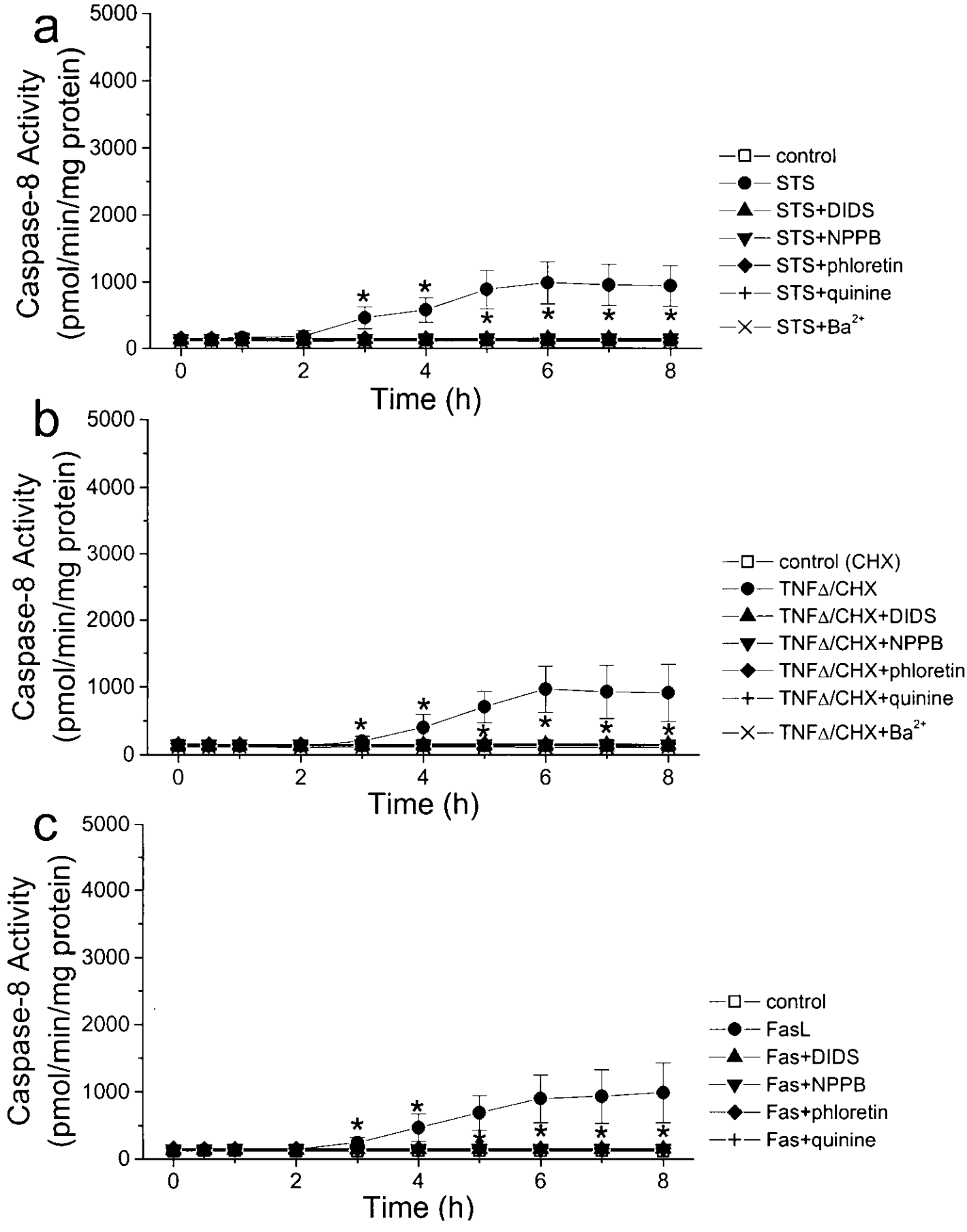
a
Caspase-8 Activity
(pmol/min/mg protein)
5000
4000
3000
2000
1000
0
0
2
4
6
8
Time (h)
control
STS
STS+DIDS
STS+NPPB
STS+phloretin
STS+quinine
STS+Ba2+
b
Caspase-8 Activity
(pmol/min/mg protein)
Time (h)
control (CHX)
TNFΔ/CHX
TNFΔ/CHX+DIDS
TNFΔ/CHX+NPPB
TNFΔ/CHX+phloretin
TNFΔ/CHX+quinine
TNFΔ/CHX+Ba2+
c
Caspase-8 Activity
(pmol/min/mg protein)
Time (h)
control
FasL
Fas+DIDS
Fas+NPPB
Fas+phloretin
Fas+quinine

9C PC12

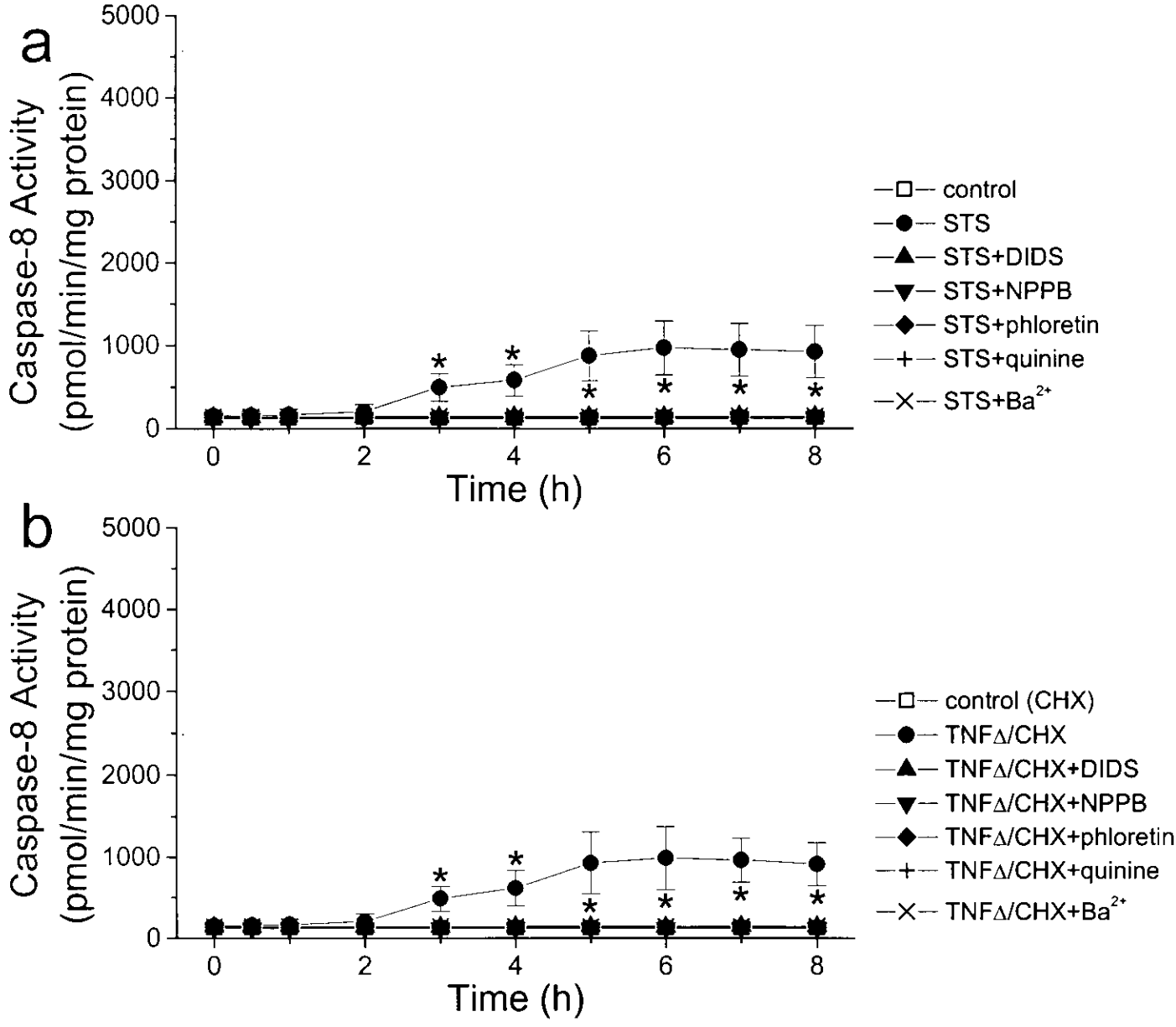
a
Caspase-8 Activity
(pmol/min/mg protein)
5000
4000
3000
2000
1000
0
0
2
4
6
8
Time (h)
control
STS
STS+DIDS
STS+NPPB
STS+phloretin
STS+quinine
STS+Ba2+
b
Caspase-8 Activity
(pmol/min/mg protein)
5000
4000
3000
2000
1000
0
0
2
4
6
8
Time (h)
control (CHX)
TNFΔ/CHX
TNFΔ/CHX+DIDS
TNFΔ/CHX+NPPB
TNFΔ/CHX+phloretin
TNFΔ/CHX+quinine
TNFΔ/CHX+Ba2+

9D NG108-15

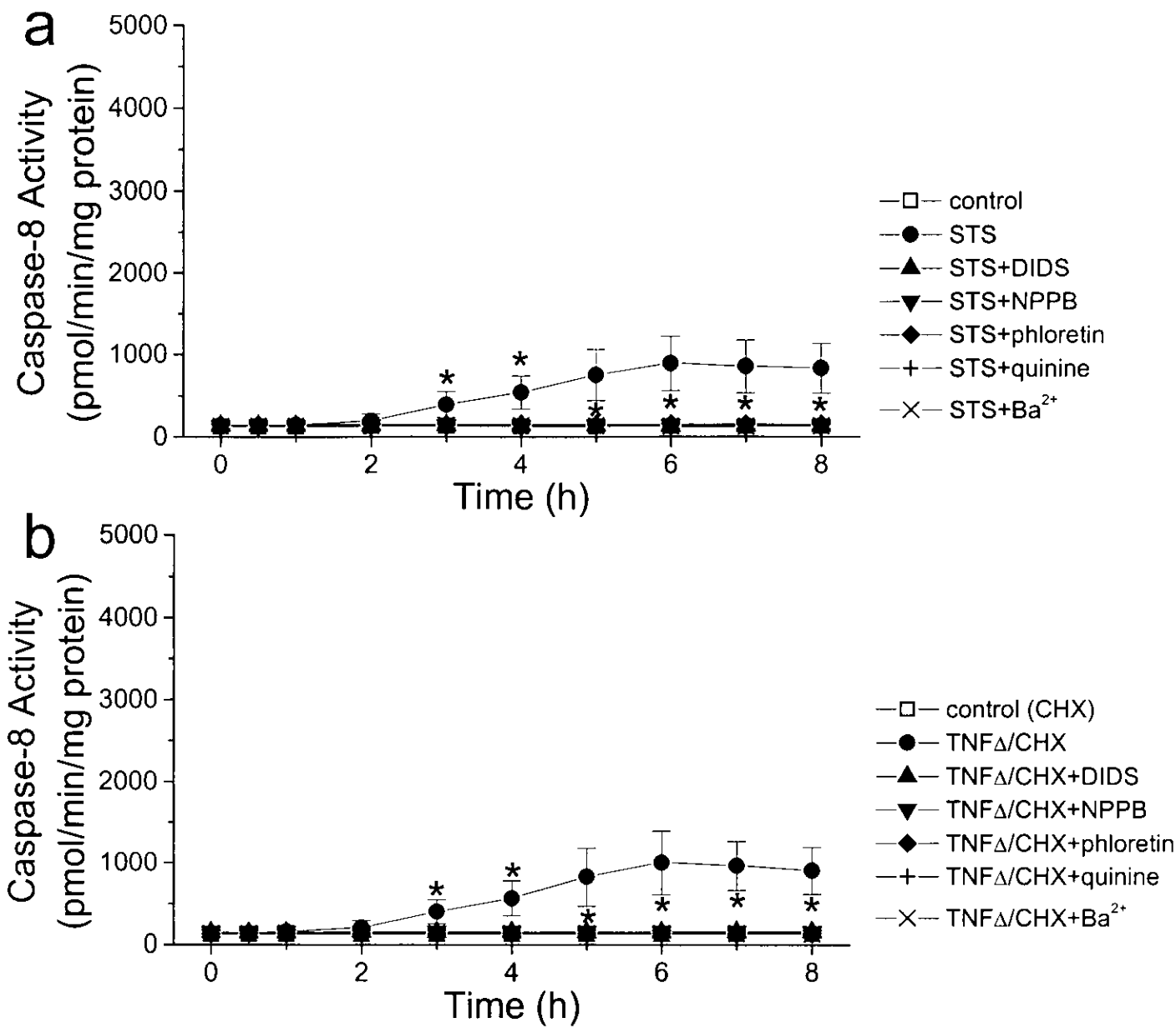
a
Caspase-8 Activity
(pmol/min/mg protein)
5000
4000
3000
2000
1000
0
0
2
4
6
8
Time (h)
control
STS
STS+DIDS
STS+NPPB
STS+phloretin
STS+quinine
STS+Ba2+
b
Caspase-8 Activity
(pmol/min/mg protein)
5000
4000
3000
2000
1000
0
0
2
4
6
8
Time (h)
control (CHX)
TNFΔ/CHX
TNFΔ/CHX+DIDS
TNFΔ/CHX+NPPB
TNFΔ/CHX+phloretin
TNFΔ/CHX+quinine
TNFΔ/CHX+Ba2+

10A U937

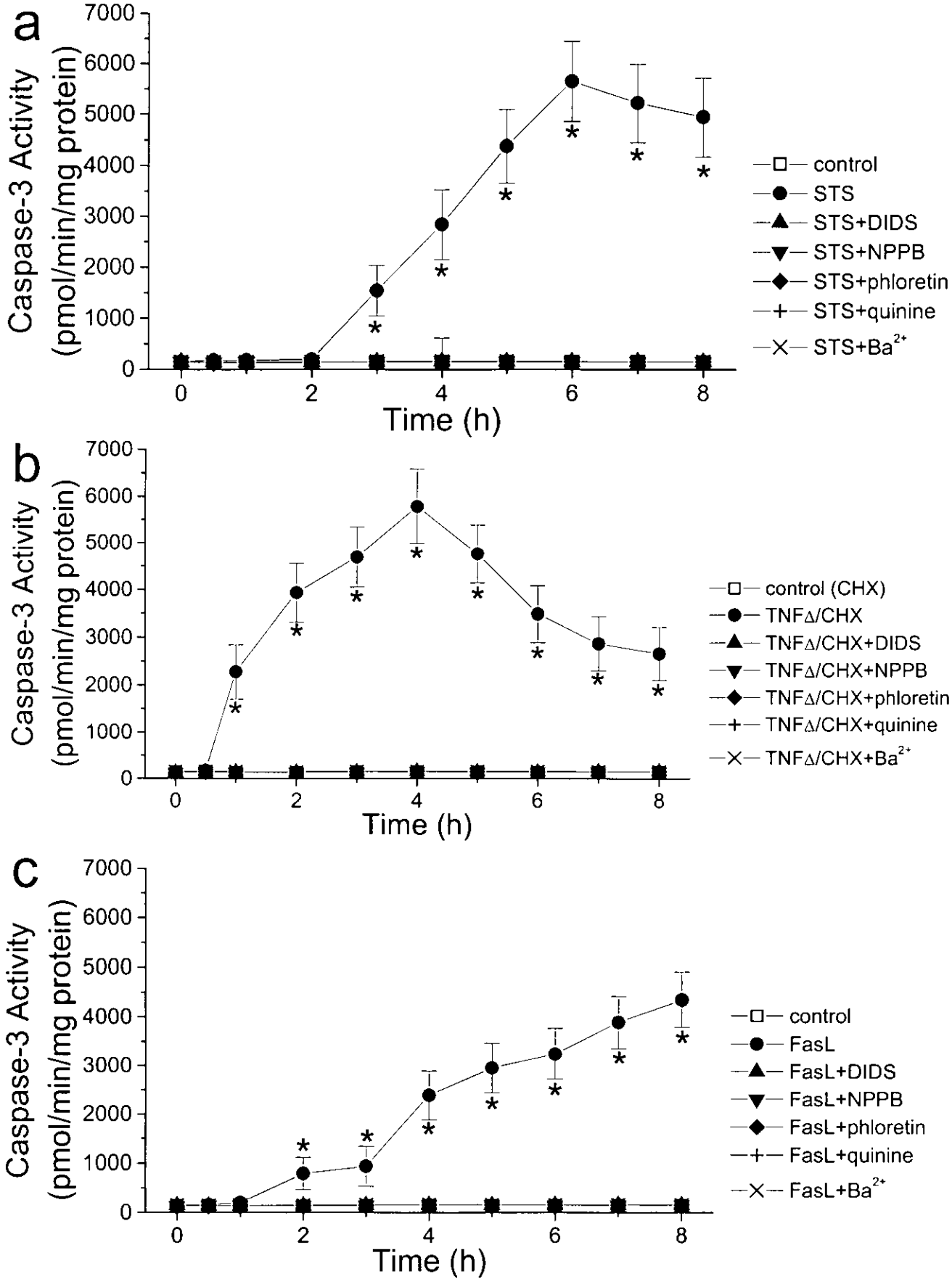
a
Caspase-3 Activity
(pmol/min/mg protein)
7000
6000
5000
4000
3000
2000
1000
0
0
2
4
6
8
Time (h)
control
STS
STS+DIDS
STS+NPPB
STS+phloretin
STS+quinine
STS+Ba2+
b
Caspase-3 Activity
(pmol/min/mg protein)
Time (h)
control (CHX)
TNFΔ/CHX
TNFΔ/CHX+DIDS
TNFΔ/CHX+NPPB
TNFΔ/CHX+phloretin
TNFΔ/CHX+quinine
TNFΔ/CHX+Ba2+
c
Caspase-3 Activity
(pmol/min/mg protein)
Time (h)
control
FasL
FasL+DIDS
FasL+NPPB
FasL+phloretin
FasL+quinine
FasL+Ba2+

10B HeLa

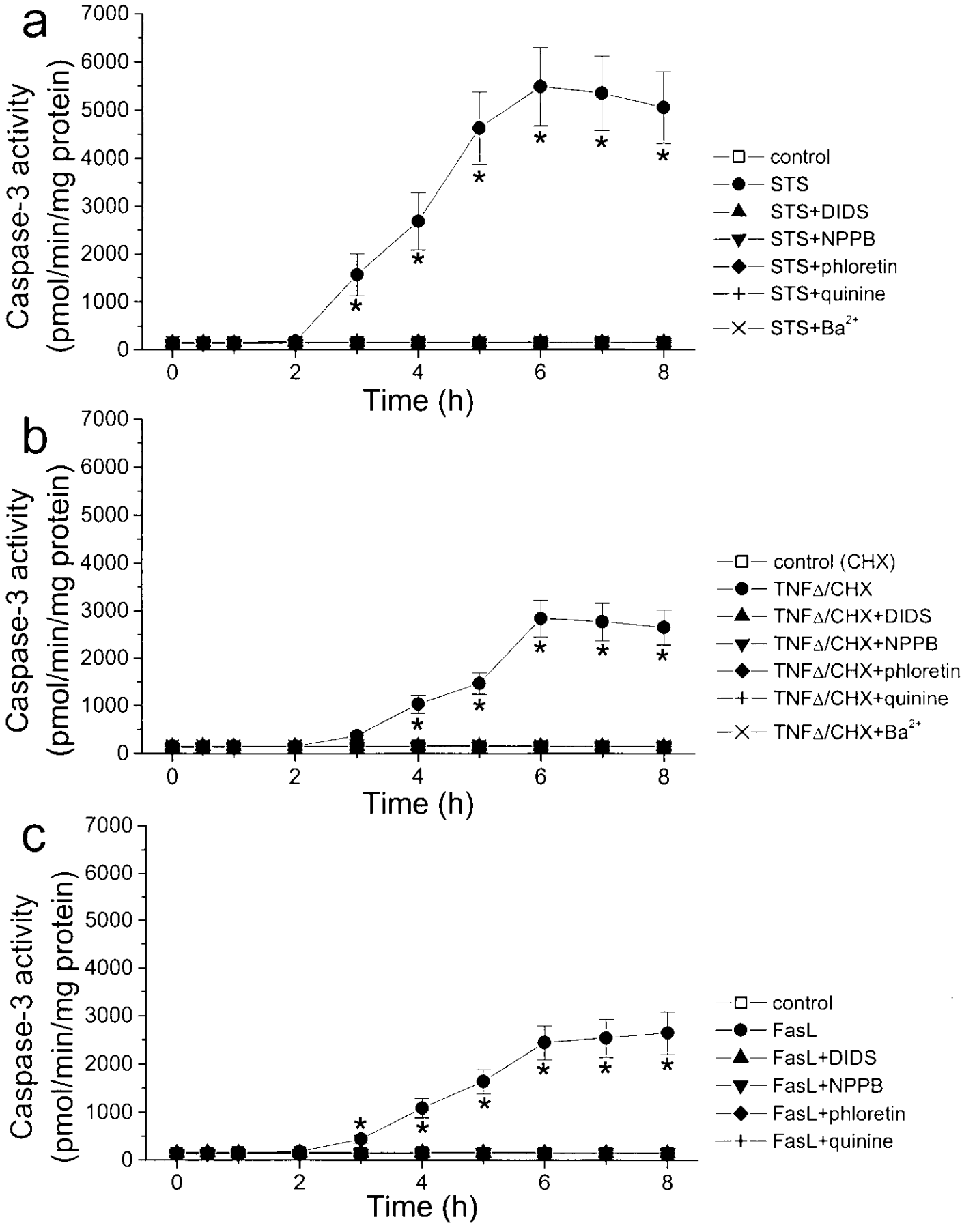
a
Caspase-3 activity
(pmol/min/mg protein)
7000
6000
5000
4000
3000
2000
1000
0
0
2
4
6
8
Time (h)
control
STS
STS+DIDS
STS+NPPB
STS+phloretin
STS+quinine
STS+Ba2+
b
Caspase-3 activity
(pmol/min/mg protein)
Time (h)
control (CHX)
TNFΔ/CHX
TNFΔ/CHX+DIDS
TNFΔ/CHX+NPPB
TNFΔ/CHX+phloretin
TNFΔ/CHX+quinine
TNFΔ/CHX+Ba2+
c
Caspase-3 activity
(pmol/min/mg protein)
Time (h)
control
FasL
FasL+DIDS
FasL+NPPB
FasL+phloretin
FasL+quinine

10C PC12

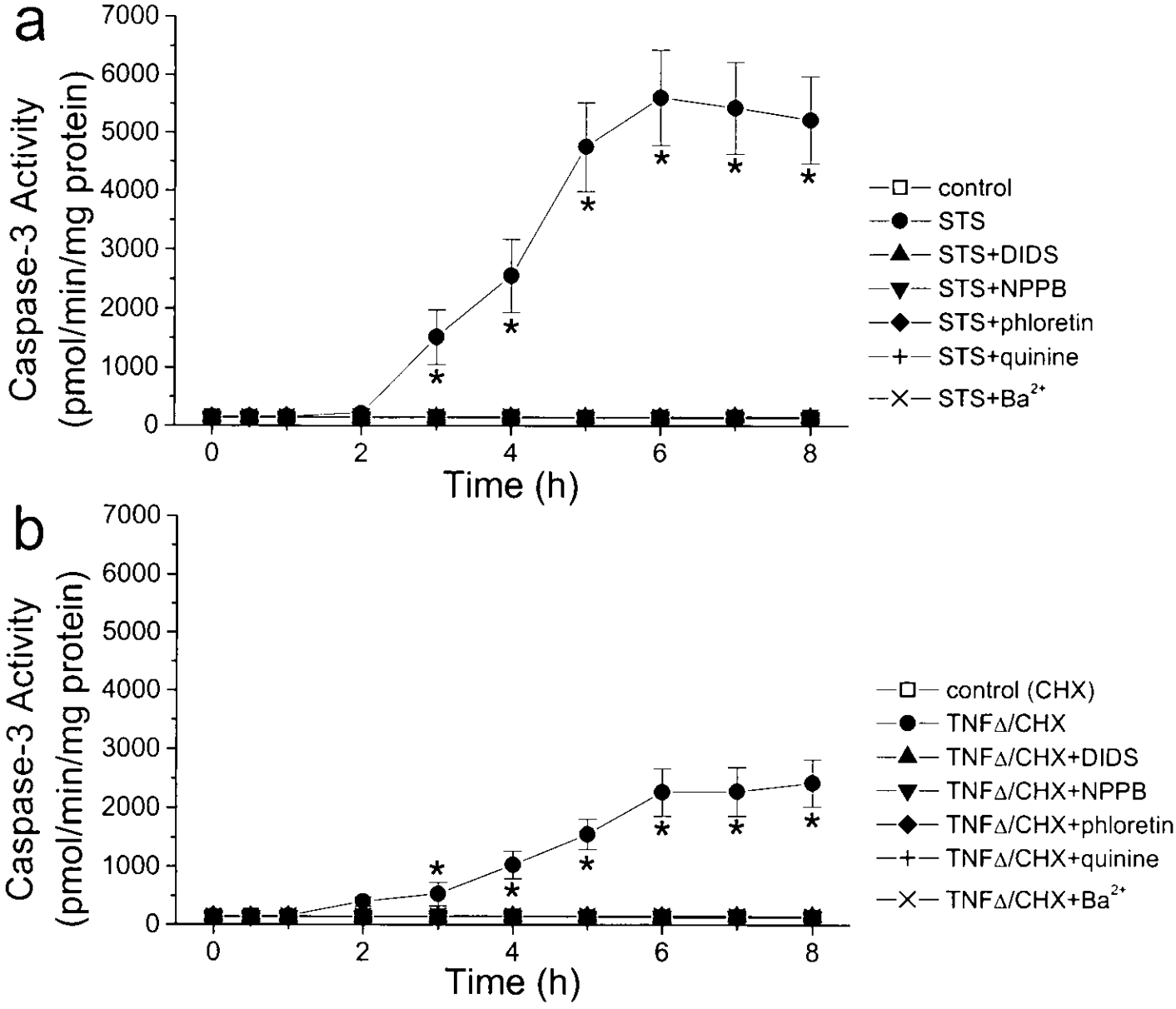
a
Caspase-3 Activity
(pmol/min/mg protein)
7000
6000
5000
4000
3000
2000
1000
0
0
2
4
6
8
Time (h)
control
STS
STS+DIDS
STS+NPPB
STS+phloretin
STS+quinine
STS+Ba2+
b
Caspase-3 Activity
(pmol/min/mg protein)
7000
6000
5000
4000
3000
2000
1000
0
0
2
4
6
8
Time (h)
control (CHX)
TNFΔ/CHX
TNFΔ/CHX+DIDS
TNFΔ/CHX+NPPB
TNFΔ/CHX+phloretin
TNFΔ/CHX+quinine
TNFΔ/CHX+Ba2+

10D NG108-15

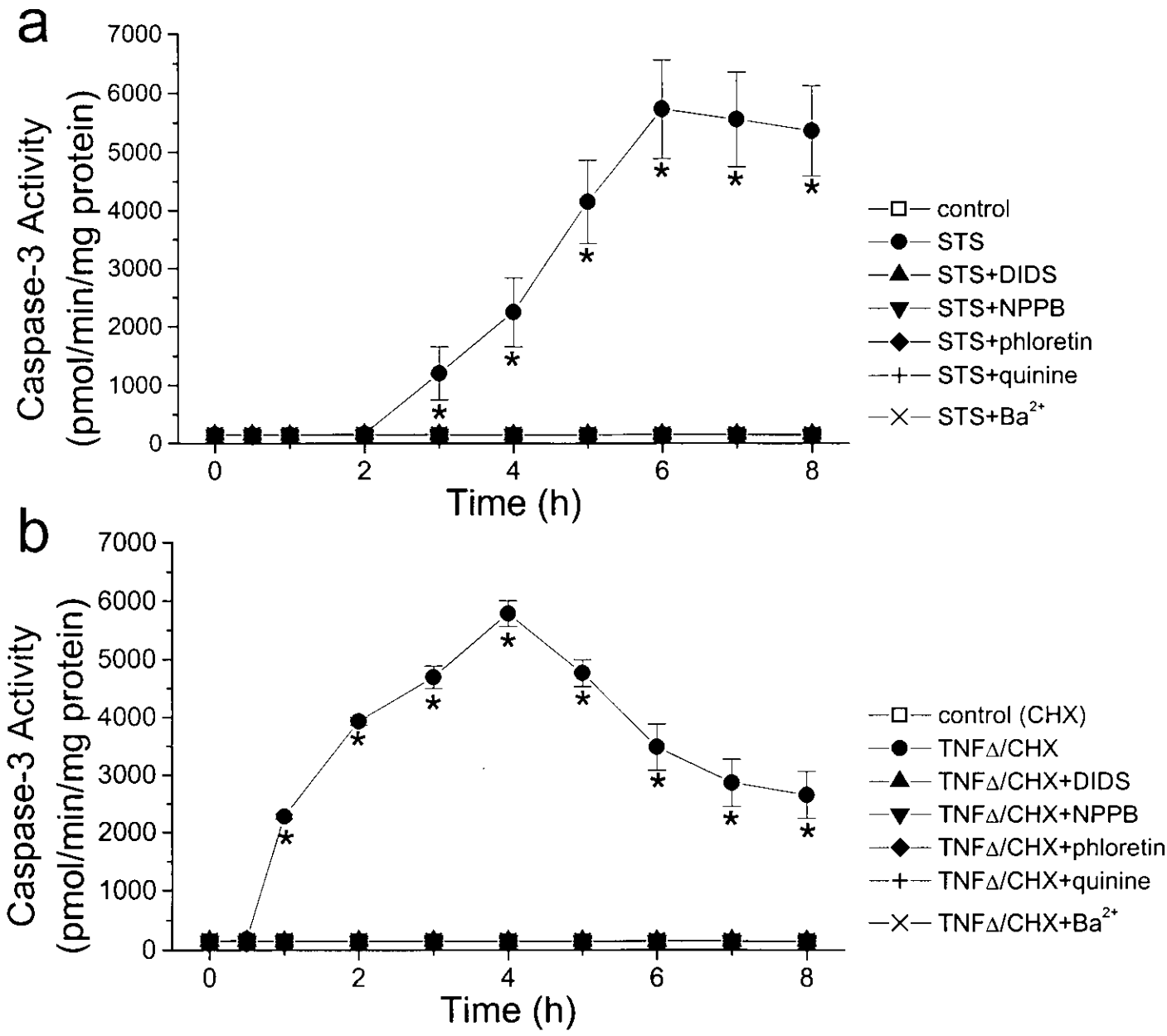
a
Caspase-3 Activity
(pmol/min/mg protein)
7000
6000
5000
4000
3000
2000
1000
0
0
2
4
6
8
Time (h)
control
STS
STS+DIDS
STS+NPPB
STS+phloretin
STS+quinine
STS+Ba2+
b
Caspase-3 Activity
(pmol/min/mg protein)
7000
6000
5000
4000
3000
2000
1000
0
0
2
4
6
8
Time (h)
control (CHX)
TNFΔ/CHX
TNFΔ/CHX+DIDS
TNFΔ/CHX+NPPB
TNFΔ/CHX+phloretin
TNFΔ/CHX+quinine
TNFΔ/CHX+Ba2+

11 U937/STS

A

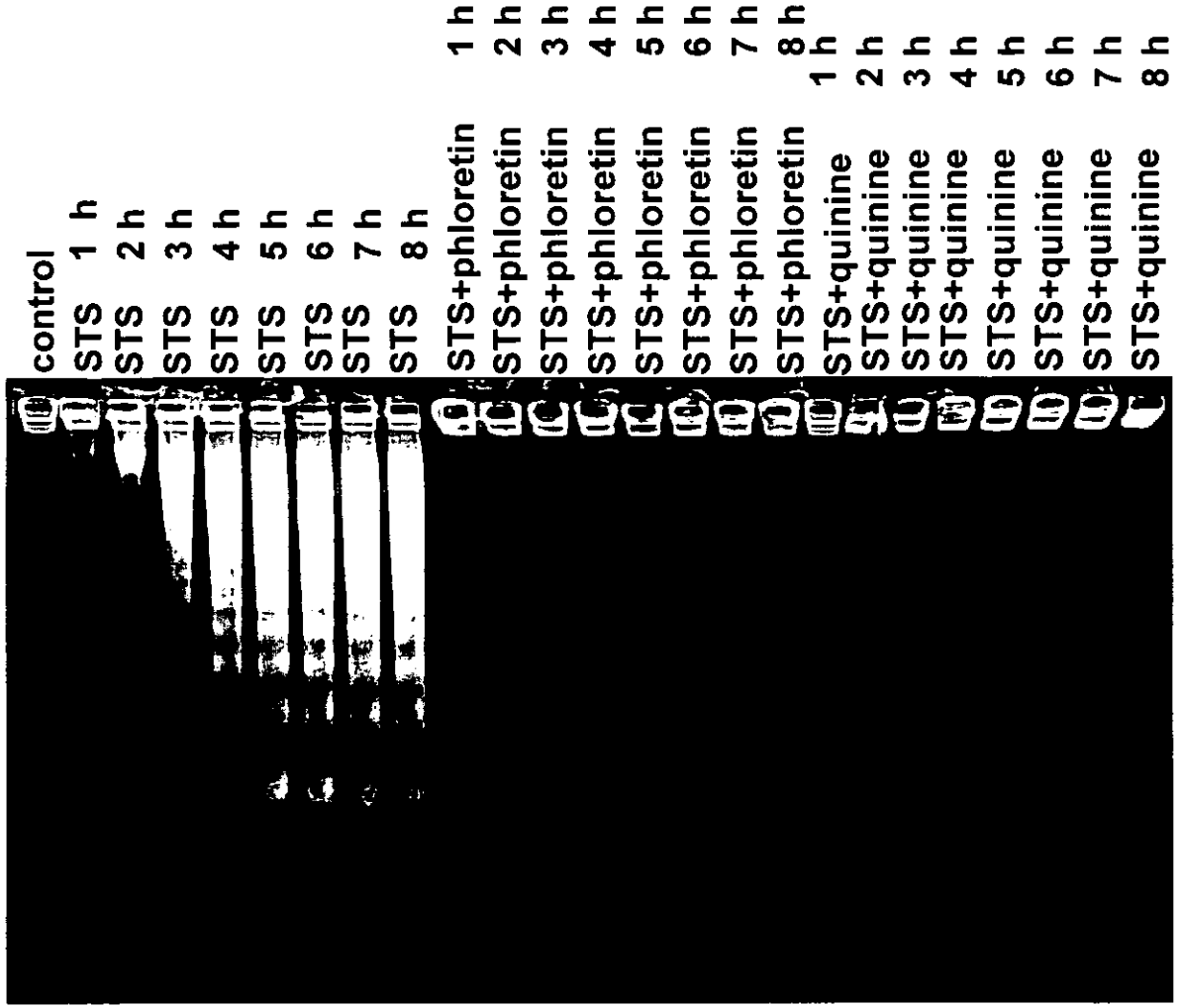
control
STS 1 h
STS 2 h
STS 3 h
STS 4 h
STS 5 h
STS 6 h
STS 7 h
STS 8 h
STS+phloretin 1 h
STS+phloretin 2 h
STS+phloretin 3 h
STS+phloretin 4 h
STS+phloretin 5 h
STS+phloretin 6 h
STS+phloretin 7 h
STS+phloretin 8 h
STS+quinine 1 h
STS+quinine 2 h
STS+quinine 3 h
STS+quinine 4 h
STS+quinine 5 h
STS+quinine 6 h
STS+quinine 7 h
STS+quinine 8 h

11 U937/TNF α

B

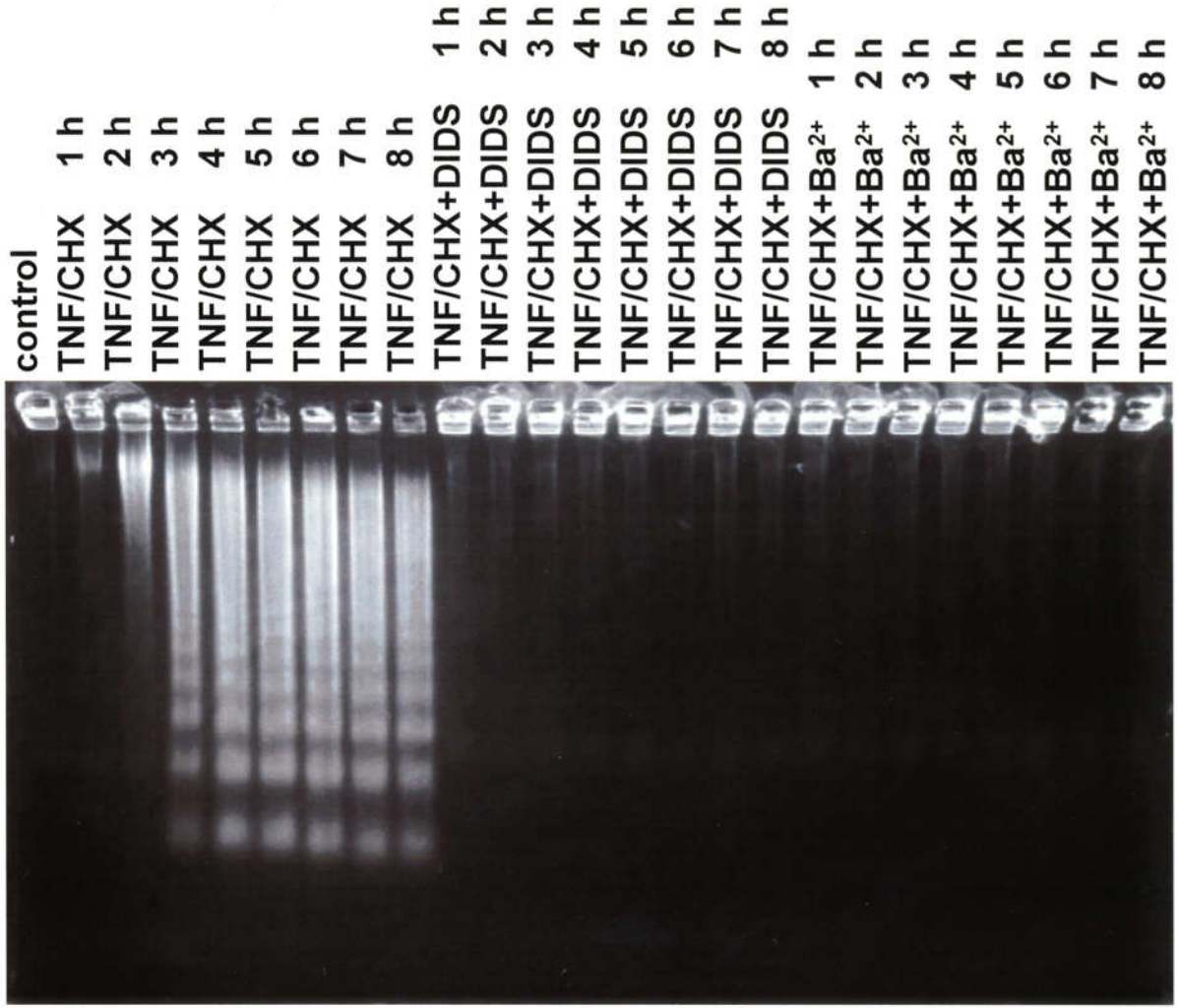

11

C

U937/FasL

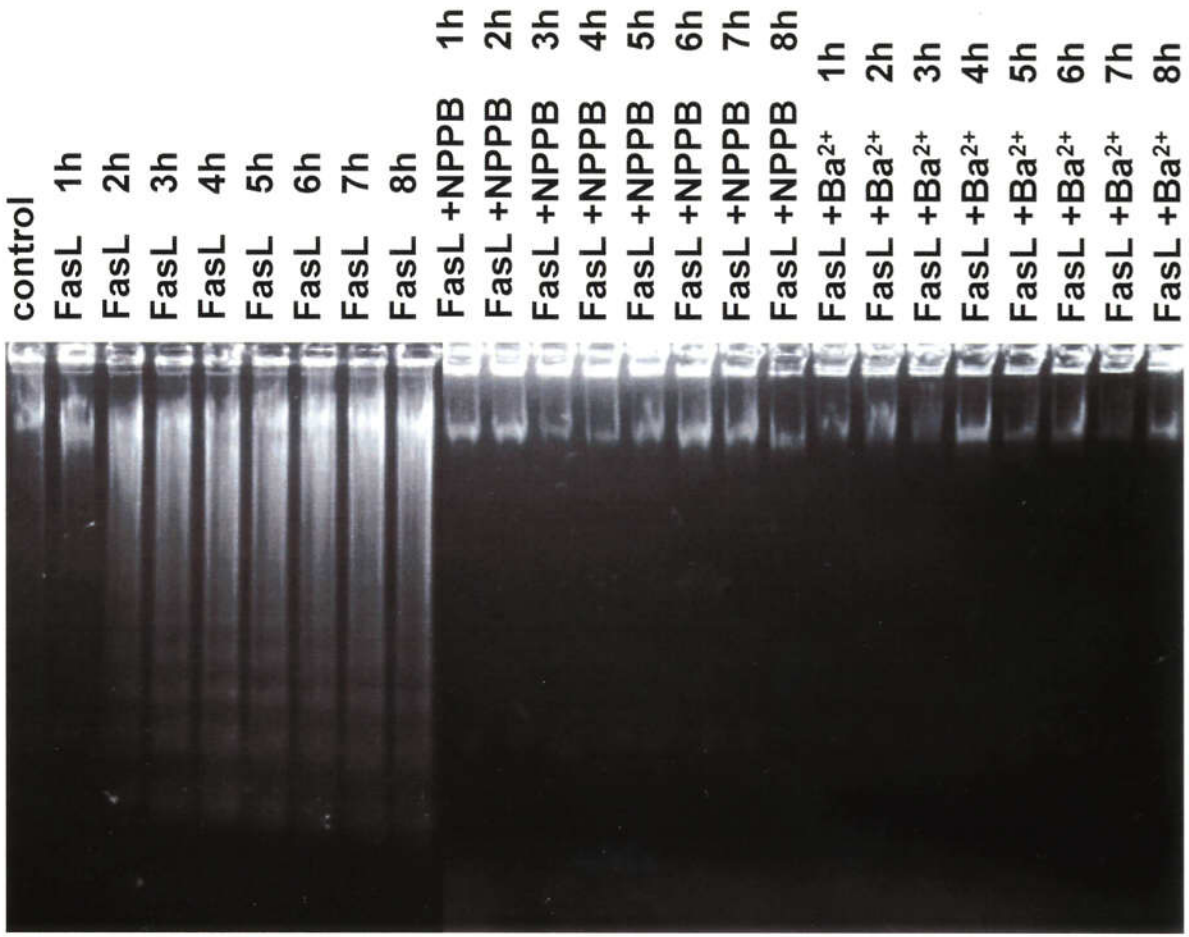

12

A U937

B HeLa

a

Control

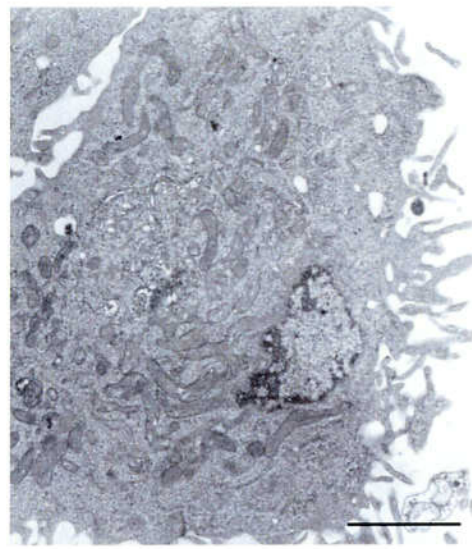

Control

b

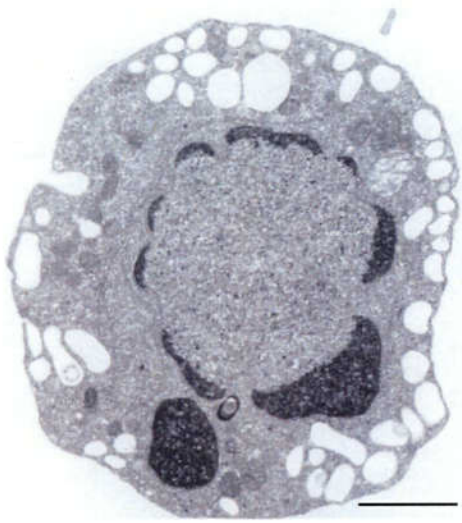

STS (4 h)

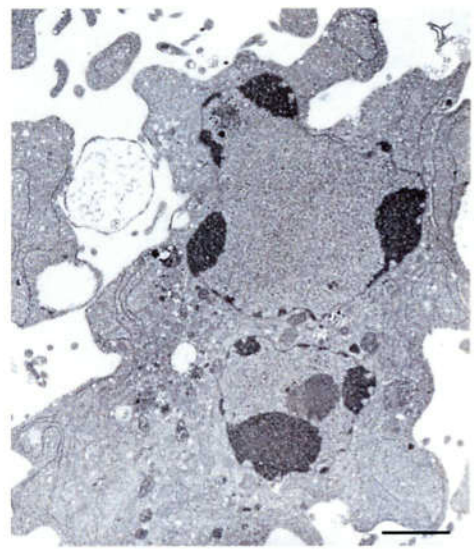

STS (4 h)

c

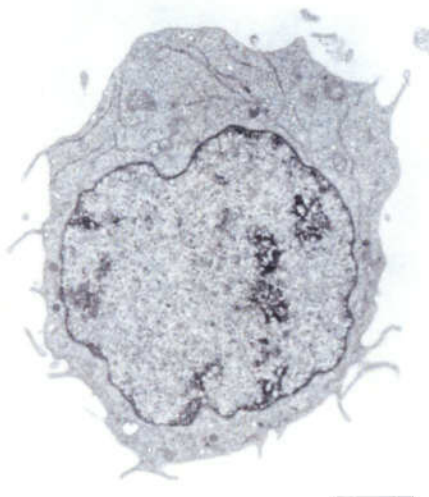

STS+DIDS (4 h)

STS+NPPB (4 h)

13A U937

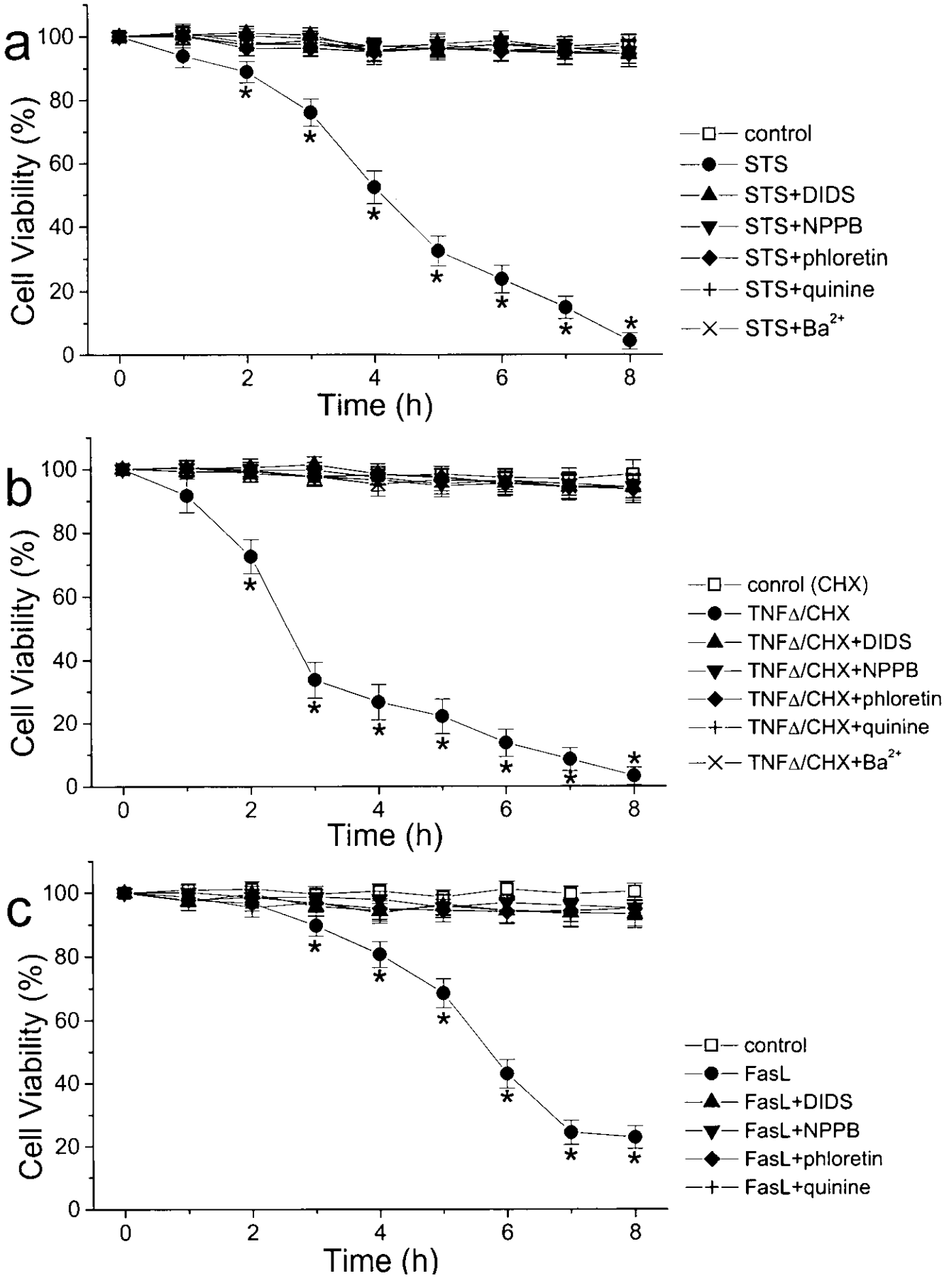
a
Cell Viability (%)
Time (h)
control
STS
STS+DIDS
STS+NPPB
STS+phloretin
STS+quinine
STS+Ba2+
b
Cell Viability (%)
Time (h)
conrol (CHX)
TNFΔ/CHX
TNFΔ/CHX+DIDS
TNFΔ/CHX+NPPB
TNFΔ/CHX+phloretin
TNFΔ/CHX+quinine
TNFΔ/CHX+Ba2+
c
Cell Viability (%)
Time (h)
control
FasL
FasL+DIDS
FasL+NPPB
FasL+phloretin
FasL+quinine

13B HeLa

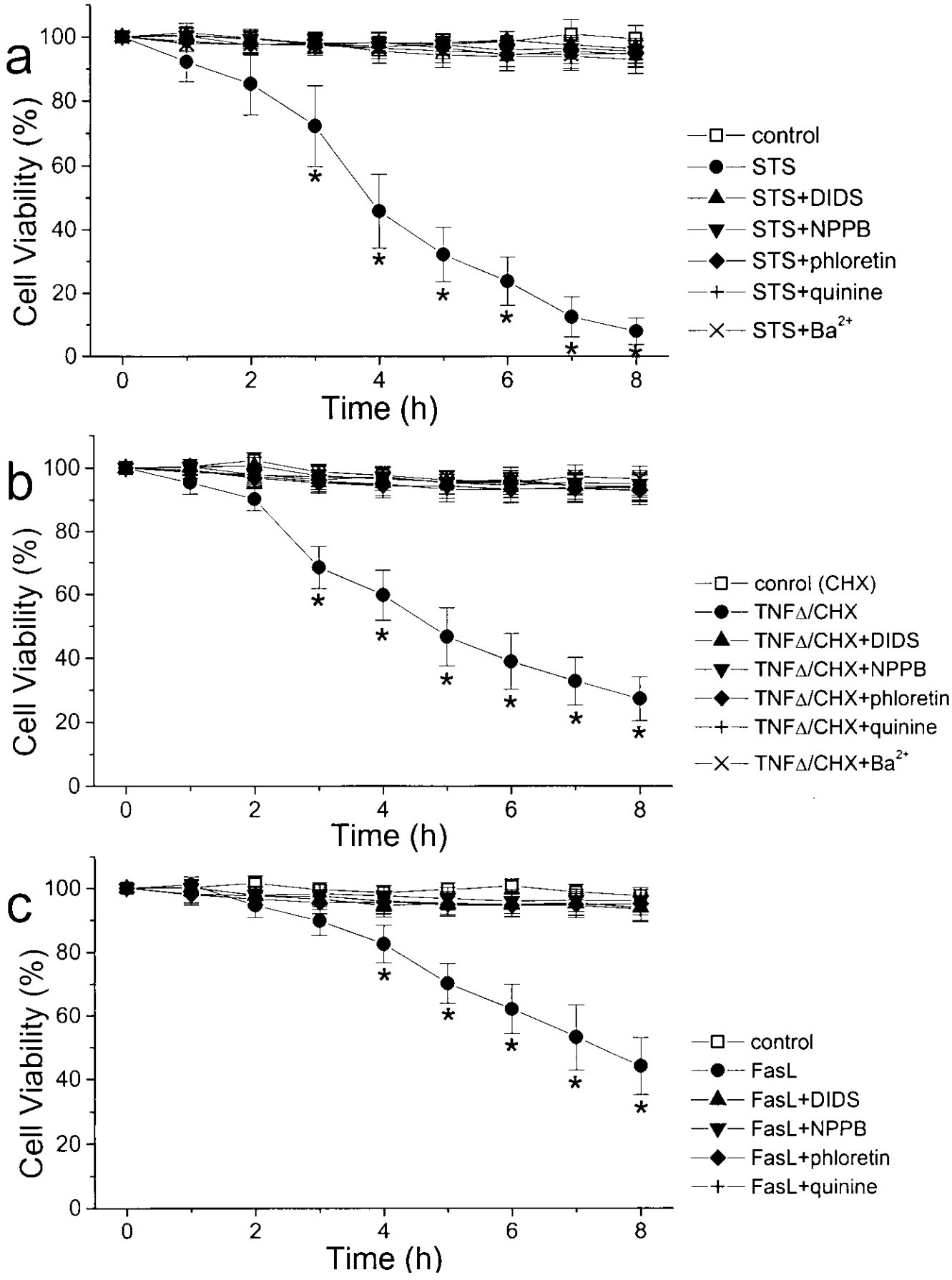
a
Cell Viability (%)
Time (h)
control
STS
STS+DIDS
STS+NPPB
STS+phloretin
STS+quinine
STS+Ba2+
b
Cell Viability (%)
Time (h)
conrol (CHX)
TNFΔ/CHX
TNFΔ/CHX+DIDS
TNFΔ/CHX+NPPB
TNFΔ/CHX+phloretin
TNFΔ/CHX+quinine
TNFΔ/CHX+Ba2+
c
Cell Viability (%)
Time (h)
control
FasL
FasL+DIDS
FasL+NPPB
FasL+phloretin
FasL+quinine

13C PC12

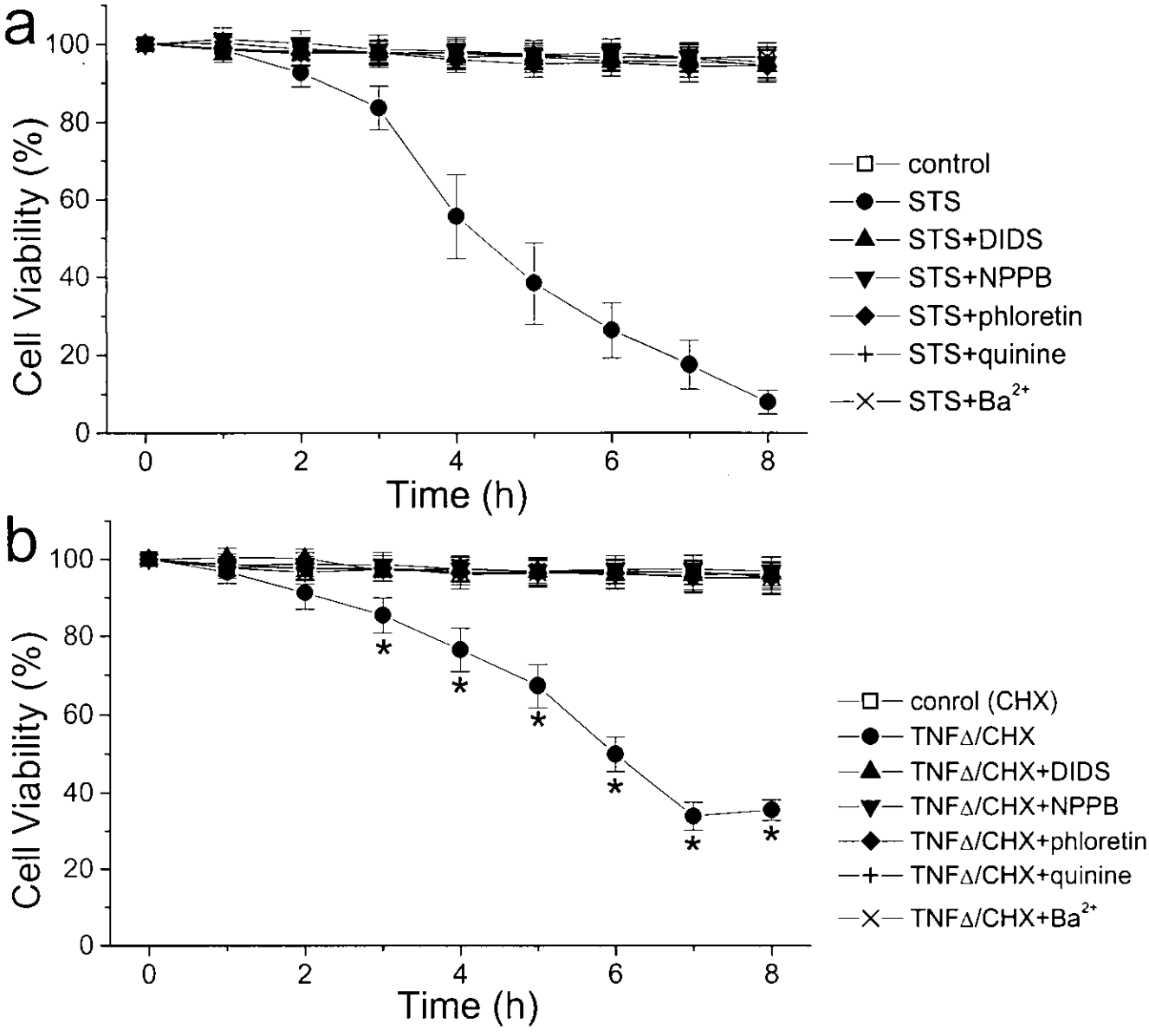
a
Cell Viability (%)
Time (h)
control
STS
STS+DIDS
STS+NPPB
STS+phloretin
STS+quinine
STS+Ba2+
b
Cell Viability (%)
Time (h)
conrol (CHX)
TNFΔ/CHX
TNFΔ/CHX+DIDS
TNFΔ/CHX+NPPB
TNFΔ/CHX+phloretin
TNFΔ/CHX+quinine
TNFΔ/CHX+Ba2+

13D NG108-15

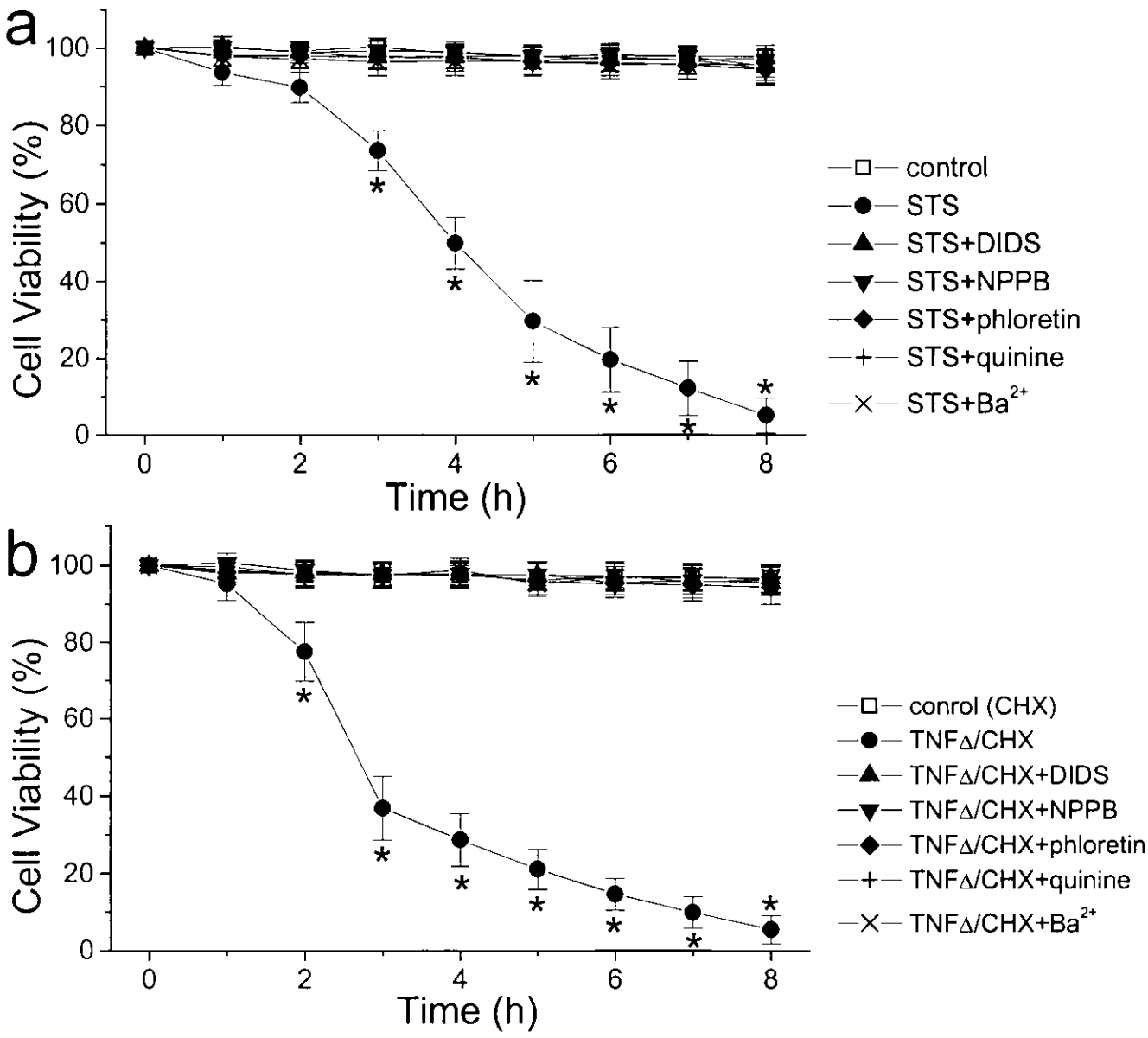
a
Cell Viability (%)
Time (h)
control
STS
STS+DIDS
STS+NPPB
STS+phloretin
STS+quinine
STS+Ba2+
b
Cell Viability (%)
Time (h)
conrol (CHX)
TNFΔ/CHX
TNFΔ/CHX+DIDS
TNFΔ/CHX+NPPB
TNFΔ/CHX+phloretin
TNFΔ/CHX+quinine
TNFΔ/CHX+Ba2+

14 SKW6.4

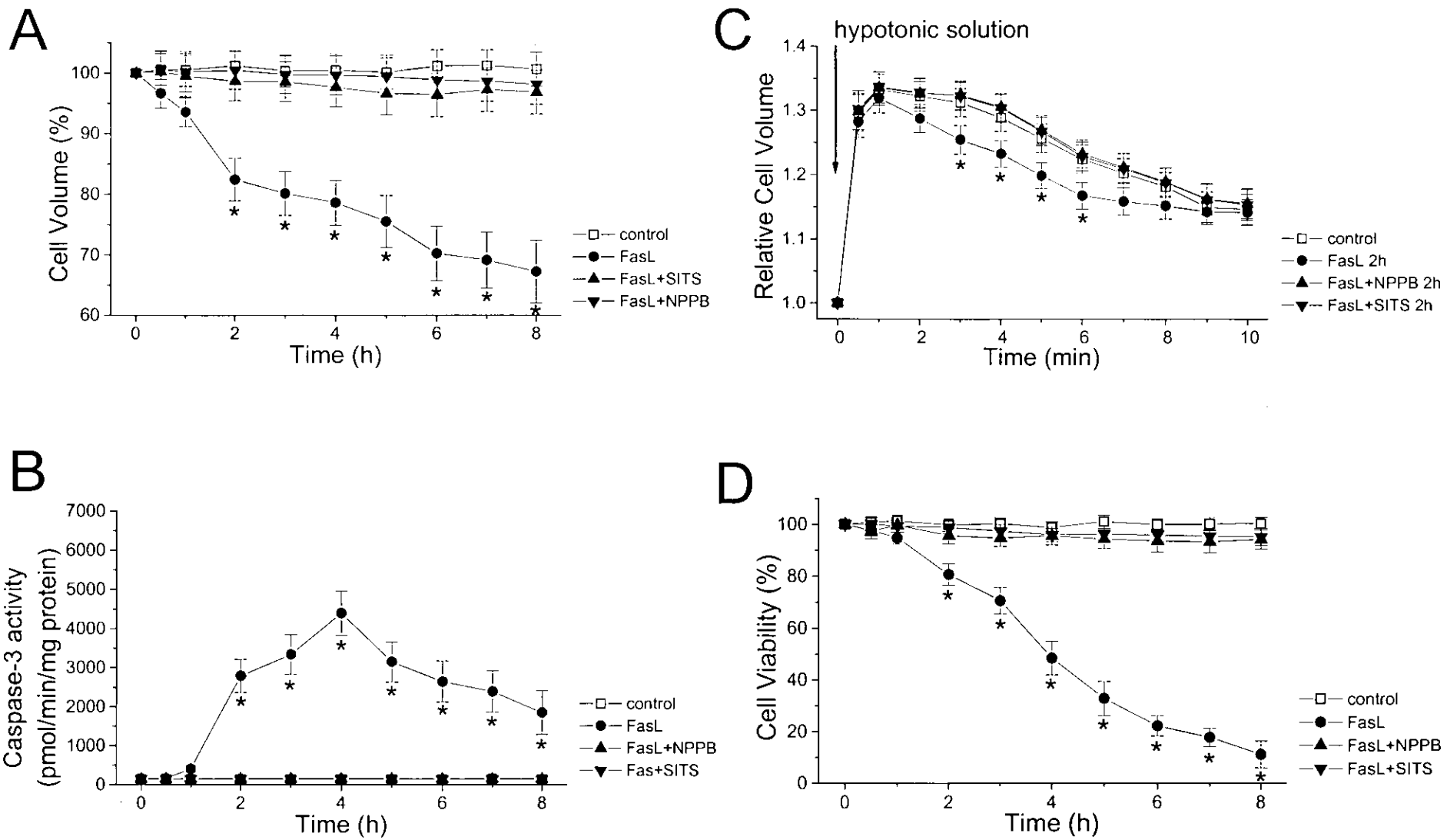
A
Cell Volume (%)
Time (h)
control
FasL
FasL+SITS
FasL+NPPB
C
hypotonic solution
Relative Cell Volume
Time (min)
control
FasL 2h
FasL+NPPB 2h
FasL+SITS 2h
B
Caspase-3 activity
(pmol/min/mg protein)
Time (h)
control
FasL
FasL+NPPB
Fas+SITS
D
Cell Viability (%)
Time (h)
control
FasL
FasL+NPPB
FasL+SITS

15

A WEHI

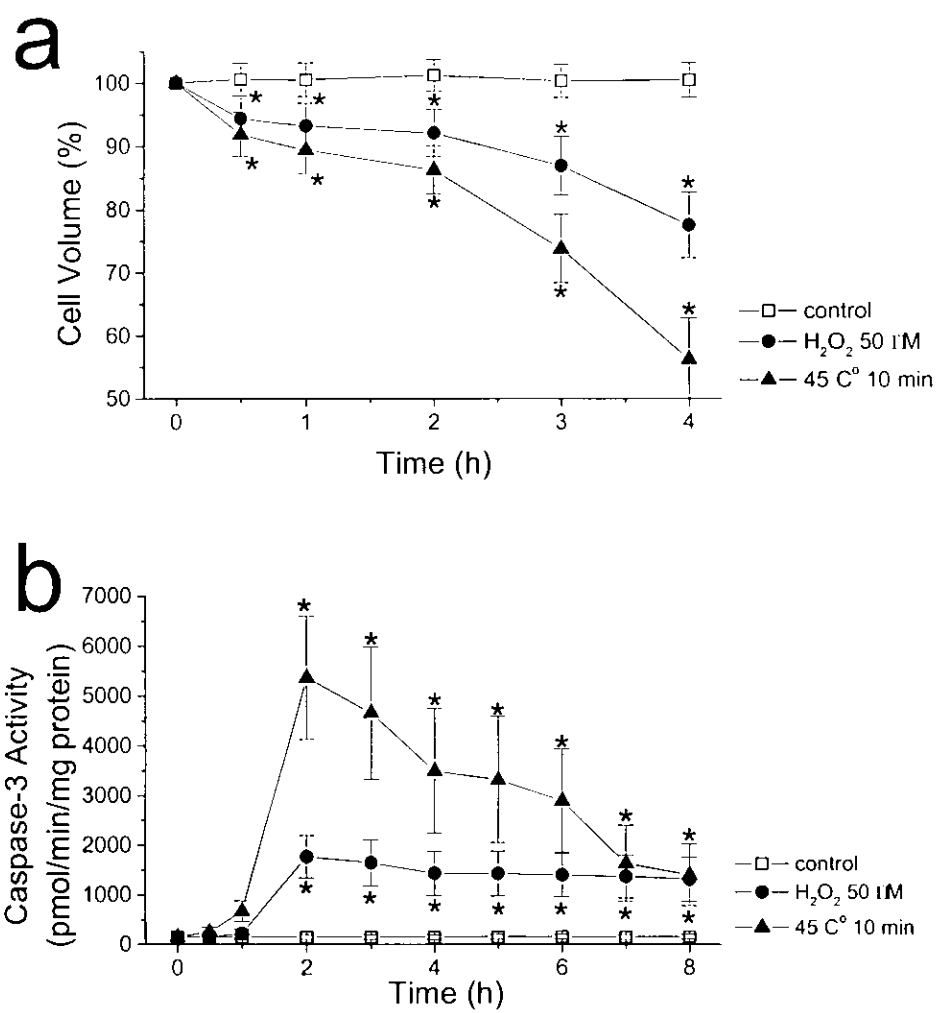

B WEHI/Bcl-2

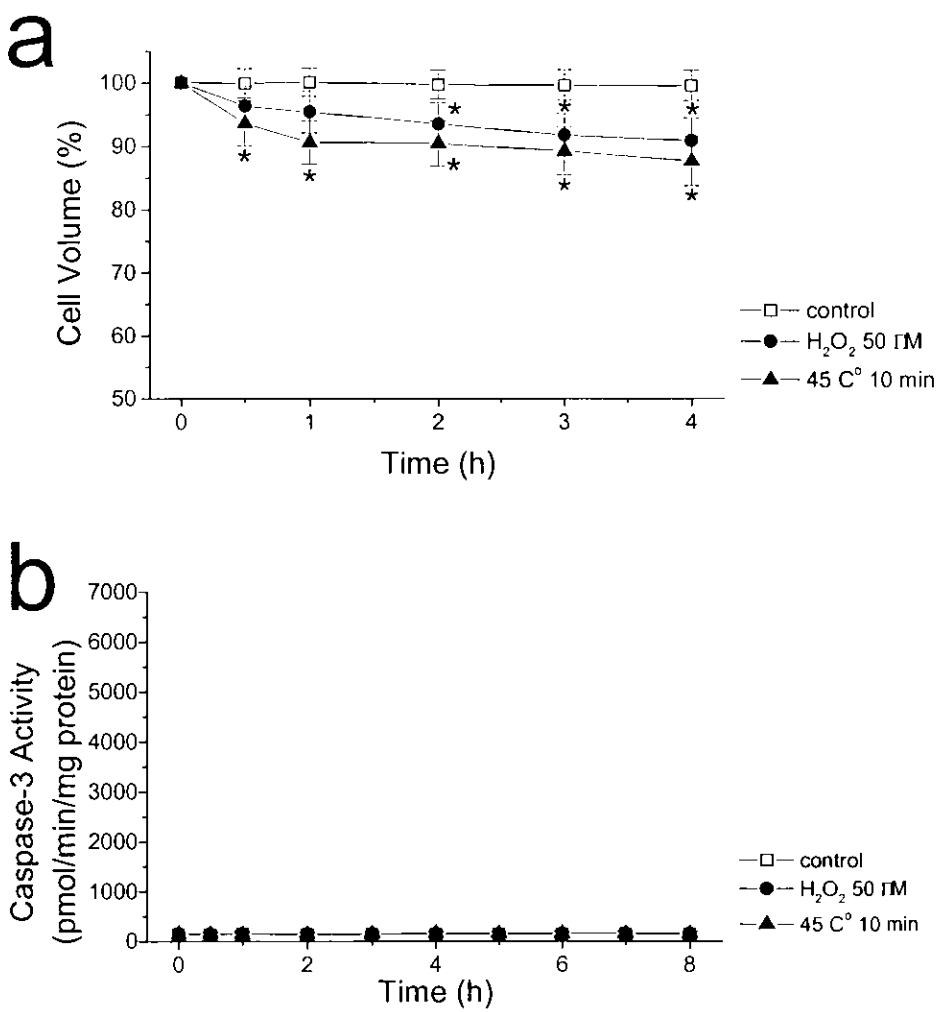

16A U937/STS

a

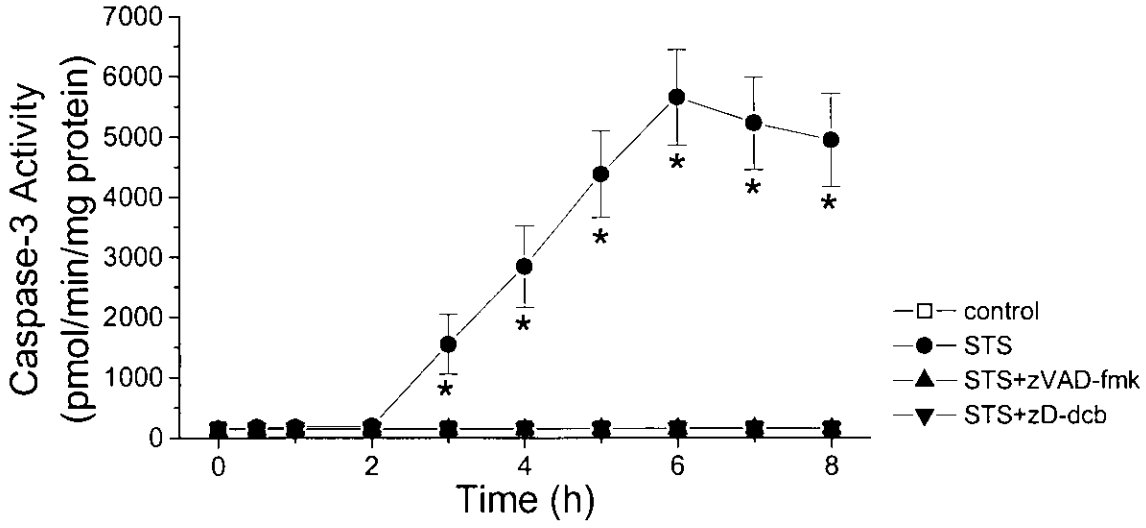

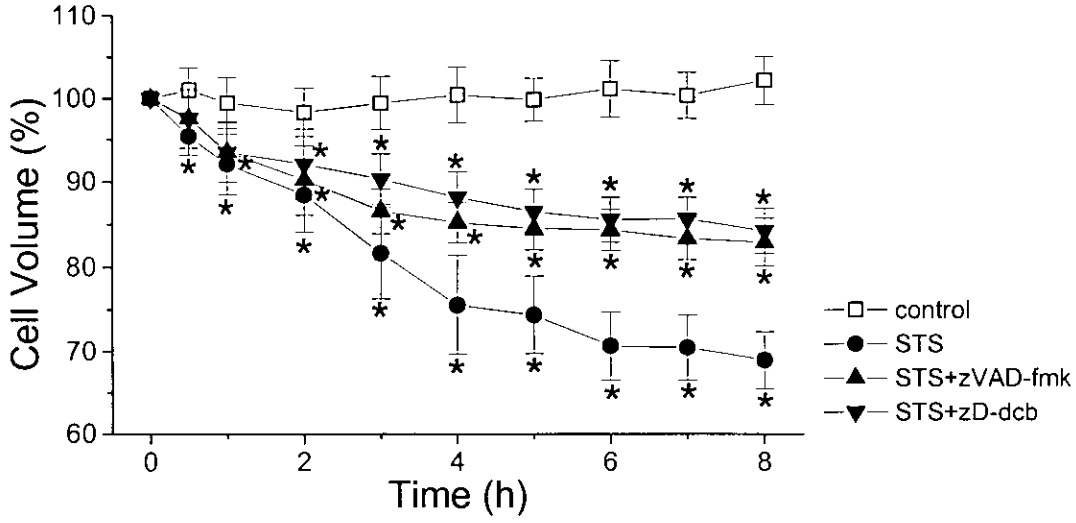

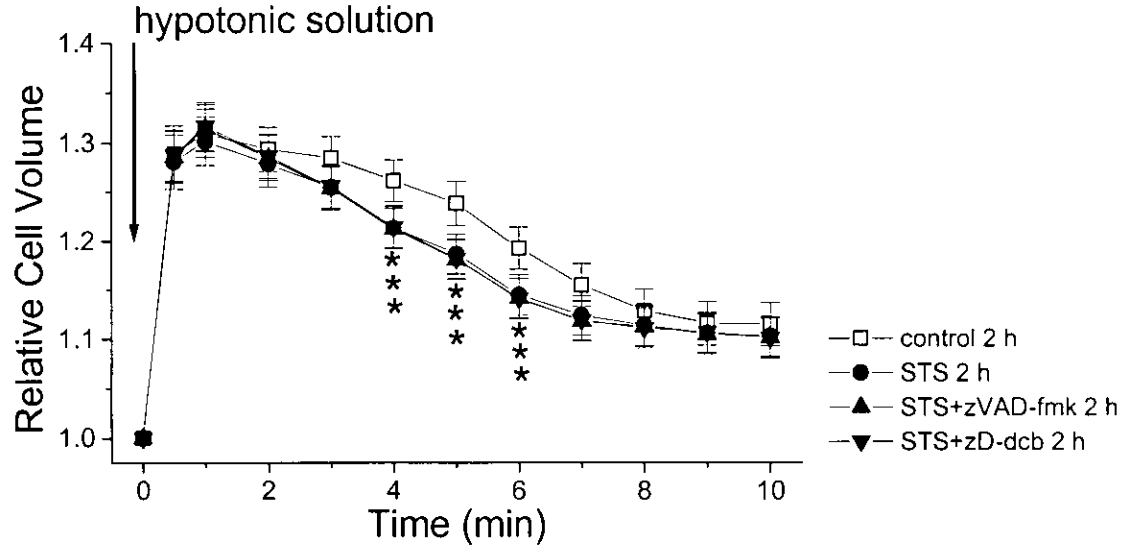

16A U937/TNF α

b

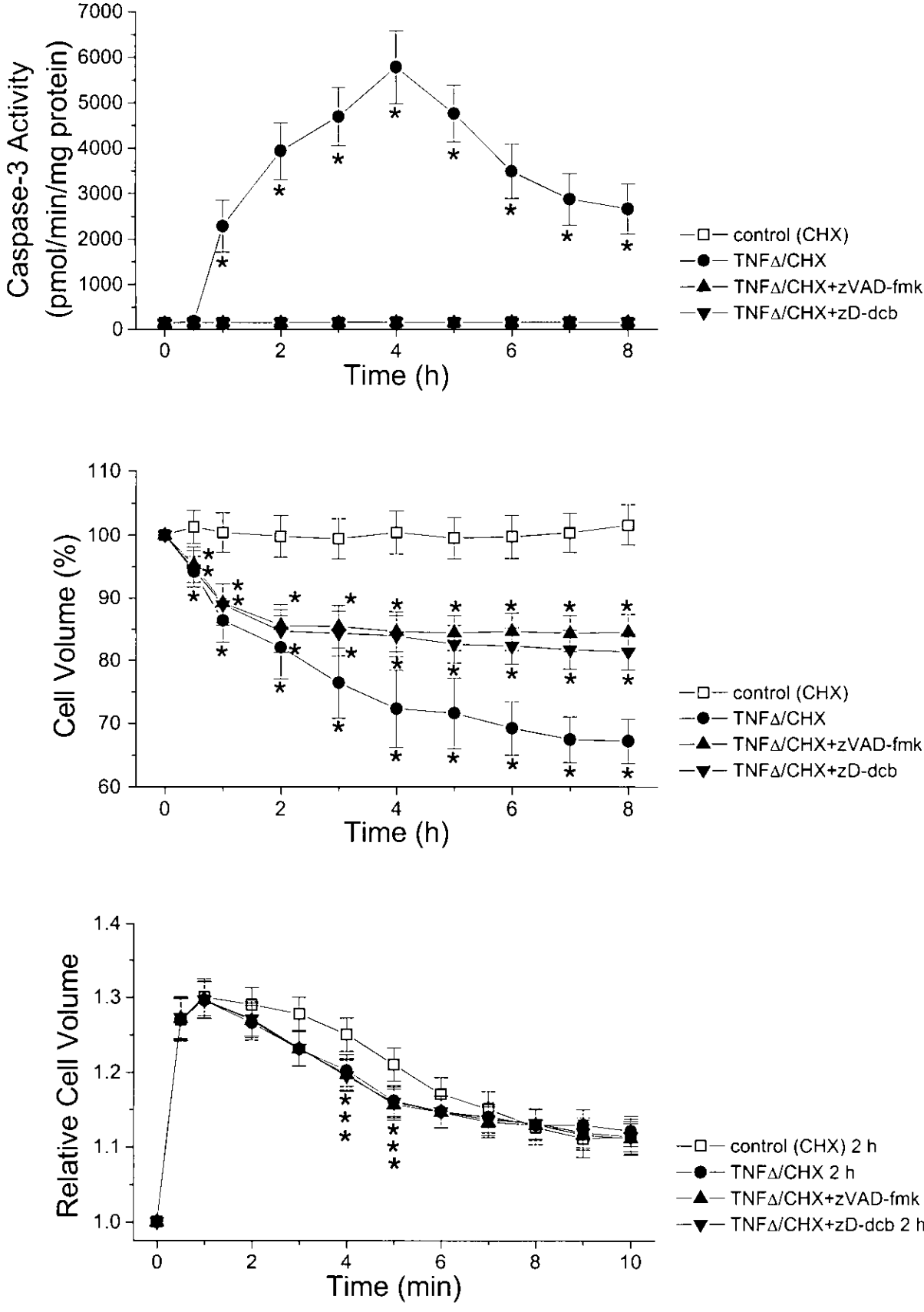

16A U937/FasL

c

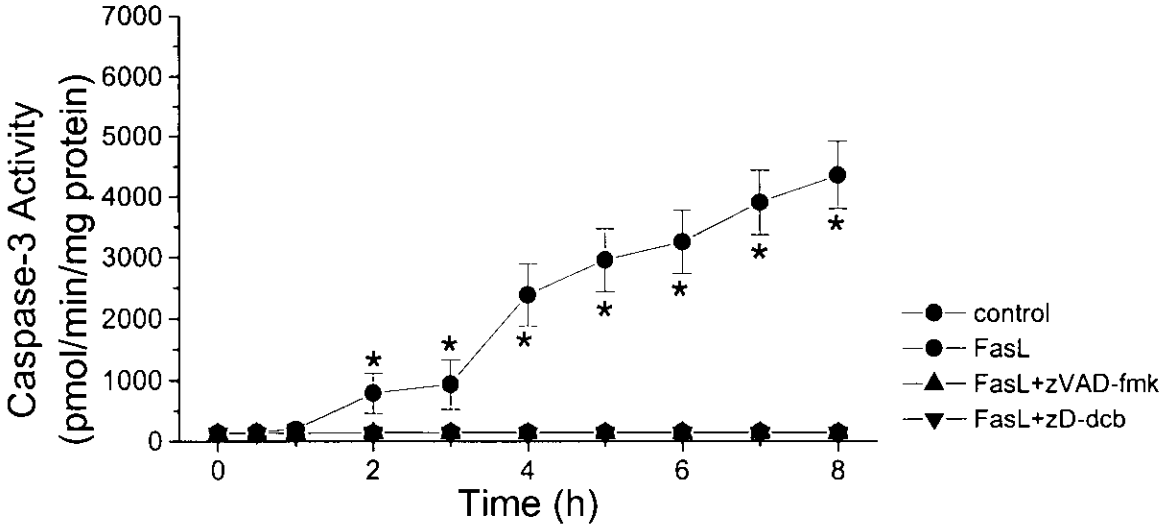

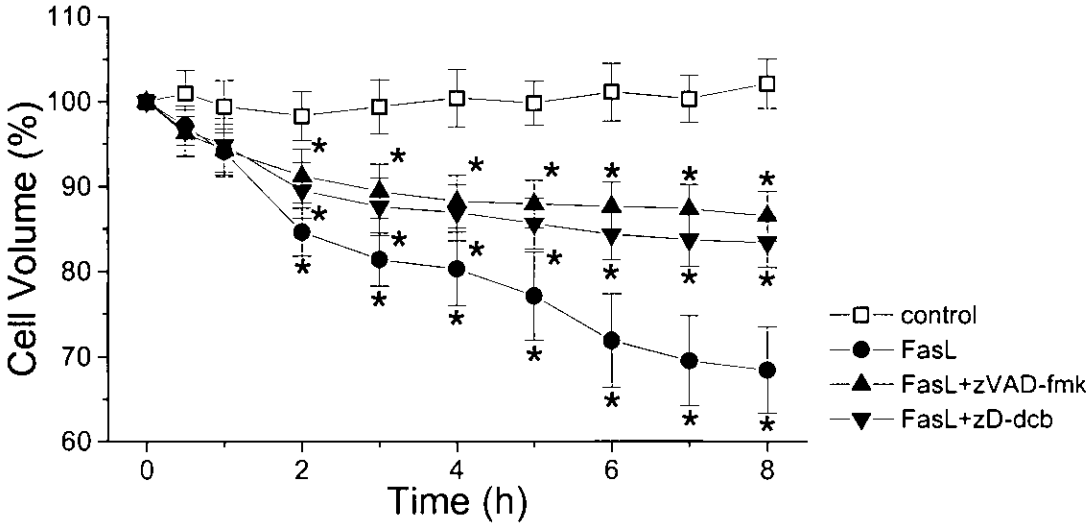

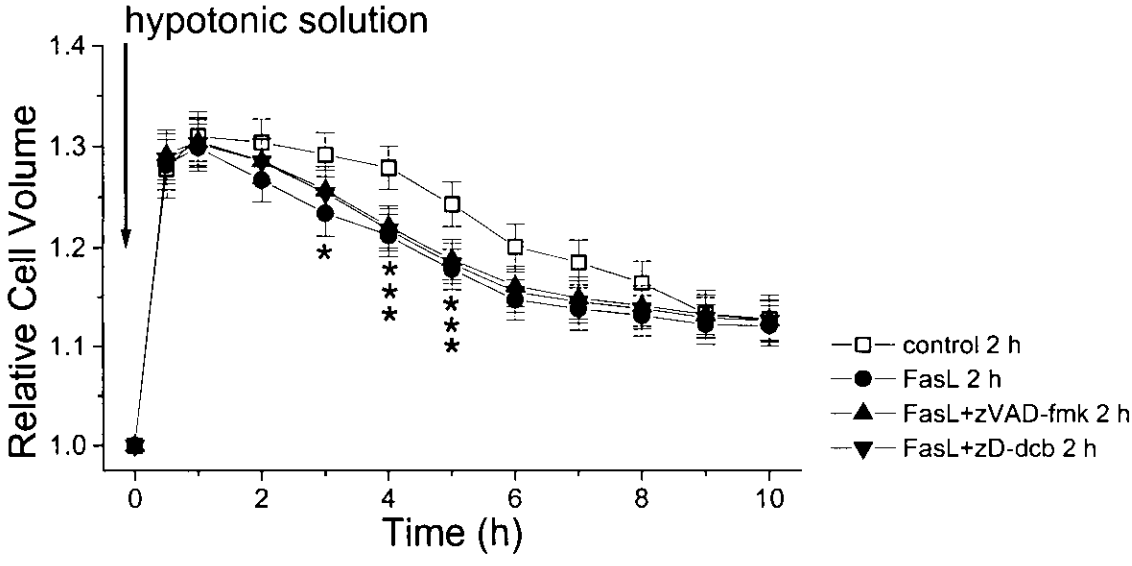

16B HeLa/STS

a

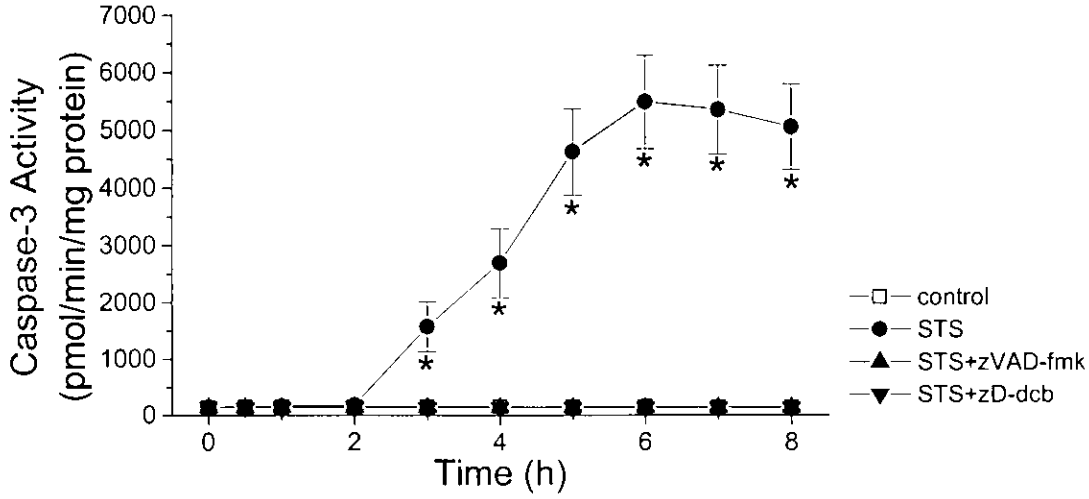

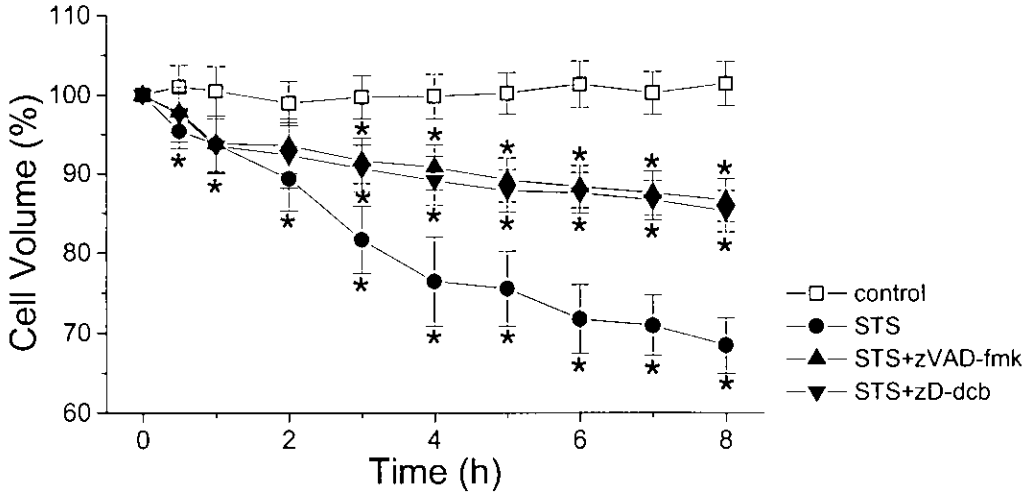

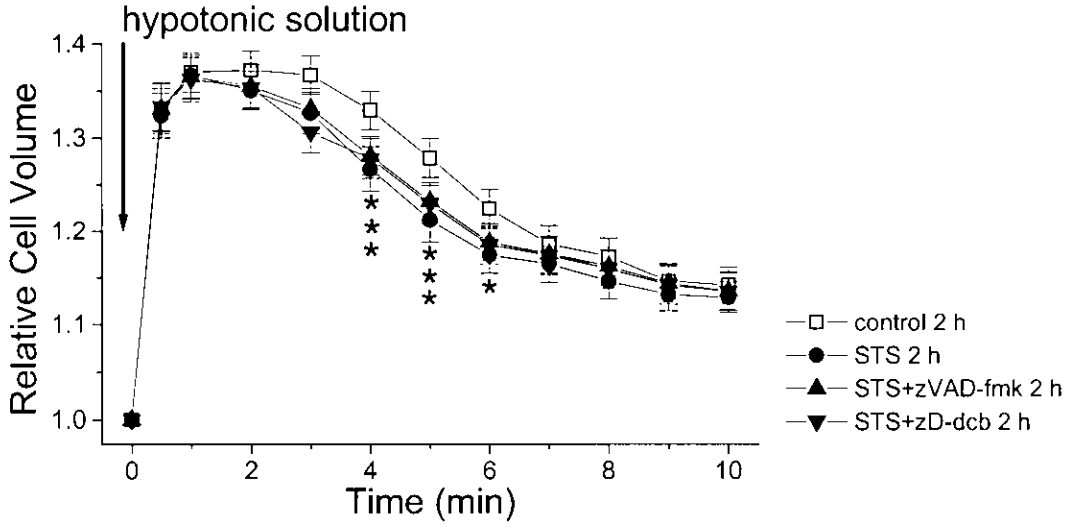

16B HeLa/TNF α

b

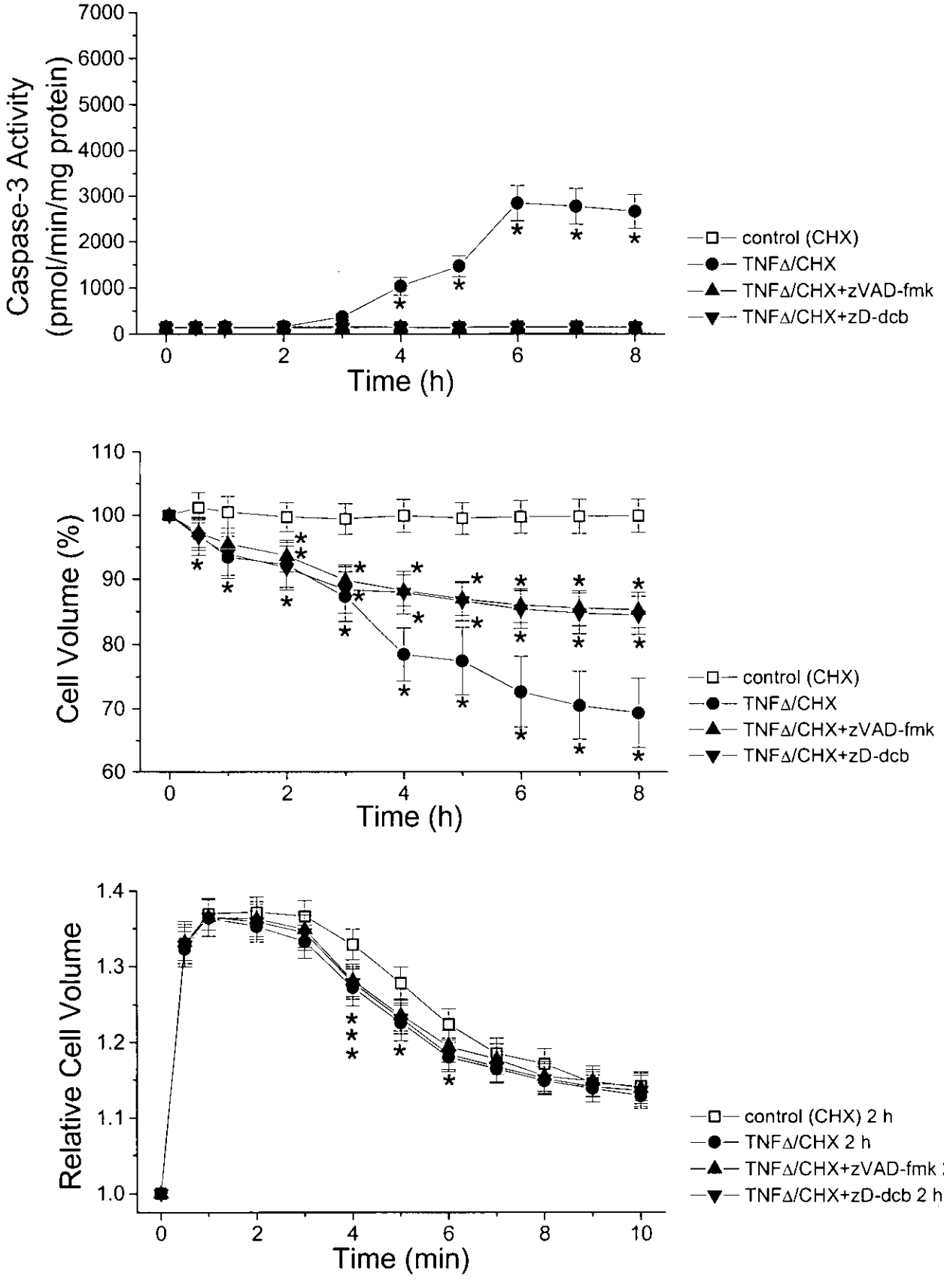

16B HeLa/FasL

c

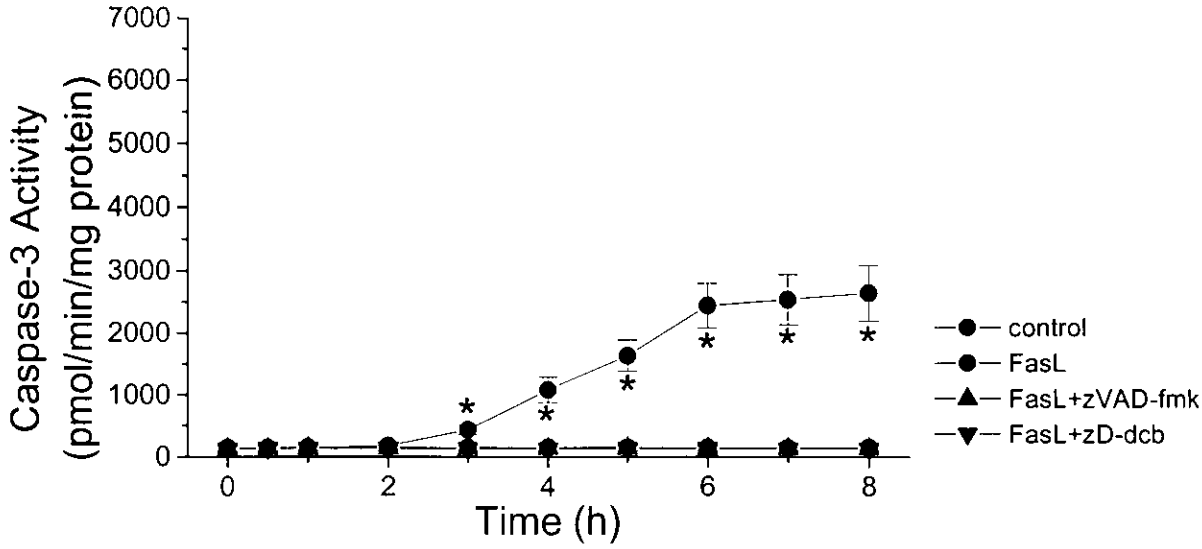

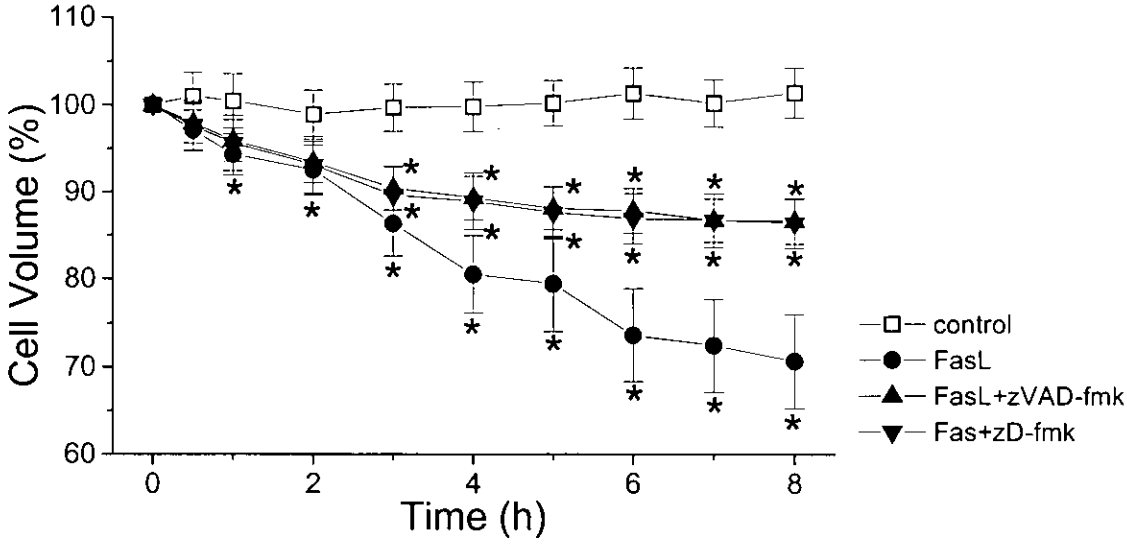

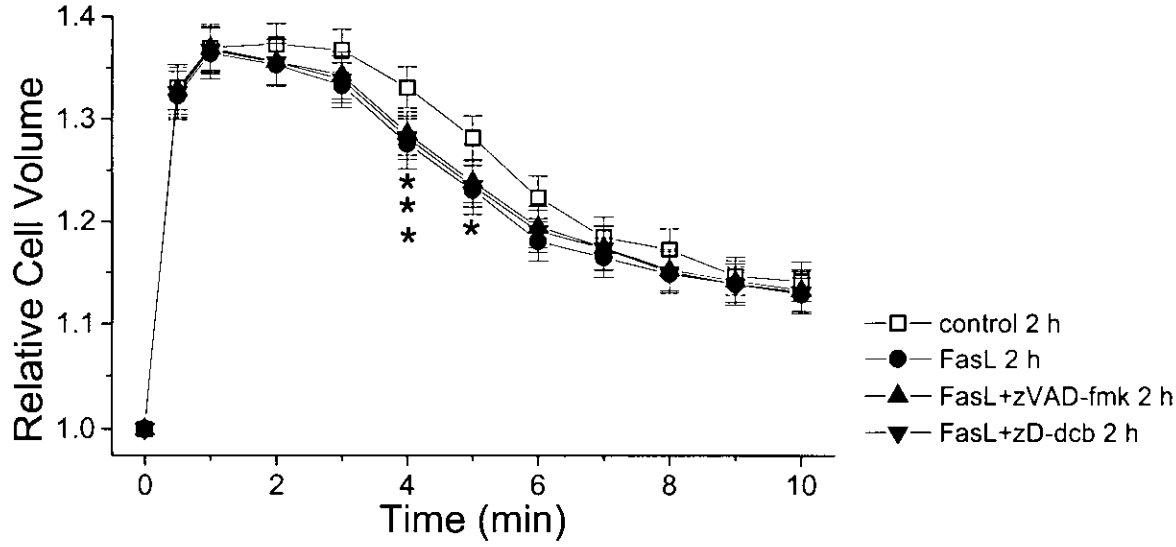

16C PC12/STS

a

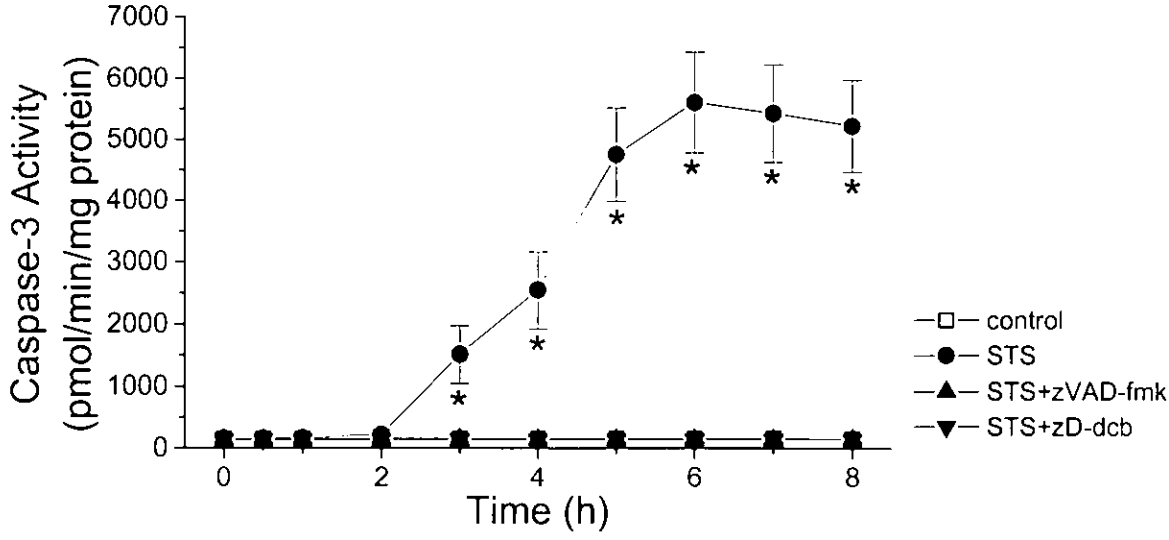

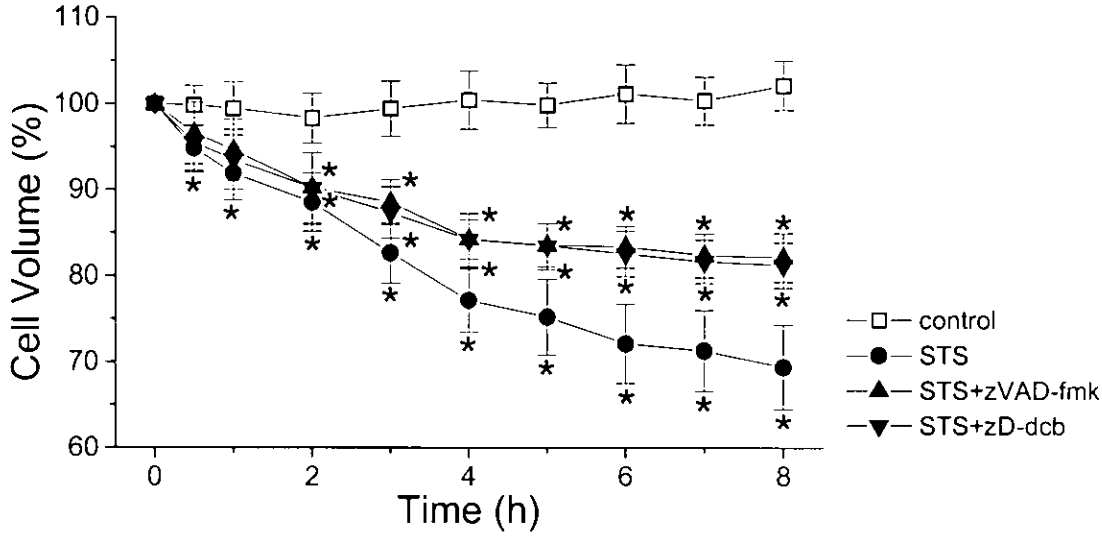

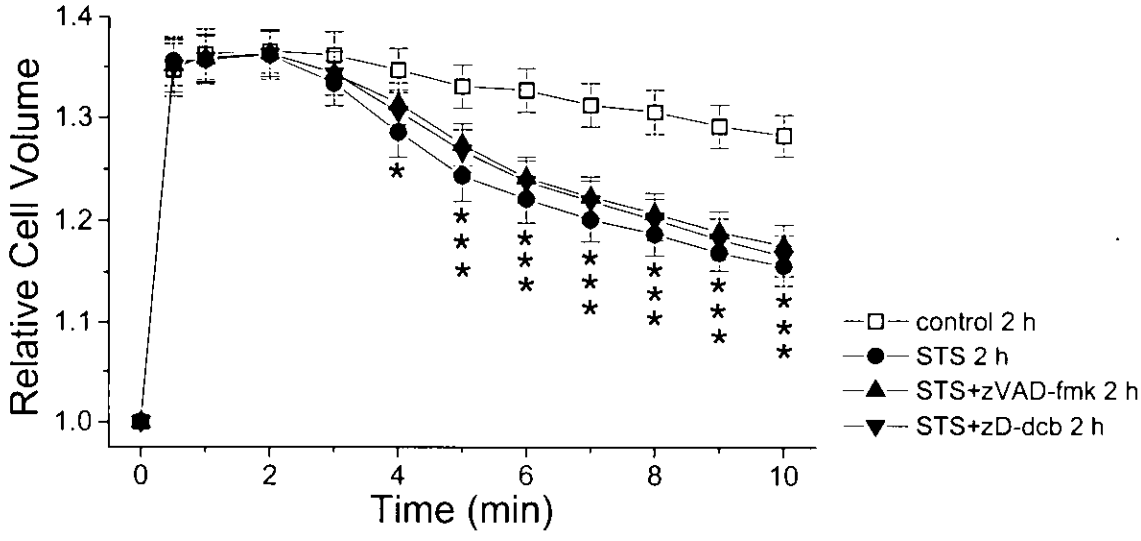

17 HeLa

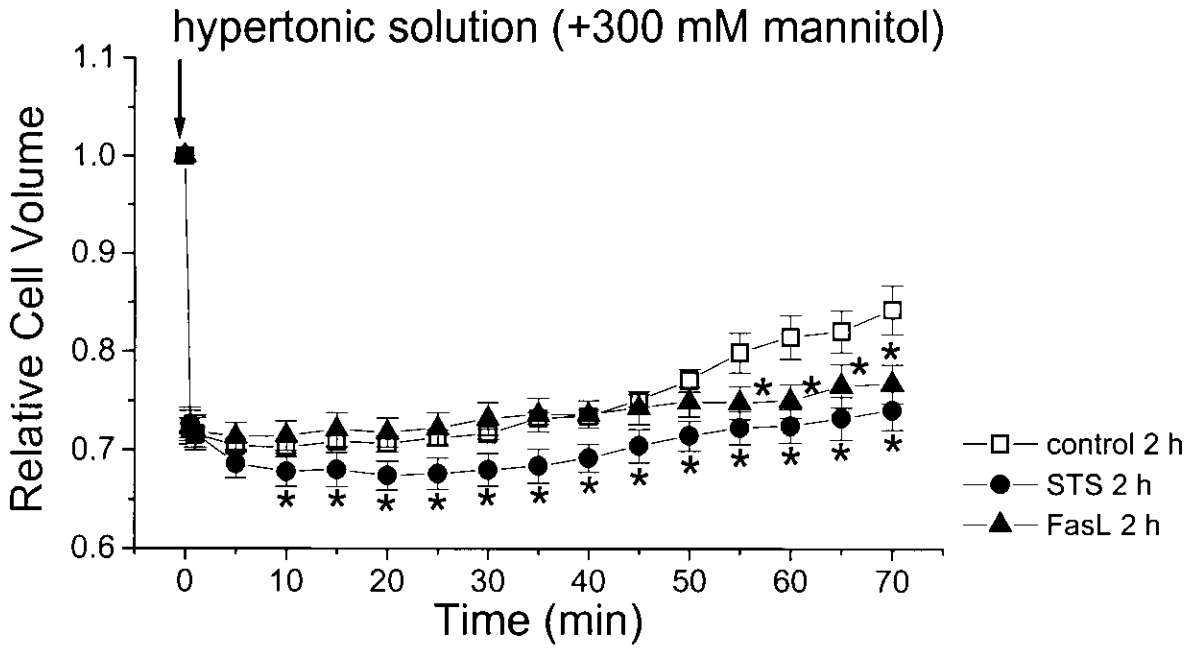
hypertonic solution (+300 mM mannitol)
Relative Cell Volume
1.1
1.0
0.9
0.8
0.7
0.6
0
10
20
30
40
50
60
70
Time (min)
control 2 h
STS 2 h
FasL 2 h

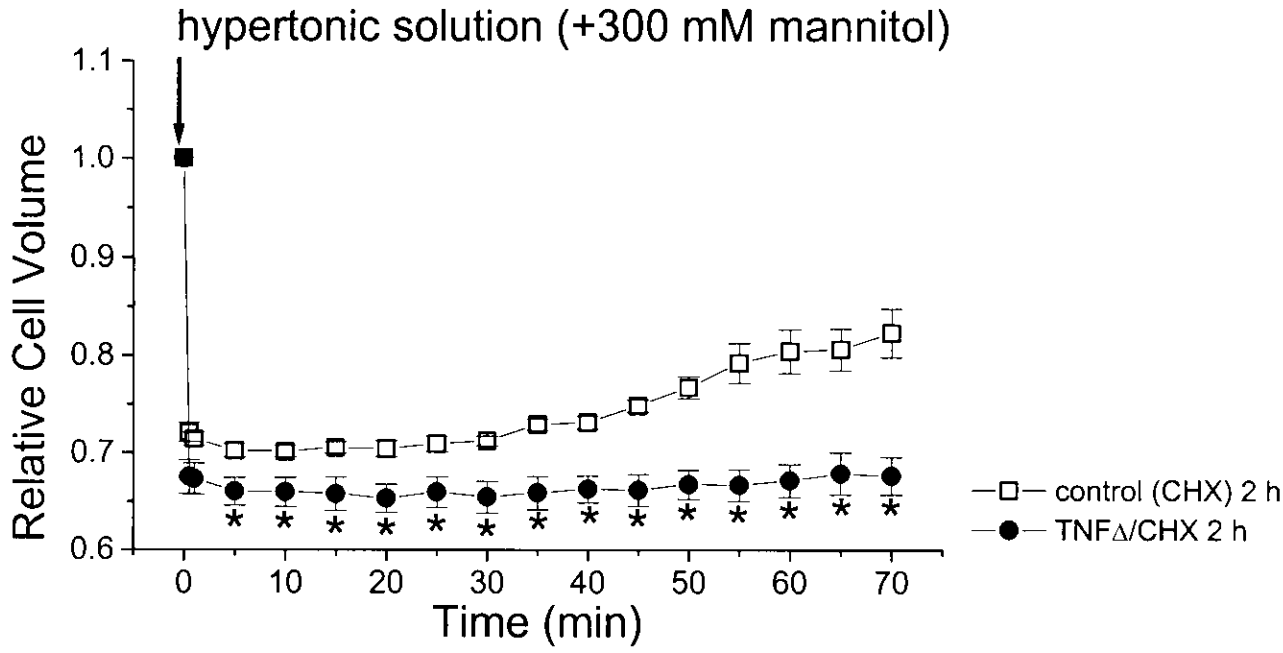
hypertonic solution (+300 mM mannitol)
Relative Cell Volume
1.1
1.0
0.9
0.8
0.7
0.6
0
10
20
30
40
50
60
70
Time (min)
control (CHX) 2 h
TNFΔ/CHX 2 h

18

A

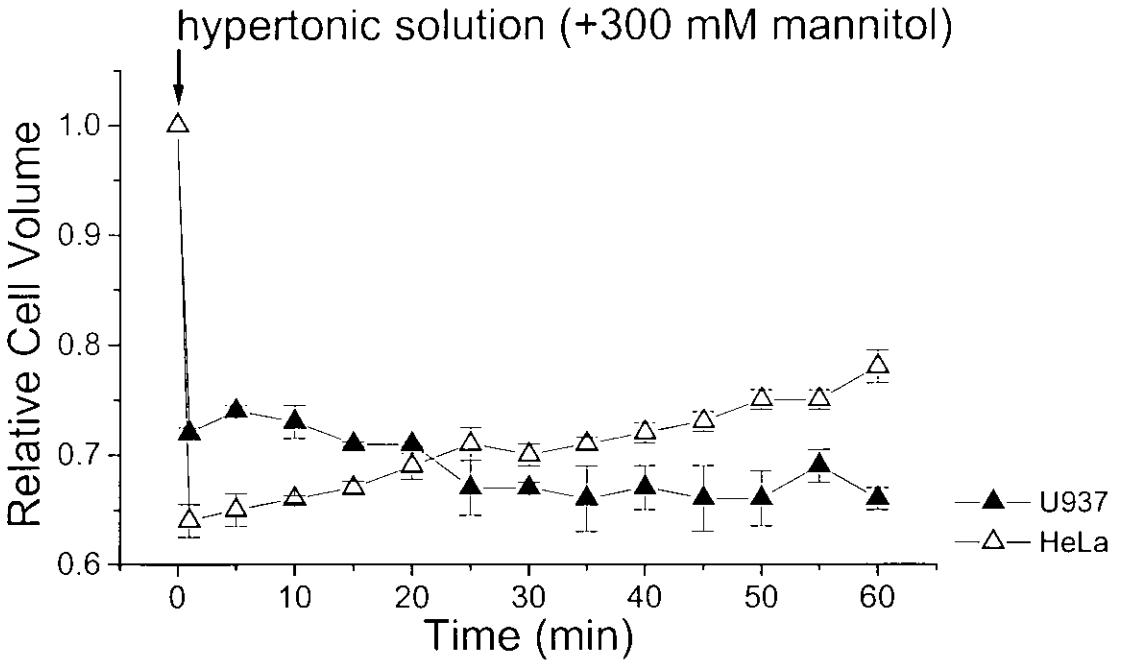
hypertonic solution (+300 mM mannitol)
Relative Cell Volume
1.0
0.9
0.8
0.7
0.6
0
10
20
30
40
50
60
Time (min)
U937
HeLa

B

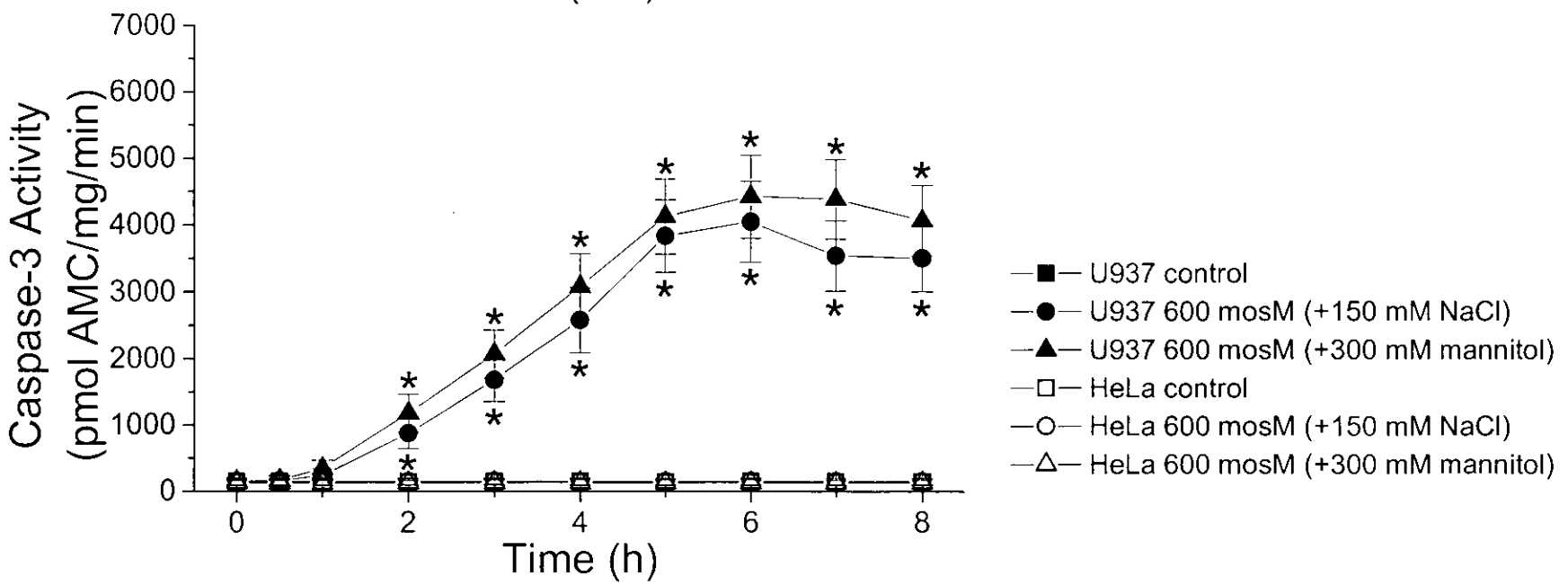
Caspase-3 Activity
(pmol AMC/mg/min)
7000
6000
5000
4000
3000
2000
1000
0
0
2
4
6
8
Time (h)
U937 control
U937 600 mosM (+150 mM NaCl)
U937 600 mosM (+300 mM mannitol)
HeLa control
HeLa 600 mosM (+150 mM NaCl)
HeLa 600 mosM (+300 mM mannitol)

19

A PS120

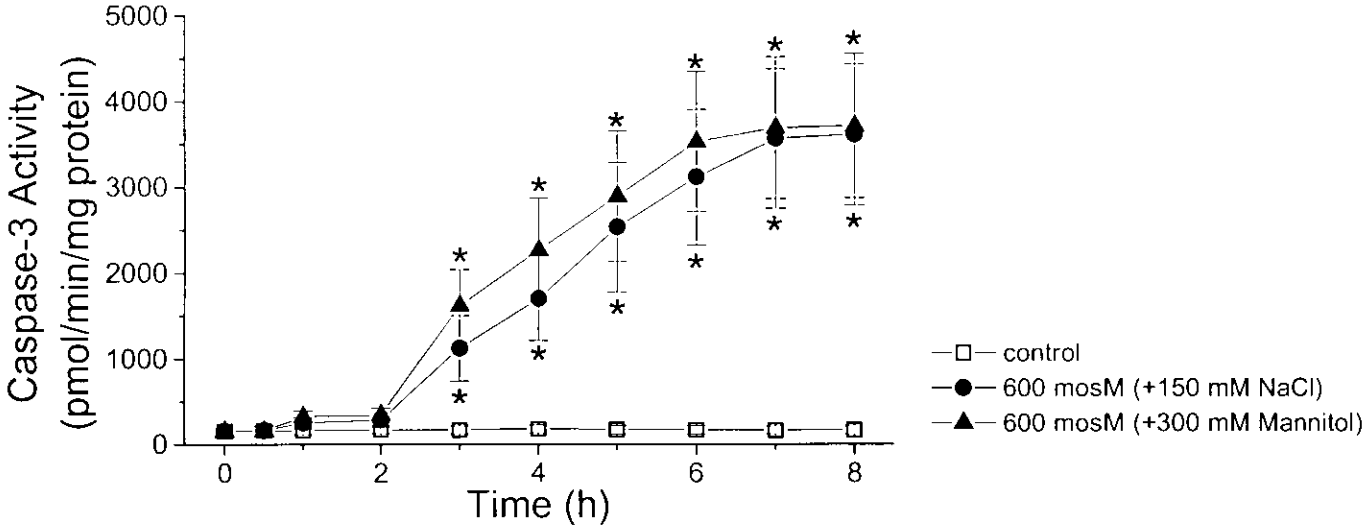

B PS120/NHE1

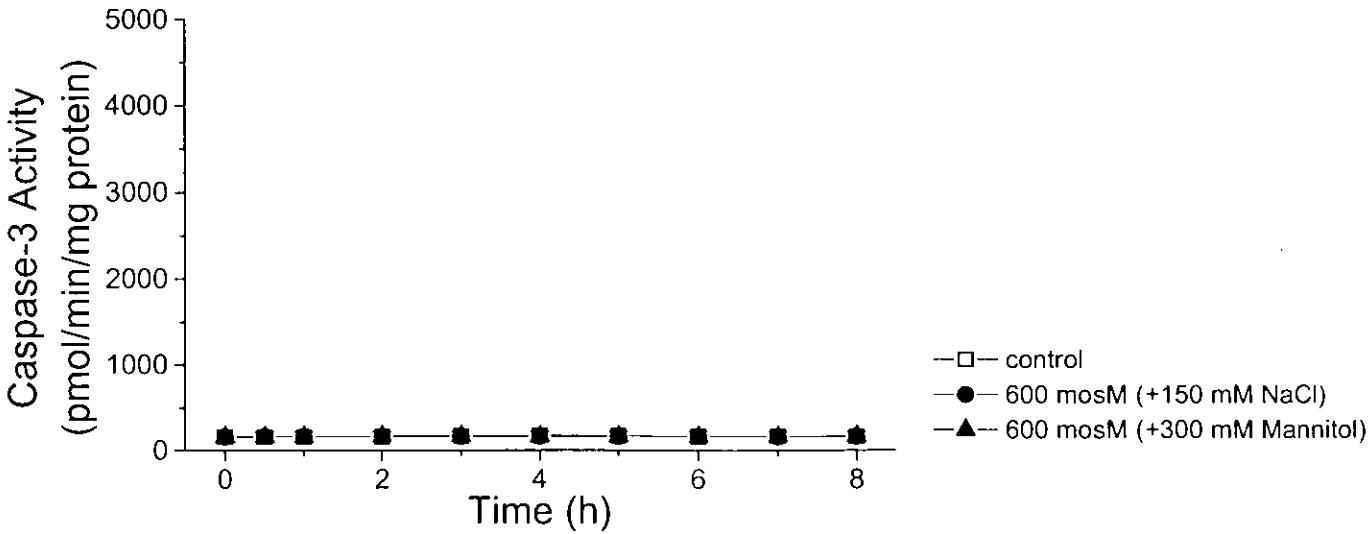

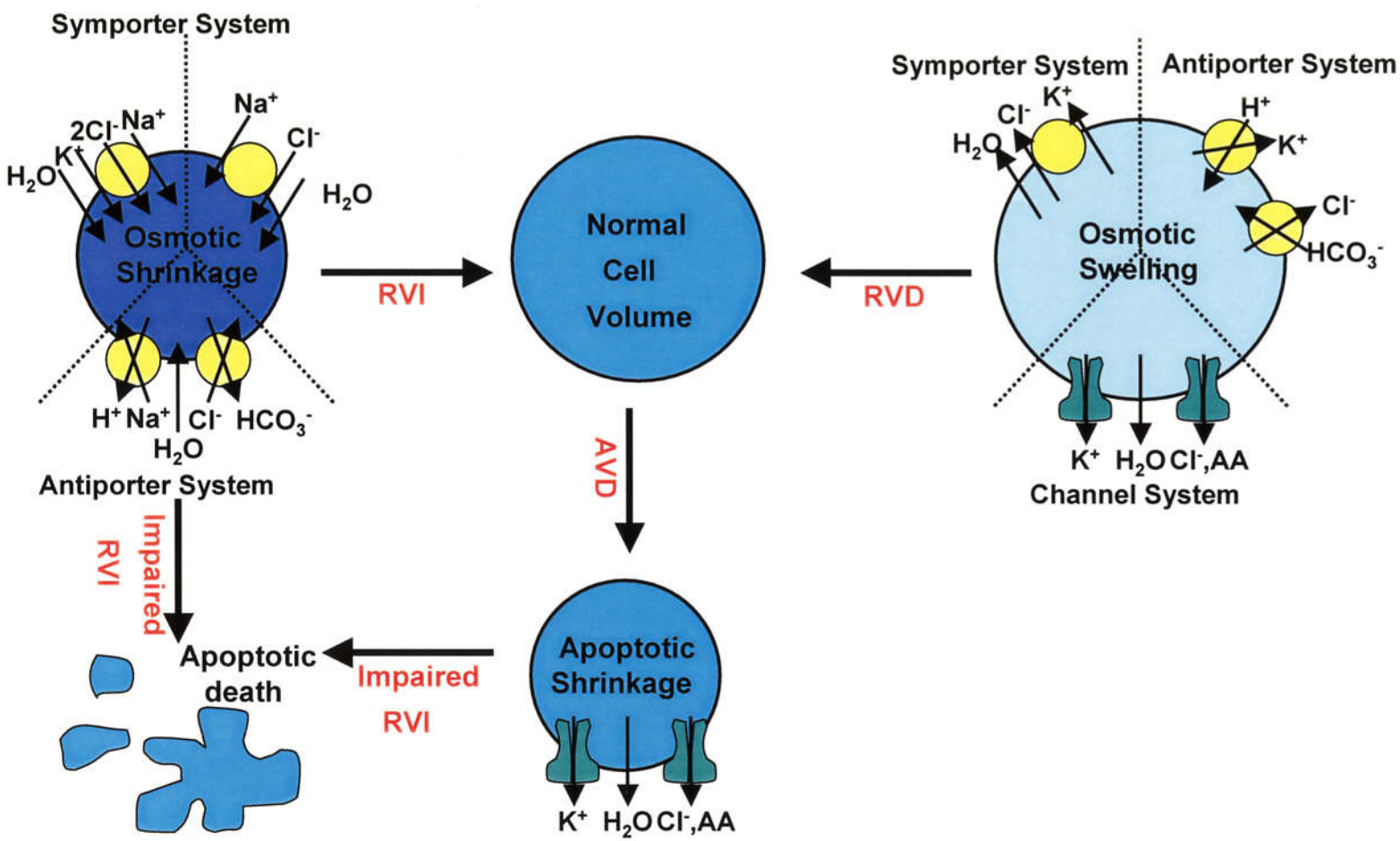
Symporter System
Na+
2Cl- Na+
Cl-
K+
H2O
H2O
Osmotic Shrinkage
H+ Na+ Cl- HCO3-
H2O
Antiporter System
RVI
Impaired
Apoptotic death
Impaired RVI
Apoptotic Shrinkage
K+ H2O Cl-,AA
AVD
Normal Cell Volume
RVD
Symporter System
Antiporter System
K+
Cl-
H2O
H+
K+
Cl-
HCO3-
Osmotic Swelling
K+ H2O Cl-,AA
Channel System